

https://dspace.org/

Palaeoclimate Reconstruction Using Charcoal from a Mid-Holocene Stratum 4b, Wonderwerk Cave, South Africa

Hlophe, Busisiwe

2024-06-18

University of the Witwatersrand, Johannesburg

https://hdl.handle.net/10539/45247

Hlophe, Busisiwe. (2023). Palaeoclimate Reconstruction Using Charcoal from a Mid-Holocene Stratum 4b, Wonderwerk Cave, South Africa. [Master's dissertation, University of the Witwatersrand, Johannesburg]. WIReDSpace. https://hdl.handle.net/10539/45247

Downloaded from a DSpace repository. https://dspace.org/

Palaeoclimate Reconstruction Using Charcoal from a Mid-Holocene Stratum 4b, Wonderwerk Cave, South Africa

by

Busisiwe Hlophe (1708117)

ORCID: 0000-0002-4123-9435

A Dissertation submitted to the Faculty of Science, University of the Witwatersrand, in fulfilment of the requirements for the degree of Master of Science

Supervisor: Prof. Marion Bamford

18 June 2024

Declaration

I declare that this dissertation is my own, unaided work. It is being submitted for the Degree of Master of Science, at the University of the Witwatersrand, Johannesburg. It has not been submitted before for any degree or examination at any other University.



(Signature of candidate)

18th day of June 2024 at Johannesburg

Abstract

Caves are often sources for palaeoenvironmental information in the dry interior regions of southern Africa. The Wonderwerk Cave, located in Northern Cape, is a national heritage site with a well-preserved, nearly complete record of the local Holocene LSA techno-complexes and past environmental indicators. Hence, it has the potential to provide valuable insights into past human behaviour as well as the local palaeoclimate and vegetation. This study examined wood charcoal from stratum 4b, Excavation 1 of the Wonderwerk Cave. The aim was to evaluate the taxonomic composition and the physiognomy of the charcoal to understand the environment around the cave 6.9-5.9 ka. The study also investigated the modern uses of the vegetation to infer how humans may have utilized the woody plants around them during that period. The results indicate the landscape cover included woody plants adapted to dry conditions and summer rainfall. However, the archaeological taxa identified also included two species that thrive in moist environments, *Halleria lucida* and *Olinia ventosa*, suggesting fluctuations in climate. The taxonomic composition also suggests an environment similar to the modern bushveld found near the cave. The low conductivity capacity as well as vulnerability and mesomorphy indices of the woods support the implication that the vegetation was adapted to low water availability or aridity. The cave's inhabitants likely used the identified plants for firewood, magical and medicinal purposes, and more between 6.9 and 5.9 ka.

Keywords: Charcoal analysis; Palaeovegetation; Palaeoclimate: Mid-Holocene; Wonderwerk Cave

Acknowledgements

I am deeply grateful to the University of the Witwatersrand and the Evolutionary Studies Institute (ESI) for providing me with the necessary resources and equipment to conduct my research. I would like to thank my supervisor, Prof. Marion Bamford, for her exceptional guidance, support, and supervision throughout this project. I also want to acknowledge and thank Liora Horwitz and Michael Chazan for leading the Wonderwerk project and giving me the opportunity to work on the charcoal.

I also thank PAST for providing Prof. Marion with funding to establish the ESI modern charcoal reference collection used in this project. I would also like to thank the NRF for funding this research project and the DSI-NRF Centre of Excellence in Palaeosciences for the intellectual support they have provided me during my postgraduate journey.

I am grateful to my family, friends, and colleagues for their unwavering support throughout my academic journey.

Table of Contents

Declaration ii
Abstract iii
Acknowledgements iv
Table of Contents v
List of Figures viii
List of Tables xi
CHAPTER ONE 1
Introduction 1
1.1 General introduction 1
1.2 Research Aims and Objectives 3
1.3 Dissertation outline 4
CHAPTER TWO 6
Literature Review 6
2.1 Plant-based environmental reconstructions 6
2.2 Physiognomy 18
2.3 Review of Holocene Environments 21
2.4 Summary of the chapter 24
CHAPTER THREE 26
Site background 26
3.1 Wonderwerk Cave and its location 26
3.2 The environmental context of the cave 27
3.3 Climate 31
3.4 Excavation history of the Wonderwerk Cave 32
3.5 Dating of the cave strata 36
3.6 Summary of the chapter 38
CHAPTER FOUR 39
Materials and Methods 39

4.1 Material 39
4.2 Methods 40
4.3 Summary of the chapter 46
CHAPTER FIVE 47
Results 47
5.1 Description of the archaeological charcoal specimens 47
5.3 Distribution of the species across the grid squares 95
5.4 Ecology of the taxa 97
5.5 Wonderwerk charcoal record 101
5.6 Physiognomy 102
5.7 Summary of the chapter 107
CHAPTER SIX 108
Discussion 108
6.1 Taxonomic implication of Mid-Holocene Wonderwerk Cave environment 108
6. 2 Interpretations of the wood physiognomy 113
6.3 Comparison with other southern African records 115
6.4 Implications on human subsistence and activities in the combustion features 117
6.5 Limitations and future research 121
6.6 Summary of the chapter 122
CHAPTER SEVEN 123
Conclusion 123
References 125
Appendix A: List of woody vegetation growing in the adjacent biozones; SVk 7, 8 and 9 (Rutherford *et al.,* 2006). 141
Appendix B: Summarized descriptions of the comparative charcoal anatomy. Charcoal described using the numbered features descriptions from Wheeler *et al.,* (1989). 145
Appendix C: Photomicrographs of (1-3) *Olinia ventosa*, (4-6) *Searsia lancea* and (7-9) *Ziziphus mucronata.* 147
Appendix D: Photomicrographs of (10-12) *Commiphora schimperi*, (13-15) *Olea europaea* subsp. *africana* and (16-18) *Ozoroa paniculosa.* 148
Appendix E: Photomicrographs of (19-21) *Tarchonanthus camphoratus*, (22-24) *T. parvicapitulatus* and (25-27) *T. trilobus.* 149

Appendix F: Photomicrographs of (28-30) *Searsia pyroides*, (31-33) *Vachellia mellifera* and (34-36) *V. tortilis.* 150

Appendix G: Venn diagram showing the deciduous and evergreen taxa identified in stratum 4b, Excavation 1, Wonderwerk Cave. 151

Appendix H: The distribution of the charcoal taxa across the cave floor. 152

Appendix I: Distribution of taxa in South African bioregions and biomes (Mucina and Rutherford, 2006; van Wykand van Wyk, 2013). 153

Appendix J: Climate of the Wonderwerk Cave locality between 6.9-5.9 ka cal BP. SRZ = Summer Rainfall Zone, WRZ= Winter Rainfall Zone, YRZ= Year-Round Zone. 154

List of Figures

Fig. 2.1: A schematic illustration of how archaeological charcoal is formed.

Fig. 2.2: Taphonomic filters affecting charcoal assemblages from live vegetation till analysis in the laboratory.

Fig. 3.1: Map of South Africa showing the situation of Wonderwerk Cave.

Fig. 3.2: The location of the Wonderwerk Cave in the Kuruman Mountain Bushveld and the other savanna vegetation units around the cave.

Fig. 3.3: Image showing the current environment around the Wonderwerk Cave.

Fig. 3.4: Map showing the mean annual rainfall of Southern Africa (in mm) with winter rainfall increasing towards the left.

Fig. 3.5: Image showing Wonderwerk Cave.

Fig. 4.1: The profiles of the Wonderwerk Cave.

Fig. 4.2: The three anatomical planes of wood charcoal.

Fig. 5.1: Photomicrographs of *Ozoroa paniculosa* WW-4b-R25G charcoal from stratum 4b of Excavation 1, Wonderwerk Cave.

Fig. 5.2: Photomicrographs of *Searsia lancea* WW-4b-Q22K charcoal from stratum 4b of Excavation 1, Wonderwerk Cave.

Fig. 5.3: Photomicrographs of *Heteromorpha arborescens* WW-4b-S25IA charcoal from stratum 4b of Excavation 1, Wonderwerk Cave.

Fig. 5.4: Photomicrographs of *Tarchonanthus camphoratus* WW-4b-Q22B charcoal from stratum 4b of Excavation 1, Wonderwerk Cave.

Fig 5.5: Photomicrographs of *Tarchonanthus parvicapitulatus* WW-4b-S23E charcoal from stratum 4b of Excavation 1, Wonderwerk Cave.

Fig. 5.6: Photomicrographs of *Ehretia* sp. WW-4b-Q22IN charcoal from stratum 4b of Excavation 1, Wonderwerk Cave.

Fig. 5.7: Photomicrographs of *Commiphora schimperi* WW-4b-S23C charcoal from stratum 4b of Excavation 1, Wonderwerk Cave.

Fig. 5.8: Photomicrographs *of Olea europaea* subsp. *africana* WW-4b-R21B charcoal from stratum 4b of Excavation 1, Wonderwerk Cave.

Fig. 5.9: Photomicrographs of *Olinia ventosa* WW-4b-Q22IL charcoal from stratum 4b of Excavation 1, Wonderwerk Cave.

Fig. 5.10: Photomicrographs of *Senegalia caffra* WW-4b-S21IIH charcoal from stratum 4b of Excavation 1, Wonderwerk Cave.

Fig. 5.11: Photomicrographs of *Vachellia* cf. *tortilis* WW-4b-Q24G charcoal from stratum 4b of Excavation 1, Wonderwerk Cave.

Fig. 5.12: Photomicrographs of *Vachellia* cf. *karroo* WW-4b-S21IIIK charcoal from stratum 4b of Excavation 1, Wonderwerk Cave.

Fig. 5.13: Photomicrographs of *Berchemia* cf. *zeyheri* WW-4b-S25ID charcoal from stratum 4b of Excavation 1, Wonderwerk Cave.

Fig. 5.14: Photomicrographs of *Ziziphus mucronata* WW-4b-R24D charcoal from stratum 4b of Excavation 1, Wonderwerk Cave.

Fig. 5.15: Photomicrographs of *Halleria lucida* WW-4b-Q22P charcoal from stratum 4b of Excavation 1, Wonderwerk Cave.

Fig. 5.16: Photomicrographs of Type 16 WW-4b-T21G charcoal from stratum 4b of Excavation 1, Wonderwerk Cave.

Fig. 5.17: Photomicrographs of Type 17 WW-4b-S21IIA charcoal from stratum 4b of Excavation 1, Wonderwerk Cave.

Fig. 5.18: Photomicrographs of Type 18 WW-4b-Q24C charcoal from stratum 4b of Excavation 1, Wonderwerk Cave.

Fig. 5.19: Photomicrographs of Type 19 WW-4b-S21IIH charcoal from stratum 4b of Excavation 1, Wonderwerk Cave.

List of Tables

Table 3.1: A list of important woody taxa growing near the Wonderwerk Cave.

Table 3.2: The dominant lithic technology, revised ages, and the estimated abundance of charcoal packets and pieces recovered from the Holocene strata of the Wonderwerk Cave.

Table 5.1: Summary of the charcoal types from stratum 4b, Excavation 1, Wonderwerk Cave.

Table 5.2: Species distribution in the different grid squares of stratum 4b.

Table 5.3: The description, ecoregion and geographical distribution of the modern taxa.

Table 5.4: An updated record of the taxa identified from stratum 4b of the Wonderwerk Cave.

Table 5.5: The physiognomy of the charcoal (Vulnerability index, VI; Conductivity capacity, CC; Mesomorphy index, MI).

CHAPTER ONE

Introduction

1.1 General introduction

Much of the research on the Later Stone Age (LSA) in southern Africa has been focused on the mesic coastal regions, while only a small portion has been directed towards the arid interior (Ecker *et al.,* 2017). The arid interior lacks the necessary lakes and swamps to preserve palaeoenvironmental proxies, such as fossil wood, pollen, and phytoliths, which are typically used in palaeoclimate reconstruction studies (Scott and Thackeray, 2015). As a result, cave deposits such as those from Equus Cave (Scott, 1987) have been used as an alternative source for such evidence. However, dating the sediments in most caves is often a challenge, which makes it difficult to conduct precise temporal reconstruction studies.

The Wonderwerk Cave is a significant archaeological and palaeontological site that provides valuable insights into human evolution. The cave was first studied in the 1940s, before its excavation between 1970s and mid-2000s. Seven areas were excavated within the cave and Excavation 1, close to the cave entrance, had a long cultural sequence associated with well-preserved faunal and botanical remains, including pollen, phytoliths, and wood. These remains can be used to date sediments and study past environments (Horwitz and Chazan, 2015). Important findings include some of the earliest evidence of humans controlling fire, from 1 Ma (Berna *et al.,* 2012). The cave also recorded the last known appearance of *Antidorcas bondi,* an extinct Pleistocene springbok (Ecker *et al.,* 2017). Other extinct taxa discovered include extinct animals such as a large zebra (*Equus capensis*), a large alcelaphine (*Megalotragus priscus*) and a hyrax (*Procavia antiqua*) (Thackeray, 2015). The site also preserves some of the oldest *art mobilier* in southern Africa from 10,200±90 BP (Rhodes *et al.*, 2022).

Previous studies conducted at Excavation 1 of Wonderwerk Cave suggest that the Holocene period (11.8-0 ka) in the interior of southern Africa was mainly dominated by dry climate conditions (Brook *et al.,* 2010; 2015; Bamford, 2015b; House *et al.,* 2022). However, the analysis of stratum 4b reveals a wet phase during the Mid-Holocene. Pollen data suggest that climate conditions associated with dry karroid vegetation existed near the cave during the Early Holocene before shifting to moist, grassy conditions in the Mid-Holocene, around 6.5 ka (Scott and Thackeray, 2015). Isotope data from ostrich eggshells and herbivore tooth enamel as well as macro-faunal composition data from stratum 4b suggest that a dry savanna woodland with C_3 trees/shrubs and C_4 grasses existed in the Early Holocene from 12.5-6.2 ka, later shifting to a wetter savanna grassland as C_4 grasses expanded (Lee-Thorp and Ecker, 2015; Ecker *et al.,* 2018). This wet phase is consistent with the occurrence of abnormally high concentrations of occupational material such as artifacts, charcoal, faunal remains, and burnt stones discovered in stratum 4aLH (dated to 6.2-5.4 ka cal BP, found between stratum 4b and 4a). Furthermore, a shift in artifact type and material was also noted in stratum 4aLH (Ecker *et al.,* 2017).

Charcoal remains are the most abundantly preserved macro-botanical remains in cave sites, particularly in the LSA sequences (Bamford, 2015b; Puech *et al.,* 2020; Zwane and Bamford, 2021). This is because caves are dry and ideal for the preservation of plant matter and charcoal (Chikumbirike and Bamford, 2021). The Wonderwerk Cave in particular has an abundance of charcoal recovered from the Holocene strata (5-1) (Bamford, 2015b). The taxonomic composition of a charcoal assemblage can reveal essential information about past environmental contexts when interpreted using the environmental requirements of the modern analogs (Utescher *et al.,* 2014). Charcoal inside caves are the burnt remains of woods that were collected by the cave inhabitants and they represent a subset of the woody plants in the vicinity of the cave. Based on the principle of least effort (Shackleton and Prins, 1992), the woods most likely were collected from within an accessible

radius of the site, but acknowledging other determinants for the selection of woods. The diversity of woody taxa, therefore, represents the local vegetation which in turn reflects the local climate.

Charcoal assemblages from Wonderwerk Cave have been analysed previously by Bamford (2015b) and House *et al.* (2022). About 200 charcoals from stratum 4b were analysed in House *et al.* (2022) but only 75 charcoals could be identified and represented five species. Hence, there is a need to analyse more samples from this archaeological stratum and at a higher resolution by employing other techniques such as physiognomic analysis. This method relies on the close relationship between climate and the internal anatomy of the wood to infer climate and does not require taxonomic determinations (Carlquist, 1977; Baas *et al.,* 1983; Wiemann *et al.,* 1998). Additionally, charcoal can reveal information on past human subsistence.

1.2 Research Aims and Objectives

This study aims to examine the charcoal deposits from stratum 4b at Wonderwerk Cave to understand the vegetation, climate, and subsistence patterns of the hunter-gatherer communities in the interior region of southern Africa during the Mid-Holocene period. The study will use the types of vegetation present in the charcoal assemblage to develop an understanding of the climate patterns and wood usage by the hunter-gatherer communities during this time.

The objectives are as follows:

1) Identify the taxa present in the Wonderwerk Cave charcoal assemblage and determine the paleoclimatic conditions based on the environmental requirements of their modern analogs.

2) Study the anatomy of the wood charcoal and physiognomy to establish a correlation between wood anatomy and local water availability/rainfall patterns.

3) Investigate the possible ways in which the cave occupants may have used the woody plants in their surroundings.

It is hypothesized that vegetation and environmental conditions associated with dry climate will be reflected by the charcoal and the results will be in accordance with the interpretation from pollen and fauna. The results of this study might also address the question of the cultural shift in Wilton industries occurring in stratum 4aLH, which is coincident with an interval of a moist climate and a maximum expansion of a C_4 grassland shown by pollen data, ostrich eggshells isotopes and the abundance of large grazer taxa.

1.3 Dissertation outline

The rest of this dissertation is divided into six chapters which include the following:

Literature review

This chapter reviews the various methods using botanical remains in palaeoenvironmental studies conducted worldwide. Additionally, it highlights previous palaeo- and archaeological studies carried out in southern Africa and Wonderwerk Cave while pointing out the gaps in knowledge.

Site Background

This chapter contains details about the Wonderwerk Cave's location, excavation history, archaeological layers, contemporaneous vegetation, and climate.

Materials and Methods

This chapter details the sampling and data exploration techniques employed to analyse charcoal from stratum 4b of the Wonderwerk Cave. Two methods are usually used to infer palaeoclimatic conditions from wood. These methods were employed in this study, one focuses on the analysis of the physiological adaptations that permit woody plants to grow under specific climatic conditions and the other on the botanical identification of archaeological charcoal, and infers past climatic conditions based on the environmental requirements of the modern analogs.

Results

The results chapter contains descriptions of the archaeological charcoal, its spatial distribution across the cave floor, the ecology of modern analogues, an updated record of Wonderwerk Cave charcoal, and the physiognomy of the wood charcoal.

Discussion

This chapter details the implications made from the archaeological charcoal about the vegetation, climate and exploration of woody plants at the cave around 6.9-5.9 ka. It concludes by giving a broad summary of the environmental conditions in the interior of southern Africa during the Holocene.

Conclusion

The concluding chapter summarises the whole dissertation.

CHAPTER TWO

Literature Review

2.1 Plant-based environmental reconstructions

2.1.1 Botanical palaeoenvironmental reconstructions

Since the 19th century, botanical remains have been utilized to study past climates and environments. This method now has various approaches for reconstructing and quantifying paleoclimatic and paleoenvironmental parameters. One such approach involves examining the physiognomy or expression of specific plant traits. This approach is independent of taxonomic determinations and relies solely on the correlation between specific climate parameters and the anatomy of plant organs, such as leaves or wood (Bailey and Sinnott, 1915; Wolfe and Upchurch, 1987; Conran *et al.,* 2016).

Physiognomic implications have been used as a climate reconstruction method since the early 1900's. For example, Bailey and Sinnott (1915) proposed the analysis of dicotyledonous fossil leaf assemblages to construct a relationship between leaf anatomy and climate. This study finds that leaves in plants adapted to mesic, tropical environments have entire margins, whereas leaves in mesic, temperate habitats have non-entire margins. Wheeler and Baas (1993) studied wood features to interpret past climate and long-term climate change. This study finds ecologically significant differences between wood from the southern and northern hemispheres, similar to today.

The second plant-based reconstruction approach requires the taxonomic determinations of the fossil plants, and the results are interpreted using the nearest living relative method. This approach assumes there is a relationship between the fossil and modern plant taxa and that the climatic requirements of the plants have

remained the same over time. So, past climate regimes can be inferred by using the environmental requirements of modern plants with a known climatic distribution. This method is most effective when applied to Quaternary and Neogene plants, where the changes in environmental requirements are minimal (Utescher *et al.,* 2014). Several methods have been developed for this approach, including CLIMBOT (co-existence approach) (Mosbrugger and Utescher, 1997), Climate Amplitude Method (Fauquette *et al.,* 1998), Wood anatomical approach (Wiemann *et al.,* 1998), Probability Density Functions (Kühl *et al.,* 2002) and Pastclim (Leonardi *et al.,* 2023).

Different structures in plants can be informative about the climate. Pollen is the most used source for reconstructing past environmental conditions (*Guiot et al.,* 1993; Mauri *et al.,* 2015). In southern Africa, pollen has been successfully employed in studies like Scott (1987), Scott *et al.* (2003), Brook *et al.* (2010, 2015) and Scott and Thackeray (2015). While pollen is an excellent data source, its use as a localized environmental indicator is often debated due to its susceptibility to transport over long distances, given its light weight. Additionally, pollen types are challenging to identify to species, which might influence data interpretation (Hubau *et al.,* 2012). Phytoliths, on the other hand, also offer information about past ecosystems. Rossouw (2016) employed grass phytoliths found in the Pleistocene sequence of the Wonderwerk Cave to reconstruct the environment surrounding the cave. However, this method also has limitations, as not all plant species produce phytoliths (Rossouw, 2016).

2.1.2 History of anthracology

Archaeological macrocharcoal represents the remains of purposeful firewood collection and use by past humans (Asouti and Austin, 2005; Braadbaart and Poole, 2008). The process that forms charcoal, known as charcoalification, occurs

by charring or carbonization of wood with limited oxygen or in its absence, respectively. Additionally, charcoal is formed when wood is burnt in an open fire with an abundant oxygen supply, but only if combustion is incomplete/interrupted. If combustion is complete/uninterrupted, ash is formed instead (Fig. 2.1). Ash is helpful in identifying hearths but not in reconstruction studies as it cannot be identified (Braadbaart and Poole, 2008).

Charcoal is a chemically stable product that is highly resistant to chemical weathering (Braadbaart and Poole, 2008), which enables its long-term preservation in soil profiles. It preserves wood's internal structure, allowing for identification through direct comparison with modern charcoal, as wood retains a maximum number of anatomical features after carbonization (Zicherman and Williamson, 1981). However, caution is necessary when dealing with absolute measurements, as burning can cause shrinkage (8-20%) and fissures, depending on factors like wood type, moisture content, and fire temperature. While most wood features' sizes are not affected by carbonization, the tangential vessel diameter can be reduced by 17% (Prior and Alvin, 1986; Prior and Gasson, 1993; Gonçalves *et al.,* 2012). Additionally, charcoal is very pressure-resistant, withstanding up to 13.7 MPa pressure before fracturing (Chrzavzez *et al.,* 2014), which allows it to survive the trampling that occurs in caves or shelters.

Firewood has been used as a fuel source since the Early Paleolithic age. This is evidenced by the increased occurence of carbonized material globally from this time (Gelabert *et al.,* 2011). Archaeological and ecological studies suggest that *Homo erectus*, a hominin species adapted to a cooked meal diet and lived around 1.9 Ma, was the first to use fire in the Early-Middle Pleistocene in the Levant and Africa (Karkanas *et al.,* 2007; Berna *et al.,* 2012). By the Late Paleolithic period, around 400-500 thousand years ago, fire had become a habitual tool for humans and is linked with increasing social and intellectual complexity. Potential uses of fire during that time might have included cooking and roasting food, providing light, and safeguarding against predators. It is possible that fire also played a role in

human migration, as pre-modern humans likely used it to explore and settle in unfamiliar, colder environments (Karkanas *et al.,* 2007).

During the Paleolithic era, fire was widely used as a sustainable technology in caves, rock shelters, and open-air sites. For instance, researchers discovered ash-rich sediments in Qesem Cave in Israel, dating back to the Middle Pleistocene period. Another study by Zwane and Bamford (2021) analysed charcoal from the Middle Paleolithic period in Sibudu Cave, South Africa. Vidal-Matutano (2017) studied materials from Middle Paleolithic hearths in El Salt Rock Shelter in Eastern Iberia. This indicates that people were already collecting wood from their surroundings to burn inside caves during the Paleolithic era (Karkanas *et al.,* 2007).

Anthracology is a significant field that sheds light on past environments and human-plant interactions by analysing charcoal remains (Théry-Parisot and Henry, 2012; Dotte-Sarout *et al.,* 2015). Before its potential as an environmental indicator was known, charcoal was primarily used for radiocarbon dating (Vogel *et al.,* 1986) and studying past fire patterns (Hoffman *et al.,* 2016). During the 1940s and 1950s, researchers in the United Kingdom and France published the first studies proposing macrocharcoal as a source of palaeoenvironmental data (Salisbury and Jane, 1940; Godwin and Tansley, 1941; Balout, 1952). The availability of light-reflected microscopes in the late 1960s was a significant milestone in anthracology, enabling detailed analysis of charcoal assemblages (Leney and Casteel, 1975). By the 1980s and 1990s, the field's growth continued as it became widely used for reconstructing past ecologies and human interactions with plants (Deacon *et al.,* 1984; Chabal, 1997; Cowling *et al.,* 1999). Anthracology assumes that the anthracological hypothesis, suggesting that charcoal assemblages represent past vegetation compositions, is true (Dotte-Sarout *et al.,* 2015). Chabal (1997) developed the first reliable methodological approach and quantification methods supporting charcoal as an indicator of past environmental conditions, forming the analytical framework used by anthracologists today.

The International Association of Wood Anatomists (IAWA) has devised a specific protocol to aid in identifying and describing wood (Wheeler *et al.,* 1989). The protocol includes a comprehensive list and descriptions of all microscopic tissues in both softwood and hardwood, and each is assigned a unique number (Wheeler *et al.,* 1989). Additionally, the committee provides guidance on the proper way to view these features, as some are best seen from the tangential longitudinal section, while others are best viewed in the transverse section at varying magnifications.

InsideWood (Wheeler, 2011), a searchable online database that provides a list of wood features accompanied by photographs and descriptions, was developed for automated assistance with wood identification. This database is helpful in identifying and comparing fossil wood and charcoal. To identify a particular type of wood, the user needs to select its features from the numbered list of tissue features. The system then uses a combination of these features to provide a potential identification of the wood. However, this database is not very helpful for identifying South African woody plants, because it doesn't include many of the species found in the region. In this region, identification is done by comparison with charcoal from the contemporary woody vegetation.

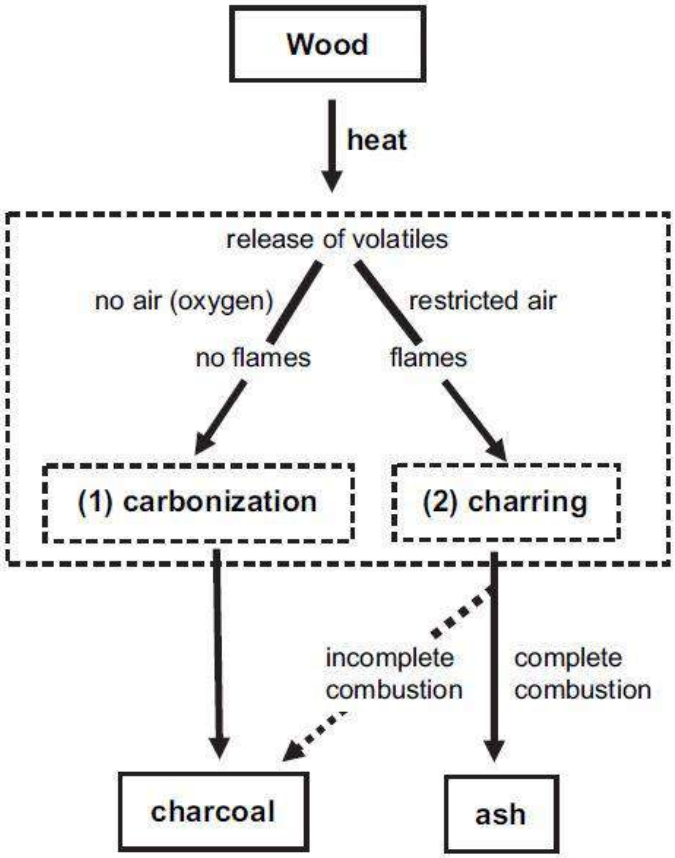


Fig. 2.1: A schematic illustration of how archaeological charcoal is formed. When burnt, wood releases volatiles and undergoes either carbonization or charring. (1) Carbonization occurs when there is no oxygen. (2) Charring occurs when oxygen is limited, and the volatiles ignite, thus releasing flames. Incomplete or interrupted combustion with oxygen supply results in the formation of charcoal, while complete combustion forms ash. (Source: Braadbaart and Poole, 2008).

2.1.3 Taphonomic filters

The legitimacy of the sub-discipline has been the subject of much debate, with concerns such as: Is archaeological charcoal a reliable representation of past vegetation? What factors can distort the signal from past vegetation to charcoal spectrum? How are valid charcoal assemblages formed? It has been suggested that past human societies may have selectively collected wood, which raises

questions about the representativeness of the archaeological charcoal (Delhon, 2018).

When attempting to reconstruct the original vegetation using archaeological charcoal assemblages, it is crucial to identify three primary taphonomic filters. The first filter takes place when vegetation is transferred from live to burnt. This can occur either through on-site fires, such as bushfires, or off-site fires created by humans using firewood in their habitation sites. The second filter occurs during the transition from total vegetation burnt to charcoal deposited. During the burning process, information on the total vegetation burnt can be lost if ash is formed instead of charcoal. Additionally, charcoal fragmentation resulting from trampling can lead to significant mass loss. Lastly, more information can be filtered during the transfer from the total charcoal deposited to the charcoal recovered during archaeological excavations to charcoal sampled and studied (Théry-Parisot *et al.,* 2010; Dotte-Sarout *et al.,* 2015) (Fig. 2.2).

Firewood collection is a significant factor in anthracology as it can impact the representativeness of the assemblage. According to the principle of least effort, past humans would collect firewood from the nearest woodlands to their habitation site. This is still evident today in Bushbuckridge, South Africa, where people prefer to collect firewood from nearby woodlands and only venture further if there is a shortage (Matsika *et al.,* 2013). When selecting firewood, several factors come into play, such as the purpose of the fire. Fires could be domestic or specialized for cooking, heating, lighting, healing, or cultural purposes. People tend to be more specific in the wood taxa collected for specialized fires, which results in a few selected taxa. On the other hand, there is little selectivity, thus high species diversity for domestic fires (Dotte-Sarout *et al.,* 2015).

The selection of firewood is also influenced by the availability of wood in nearby surroundings, which can be determined by various factors such as seasonality, abundance of dead wood, and the occurrence of wood along daily routes.

Additionally, traditional beliefs and taboos can also impact wood collection. For instance, the Fang people in Equatorial Guinea avoid the African oil bean (*Pentaclethra macrophylla*) as the tree is believed to represent a highly violent spirit. It is believed that collecting firewood from this tree will cause violent quarrels between family and community members. Similarly, *Tetrorchidium didymostemon*, also known as the tree of wealth, is avoided as burning this species is considered equivalent to destroying one's wealth (Gelabert *et al.,* 2011).

Certain tree species may also be avoided due to their undesirable properties. For instance, some tree species have wood that produces unpleasant-smelling or eye-irritating smoke, or is covered in thorns that make it difficult to collect. One such example is *Spirostachys africana*, a plant that is aromatic and poisonous. It can be fatal when used for cooking, as its smoke can cause headaches and nausea, and it produces poisonous latex that can cause skin irritation and severe eye damage (Coates Palgrave and Coates Palgrave, 1983). Furthermore, the condition of the wood can have an impact on wood collection. For example, the Fang and Bushbuckridge communities have a preference for gathering small, dry logs as they burn slowly and provide sustained heat for cooking (Gelabert *et al.,* 2011; Findlay and Twine, 2018). These societal factors can influence the distribution of charcoal deposits.

Besides societal factors, the representativeness of charcoal assemblages can be influenced by combustion (Fig. 2.2). The combustion process can impact representativeness by altering the wood's morphological, physical and chemical properties as the wood undergoes charring/darkening, mass loss, shrinkage, anatomical changes, and the conversion of cellulose, hemicellulose and lignin to aromatic moieties which all result in a carbon enriched end product called charcoal. Anatomical modifications such as retraction, fusion and cracking occurring in wood during combustion can sometimes impede taxonomic identification and falsify the amount of the initially burnt wood as the wood fragments after combustion (Braadbaart and Poole, 2008).

Anthracologists can recover data on the taxonomy of charcoal because the internal morphology of the wood remains unchanged after combustion (Braadbaart and Poole, 2008). The combustion of decayed wood results in porous and easily fragmented charcoal, while the combustion of healthy wood results in well-preserved charcoal (Théry-Parisot *et al.,* 2010). Radial cracking is mainly linked with the combustion of wet wood. Although radial cracks may occur in any wood, Théry-Parisot and Henry (2012) and Caruso Fermé and Théry-Parisot (2011) experiments show that radial cracks are likely to occur in wet wood than dry wood. This is because during the combustion of wet wood, moisture evaporates and the wood shrinks, resulting in radial cracks (Théry-Parisot and Henry, 2012).

Charcoal after combustion and during/after deposition is influenced by various factors such as fragmentation (Fig. 2.2). Chabal (1997) proposed the law of fragmentation, which states that the rate at which charcoal fragments is directly related to external factors it is exposed to. These factors include whether fresh or dead wood was burnt, the combustion conditions, and the type of sediments it was deposited in. When charcoal fragments during combustion, fragments produced by less frequently burnt taxa are multiplied. However, post-depositional processes lead to the mass loss of the less frequently burnt taxa, resulting in a balance between fragments gained and lost (Chabal, 1990). To represent the vegetation accurately, charcoal sampling methods assume that frequently burnt taxa are represented by both small- and large-sized charcoals. In contrast, small-sized fragments mostly represent less burnt taxa (Chabal, 1990). Therefore, different fragment size classes should be analysed for charcoal assemblages, especially small fragments.

Trampling, reworking, and cleaning activities in habitation sites are part of deposition and post-depositional processes (Théry-Parisot *et al.,* 2010). Post-depositional activities that affect charcoal assemblages include sediment disturbances caused by living organisms such as worms and burrowing animals, leaching or colluvium formation caused by atmospheric influences such as runoff

and wind action, mechanical constraints such as pressure in the sediments caused by freeze and thawing cycles, and the rate of burial and diagenesis, which lead to chemical modifications (Théry-Parisot *et al.,* 2010). These activities can cause vertical and horizontal movements of charcoal in archaeological sediments (Fig. 2.2).

To ensure that the representation of taxa is not biased, it is crucial to use proper excavation methods. There are various ways to recover artifacts from sediments, and one of them is by using machine-assisted flotation. This method is advantageous when dealing with large volumes of sediments, as it allows for fast and easy artifact recovery in the field. However, studies have shown that this method may not recover heavier charcoal fragments (Kabukcu and Chabal, 2021). Despite this, it is still the preferred method as it enables the recovery of more artifacts and ecofacts such as charred plant material, lithics, and bones. On the other hand, the hand-picking method is the best way to recover charcoal from sediments. Unfortunately, this method is time-consuming, especially when working with large volumes of sediments (Kabukcu and Chabal, 2021).

Anthracologists must use proper sampling methods in the laboratory. It is recommended to analyse charcoal from domestic long-term deposits, usually indicated by scattered charcoals occupying various stratigraphic units. This is preferable to short-term charcoal deposits from hearths, which usually contain the last few burnt wood logs. Long-term charcoal deposits represent numerous collections and burns, making them a more reliable source of information (Chabal, 1997; Théry-Parisot *et al.,* 2010).

Scientists in temperate Europe utilize saturation curves during sampling and analysis to estimate the species richness in the assemblage and ensure the assemblages analysed accurately represent the vegetation. The frequency of the appearance of new taxa is plotted against the total number of analysed charcoal fragments. The curve plot will plateau when the minimum number of fragments that

must be analysed in that particular assemblage is reached (Dotte-Sarout *et al.,* 2015). Usually, this number is 400 in temperate and Mediterranean Europe, and 200-300 in tropical and arid to semi-arid regions (Scheel-Ybert, 2002). Southern Africa, a region that experiences both subtropical and temperate climates (Red Cross Climate Centre, 2021), has a high plant diversity, with more than 2100 indigenous species (van Wyk and van Wyk, 2013). Thus, it is difficult to determine the minimum number of fragments required as an apparent plateau is often impossible to reach.

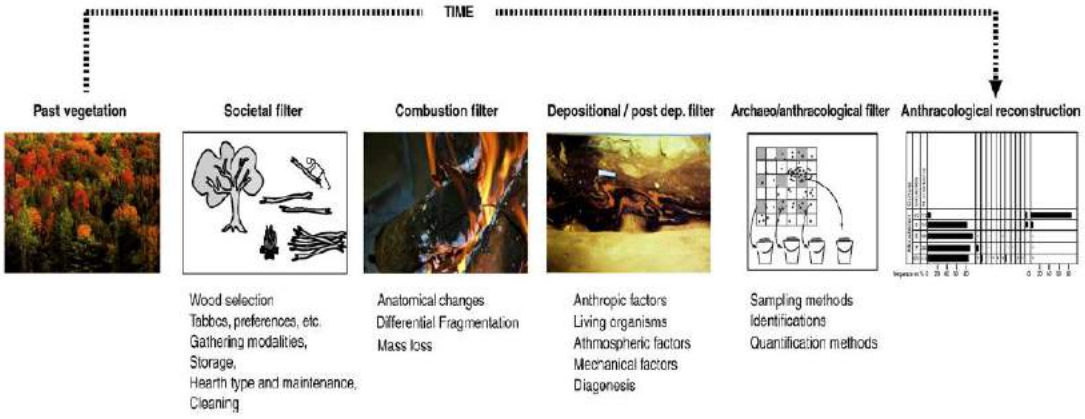


Fig. 2.2: Taphonomic filters affecting charcoal assemblages from live vegetation till analysis in the laboratory (Source: Théry-Parisot *et al.,* 2010).

2.1.4 Anthracology in southern Africa

Caves and rock shelters are the primary sources for anthracological studies. The dry environmental conditions in southern Africa, especially in internal southern Africa, prevent the preservation of most proxies, such as pollen and phytoliths, often preserved by lakes and swamps and usually used in palaeoreconstruction studies (Scott and Thackeray, 2015). Deacon *et al.* (1984) represent one of the first studies using charcoal as an indicator of Late Pleistocene and Holocene environments in South Africa. This study also showed that charcoal can be used to

understand past human behaviours and cultural practices in southern Africa. Since then, many more anthracological studies have been conducted in different parts and biomes of South Africa. Recent studies include studies from Sibudu Cave, Kwa-Zulu Natal (Lennox *et al.*, 2015; Zwane and Bamford, 2021), Ndondondwane, KwaZulu Natal (House *et al.,* 2023), Border Cave, KwaZulu Natal (Zwane and Bamford, 2021; Lennox *et al.,* 2022), Elands Bay Cave, Western Cape (Cowling *et al.,* 1999; Parkington *et al.,* 2000; Cartwright *et al.,* 2016), Diepkloof Rock Shelter, Western Cape (Cartwright, 2013), Great Zimbabwe, Zimbabwe (Chikumbirike *et al.,* 2016) and Wonderwerk Cave, Northern Cape (Bamford, 2015b; House *et al.,* 2022).

2.1.5 Wood use

Wood is an essential natural resource that can be used for fires, medicine, insect repelling and manufacturing items such as utensils, furniture, toys, figurines. Wood can be burned to produce fire for lighting, cooking, repelling insects and predators, and forging materials like silicates and metals into utensils (Karkanas *et al.,* 2007; Dotte-Sarout *et al.,* 2015). There is limited research on past human-plant interactions, or palaeoethnobotany, in southern Africa. This field is based on the assumption that past human societies understood the fire properties of the plants around them, so firewood was collected based on its fire properties and the purpose of the fire (Dotte-Sarout *et al.,* 2015). Studies such as Bamford (2015b), Zwane and Bamford (2021), House *et al.* (2022; 2023) and Lennox *et al.* (2022) identify woody species with known fuel, construction and medicinal uses in southern Africa.

2.2 Physiognomy

The internal anatomy of wood can provide crucial information about the environmental conditions of the past. The expression of internal anatomical features in wood is called wood physiognomy (Wheeler *et al.,* 2007). To infer palaeoenvironmental conditions from physiognomy, a correlation between the habitat or ecology of a given species and its internal wood anatomy needs to be established. This is possible because water is a limiting factor in plants, so plants have numerous water-related adaptations that enable them to grow in specific climatic ranges (Wolfe and Upchurch, 1987; Zwane and Bamford, 2021). That way, climate/water availability controls the internal physiognomy of the wood.

The main function of wood in woody plants is to provide mechanical support to the plant body and store and conduct water and nutrients throughout the plant. In angiosperm wood, different anatomical features are designed to carry out specific functions so the wood can be functional. For example, fibres provide mechanical support, the parenchyma is the storage compartment for nutrients and water, the rays conduct water radially, and the vessels conduct water from the roots to the leaves (Zheng *et al.,* 2019). To survive, these features must be well adapted to the environment. These features can provide critical information about rainfall patterns and the climate in which plants grew (Martínez-Cabrera and Estrada-Ruiz, 2014; Zwane and Bamford, 2021).

The efficiency of water transport in plants is closely linked to the expression of xylem conduits or vessels (Wolfe and Upchurch, 1987). Hence, they can provide past climate information. Plants that grow in environments prone to frost and drought have structural adaptations that help reduce the impact of air embolisms caused by either droughts or thawing after frosts. These adaptations include the development of clustered, smaller and numerous vessels and conductive vasicentric tracheids. Whereas, woods in environments with high precipitation and

no frost have larger and fewer vessels with simple perforation plates and nonconductive fibers (Wheeler and Baas, 1993; Wolfe and Upchurch, 1987).

Vessel length decreases from wet to dry environments and within wet floras from tropical to cool temperate or arctic latitudes (Baas *et al*., 1983). Short vessel lengths are safer as they are less likely to collapse under negative pressure compared to longer vessels (Carlquist, 1977; Baas *et al*., 1983). There is a tradeoff between efficient water transportation, usually ensured by larger, longer vessels, and safety ensured by short vessels. Safety can also be ensured by increased vessel frequency to allow wood functionality in case some vessels are blocked by air bubbles (Baas *et al*., 1983). However, woods of small trees and shrubs growing near water sources tend not to follow these trends (Baas *et al*., 1983).

Carlquist (1977) and Wolfe and Upchurch (1987) have proposed using the vulnerability index, conductivity capacity, and mesomorphy index to correlate wood physiognomy, particularly the vessels, to rainfall and temperature. Carlquist (1977) devised the measure of the plant's vulnerability by dividing the mean vessel diameter by the mean vessel frequency. This value is known as the vulnerability index. It measures the plant's vulnerability to loss of vessel function, which can be caused by air embolisms in vessels, which can impair water conduction to photosynthetic surfaces. This value is expected to range from 1.0 to 2.5 in large mesophytic trees and less than 1.0 in shrubs or small xerophytic trees. This value can also be high for shrubs and trees that grow near water or have deep roots that penetrate underground water supply as they are not subjected to droughts, so their vulnerability index values tend to be high (Carlquist, 1977).

The conductivity capacity measures the hydraulic capacity of the vessels. It can be calculated by factoring the fourth power of the vessel radius by 10^6 and multiplying it by the mean vessel frequency. Values over 200 are a syndrome of medium-large trees, while values above 500 are restricted to large trees in wet or dry environments (Wolfe and Upchurch, 1987).

The mesomorphy index proposed by Carlquist (1977) is the product of the vessel length and the vulnerability index. This index usually indicates the amount of water the plants are adapted to, i.e., whether plants are mesophytic or xerophytic. Mesophytes grow in unlimited water and nutrients, while xerophytes are adapted to grow in a limited or scarce water supply. Values above 200 usually indicate mesophytes, while values of 75 and below are typical for xerophytes (Carlquist, 1977). The three indices proposed by Carlquist (1977) and Wolfe and Upchurch (1987) are often criticized for lacking a narrow quantitative range for interpretations. However, this method is advantageous as it does not depend on the species identifications and can be used on any wood, whether identified or unidentified.

Physiognomy and taxonomy often yield consistent results (Utescher *et al.,* 2014; Bamford, 2017). Bamford (2017) identified trees from large, wet forest trees from a fossil wood assemblage from the Pleistocene of Kenya. This was consistent with the physiognomy as the woods had large and fewer vessels as well as large conductivity capacity, mesomorphy index, and vulnerability index values, typical in large trees in wet environments. Akkemik *et al.* (2023) describe and infer palaeoclimate information using fossil wood from Late Miocene-Early Pliocene of northeastern Turkey. The taxonomic composition and physiognomy implications were in an agreement, both suggesting warm climatic conditions similar to current Mediterranean conditions.

Sonsin *et al*. (2012) tested the accuracy of vulnerability and mesomorphy indices by comparing species from the Cerrado savanna biome in Brazil. Some species were collected from a dry region and some from a wet gallery forest alongside streams. The two regions shared similar environmental conditions, i.e., the same soil acidity, temperature, rainfall patterns, or seasons. The study shows species from the wet gallery had mostly solitary and large vessels and a low vessel frequency, thus higher vulnerability and mesomorphy indices, overall efficient water

conductivity. The dry region species had smaller, numerous vessels, hence lower vulnerability and mesomorphy indices, thus more safety during droughts and frosts.

Dadswell and Ingle (1954) tested the use of wood anatomy to classify *Nothofagus* trees into temperate and tropical groups. The temperate environment-adapted trees were characterized by large vessels and low vessel frequency, while the tropical trees were characterized by smaller vessels and high vessel frequency. Wheeler and Baas (1993) explored the application of wood features to interpret past climatic regimes and long-term climate change. This study shows that this method best suits Tertiary and Quaternary wood assemblages, not Cretaceous woods. This is because some wood features like ring porosity, tangential and dendritic vessel distribution patterns, and vessel clustering did not evolve until the early Tertiary (Wheeler and Baas, 1993).

2.3 Review of Holocene Environments

2.3.1 Global Environmental Conditions of the Holocene

Several reconstructions of the European Holocene climate have been conducted using different proxies, including pollen, lake levels, and other indicators. For example, a study by Mauri *et al.* (2015) used pollen to model the Holocene climate and found that the Mid-Holocene period in Central and Northern Europe was generally warmer than today, with warm summers and winters especially around 7 ka. Meanwhile, the Mediterranean and Southern Europe were cooler during that time. In Southeast, Northern, and Eastern Europe, the Mid-Holocene period was wetter, as summer and winter rainfalls were increasing, peaking around 8-6 thousand years ago, while the South-West was drier (Mauri *et al.,* 2015).

During the African Humid Period (AHP), which lasted from 14.8 ka to 5.5 ka, there was a significant increase in rainfall in North and West Africa. Various indicators from the Sahara, Sahel, and western tropical Africa show that lake levels rose, and

the environment underwent significant changes. For instance, the Sahara/Sahel belt became greener. Although several studies have shown that this period ended abruptly around 5.5 ka, leaf wax hydrogen composition isotope analysis from Ghana (West Africa) reveals a gradual termination occured between 8-5 ka (Shanahan *et al.,* 2015). Renssen *et al.* (2006) simulation of the AHP termination phase shows that North Africa was relatively humid during the Early-Mid Holocene. Grasslands, wetlands, and lakes covered the region during this time. This was followed by abrupt climate changes around 5.5 ka, leading to the formation of a desert in the area. This abrupt termination was also experienced in Northeast Africa and West Asia. The analysis of fluvial archives in the Moroccan Highlands shows that the Moulouya wetland existed in North Africa, hence suggesting wetter conditions before 5.5 ka (Depreux *et al.,* 2021).

2.3.2 Holocene Environmental Conditions of Southern Africa

While northern Africa experienced increased rainfall, dry conditions prevailed in southern Africa with sporadic wet phases. For instance, the Okavango panhandle in Botswana regressed between 7-4 ka, indicating drier conditions. However, a brief progression of the panhandle was noted at 6 ka, which aligned with the shoreline development of the Mababe depression and the Parakarungu flooding zone in Botswana between 6.8 ± 1 ka and 5.5 ± 0.6 ka BP, suggesting a phase of wetter conditions occurred (Nash *et al.,* 2006; Burrough and Thomas, 2008; 2013). During the mid-Holocene, the western part of central Namibia experienced a gradual increase in aridity during the Mid-Holocene, as per the analysis of fossil rock hyrax middens conducted by Chase *et al.* (2009). However, there were periods of significant rainfall spikes that occurred between 8.7-7.5, 6.9-6.7, 5.6-4.9 and 4.2-3.5 cal ka BP.

Pollen is a widely used proxy in southern Africa for studying Mid-Holocene climate, however, inconsistent results have been obtained from pollen data at different sites in South Africa. For example, a palynological study from Wonderkrater, located in in Limpopo (Fig. 3.1 A), showed that during the Mid-Holocene, the region underwent a transition from swampy conditions dominated by Cyperaceae species to a warm, dry, grassy woodland (Scott *et al.,* 2003). Meanwhile, the pollen analysis at Tswaing crater (Fig. 3.1 A), near Wonderkrater, indicates a humid environment dominated by broad-leaved savanna woodland species (Metwally *et al.,* 2014).

The analysis of pollen from a peat core from Braamhoek wetland (interior) in the eastern Free State, Drakensberg region (Fig. 3.1 A), suggests that the Mid-Late Holocene (7.5-2.5 ka cal BP) was primarily dry, with low sedimentation rates and plant diversity (Norström *et al.,* 2009). Norström *et al.* (2014) palynological study also found that the Drakensberg region was mostly dry from 7-2 ka cal BP, and the environment was dominated by Asteraceae species, while grasses were declining.

Pollen from hyena coprolites suggests that the environment around the Equus Cave, near Taung in the North West (Fig. 3.1 A), was warm with vegetation similar to modern savanna (Scott, 1987). The eastern Karroo (Blydefontein) was mostly dry from the early Holocene until the Mid-Holocene, around 11.0-5.4 ka cal BP (Scott *et al.,* 2005). The Florisband spring pollen data shows that the interior in the Free State Mid-Holocene was initially dry, starting from 7.0 ka cal BP. This was followed by a wet period at 6.5 ka cal BP, peaking around 6.3 ka cal. BP (Scott *et al.,* 2022) (Fig. 3.1 A).

Pollen records from the coastal region, Lake Eteza (Fig. 3.1 A), indicate that dry grassy conditions existed till 6.8 ka. This was followed by a humid period between 6.8 and 3.6 ka, indicated by a high frequency of forest trees. After 3.6 ka, dry conditions returned, indicated by an increase in Amaranthaceae, grasses, and Phoenix species and a decrease in forest trees (Neumann *et al.,* 2010).

While the aforementioned sites provide limited information on palaeoenvironmental conditions, i.e., data is mostly based on pollen, the Wonderwerk Cave has been able to preserve multiple indicators of such conditions. However, there have been differences in the interpretation of these indicators. For instance, Brook *et al.* (2015) show there was little to no stalagmite development between 13-3.5 ka, indicating aridity in the region. Other Wonderwerk Cave proxies show dry conditions lasted till 6.5/6.2 ka. For example, a high count of Asteraceae pollen in the strata 5a to 4b suggests an environment similar to the dry regions of Nama-Karroo, currently located south of the cave, existed from 12.5-6.5 ka cal BP. Subsequently, the vegetation shifted to humid and grassy conditions, peaking between 5.6 and 4.5 ka cal BP (Scott and Thackeray, 2015). The analysis of ostrich eggshell isotopes indicates that the shift from arid to wetter conditions began at 6.2 ka cal BP and lasted till 5.5 ka cal BP (Lee-Thorp and Ecker, 2015). Herbivore species composition and tooth enamel isotope data also suggest the area was semi-arid, then wetter and vegetation was dominated by C_3 trees or shrubs (Ecker *et al.,* 2018). The charcoal species composition in House *et al.* (2022) also suggests a predominantly arid Mid-Holocene environment. This study identified dry to mesic environment indicator species like *Diospyros austro-africana, Vitex rehmannii, V. mombassae, Searsia lancea* and *Commiphora schimperi*.

2.4 Summary of the chapter

This chapter presents information on various methods of utilizing plants to recreate past environments, highlighting their limitations. Different studies on the southern African Mid-Holocene conditions reveal that the region experienced climate and environment fluctuations. The chapter further demonstrates that pollen data is the primary source of information for reconstructing Holocene southern African environments, and has yielded contradictory results in the interior. Therefore, it is

essential to utilize additional proxies, which are well-preserved at the Wonderwerk Cave.

CHAPTER THREE

Site background

3.1 Wonderwerk Cave and its location

The Wonderwerk Cave is located in the Northern Cape at 27° 50' 38" S, 23° 33' 18" E, at an altitude of 1680 meters above sea level. The site contains artifacts spanning over 2 million years of human habitation, including the Early, Middle, and Later Stone Ages. It is situated at the base of the Kuruman Hills on the edge of the Ghaap Plateau (Bamford, 2015a; Horwitz and Chazan, 2015) (Fig. 3.1 A, B & C).

Wonderwerk Cave is a large dolostone cavity covered by Banded ironstones that dates back to the Early Proterozoic to Late Archean period, 2-3 Ga. The cave is quite large, measuring about 140 meters in length, 3-7 meters in height, and 11-26 meters in width. It has only one entrance that faces north and overlooks the Ghaap Plateau, which is about 7 meters high and 15 meters wide. Inside the cave, there is a large and irregular stalagmite that partially blocks the light, located about 20 meters from the entrance (Fig. 3.5 B). The cave walls are parallel and perpendicular and covered by paintings that start from the entrance and extend about 20 meters inside (Fig. 3.5 C). You can also find some poorly formed stalactites inside the cave. The back area is dark and covered with bat guano (Malan and Cooke, 1941; Beaumont and Vogel, 2006; Bamford, 2015a) (Fig. 3.5 D).

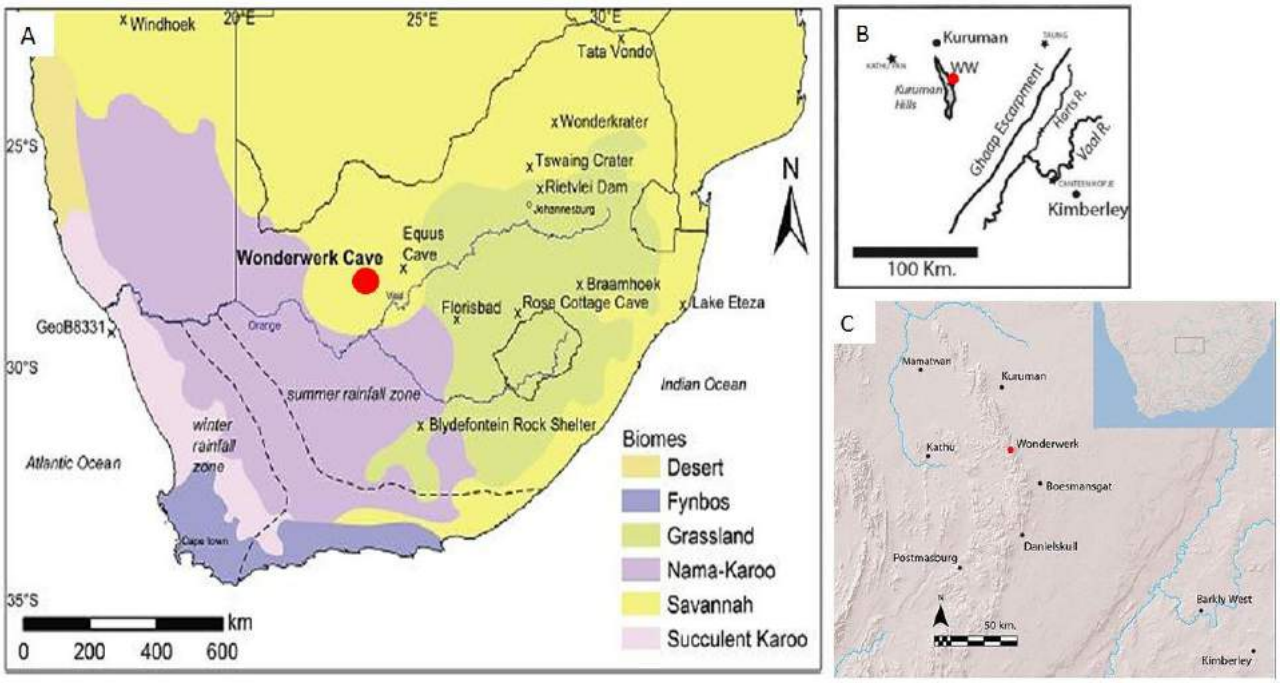


Fig. 3.1: Map of South Africa showing the situation of Wonderwerk Cave (red dots) (A) in the savanna biome and the summer rainfall zone, (B) in the Kuruman Hills at the edge of the Ghaap Plateau/Escarpment and (C) and other sites mentioned in the study i.e., Danielskuil, Boesmansgat, Kuruman and Khathu Pan shown in a terrain map (Source: Chazan *et al.,* 2008; Horwitz and Chazan, 2015; Ecker *et al.,* 2018).

3.2 The environmental context of the cave

The cave lies in a Savanna biome. The regional vegetation type is the Kuruman Mountain Bushveld (Svk 10) (Fig. 3.2). The landscape consists of gently sloping hills and an open bushland with a well-developed grass layer (Rutherford *et al.,* 2006). The plants in the region use different photosynthetic pathways: C_4 for grasses and C_3 for trees, shrubs, and herbs. Crassulacean Acid Metabolism (CAM) plants are rare (Lee-Thorp and Ecker, 2015).

The vegetation on the western side of Kuruman Hills transforms into Kuruman Thornveld (SVk 9). This region is characterized by sloping hills, with closed shrub- and open tree layers, mainly dominated by *Vachellia erioloba*. On the eastern side

of the hills, the vegetation changes into Kuruman Vaalbosveld (SVk 8). The latter is recognized by a patchy layer of grass and small and tall trees such as *V. erioloba, V. karroo, Searsia lancea* and *Ziziphus mucronata* (Rutherford *et al.,* 2006) (Fig. 3.2). A complete list of dominant woody species growing in the vicinity of the cave is provided in Table 3.1 and Appendix A. The vegetation changes to Nama-Karoo towards the south and to grassland towards the east.

The water sources in the area are limited to a natural sinkhole named Boesmansgat, situated on Mount Carmel farm, 15 km from the cave (Fig. 3.1 C). There is also a seep about 5 km away on the eastern side of Garankosa Hill (Beaumont and Vogel, 2006). The Kuruman River, whose upper drainage is in the Ghaap plateau (Smit, 1978), runs close to the cave (Fig. 3.2).

The terrain surrounding the cave is flat (Bamford, 2015a). The geological context of the area is banded ironstone of the Asbestos Hills Formation of the Griqualand West Sequence that overlies the stratified dolomitic limestone of the Ghaap Plateau (Smit, 1978; Beaumont and Vogel, 2006). The area has shallow, sandy soils of the Hutton form (Rutherford *et al.,* 2006).

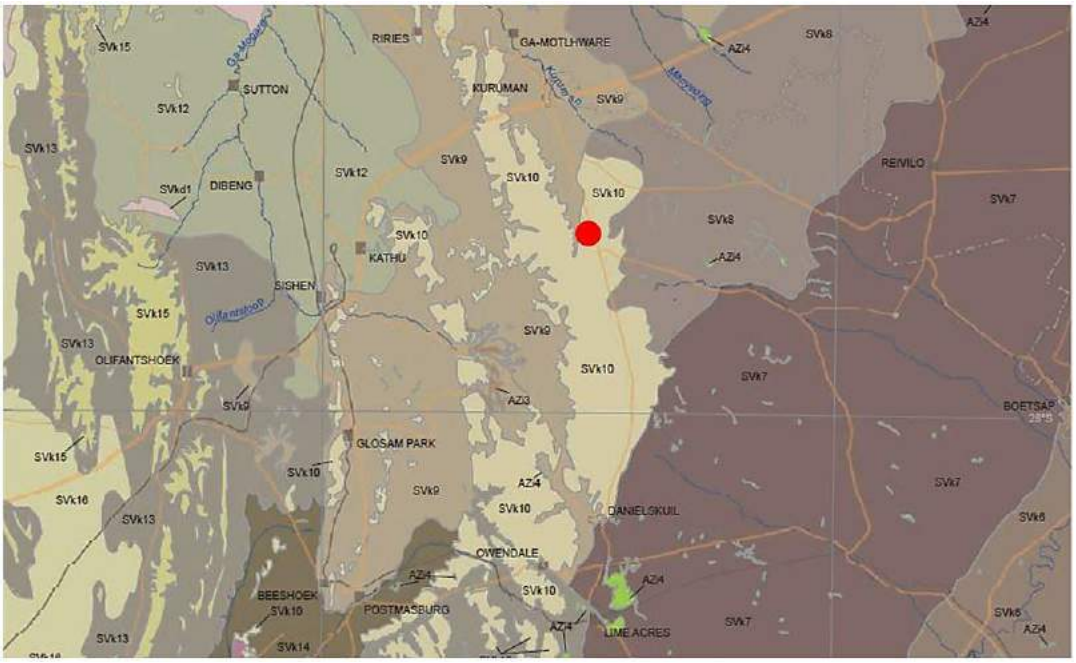


Fig. 3.2: The location of the Wonderwerk Cave in the Kuruman Mountain Bushveld (SVk10) and the other savanna vegetation units around the cave (Source: Rutherford *et al.,* 2006).

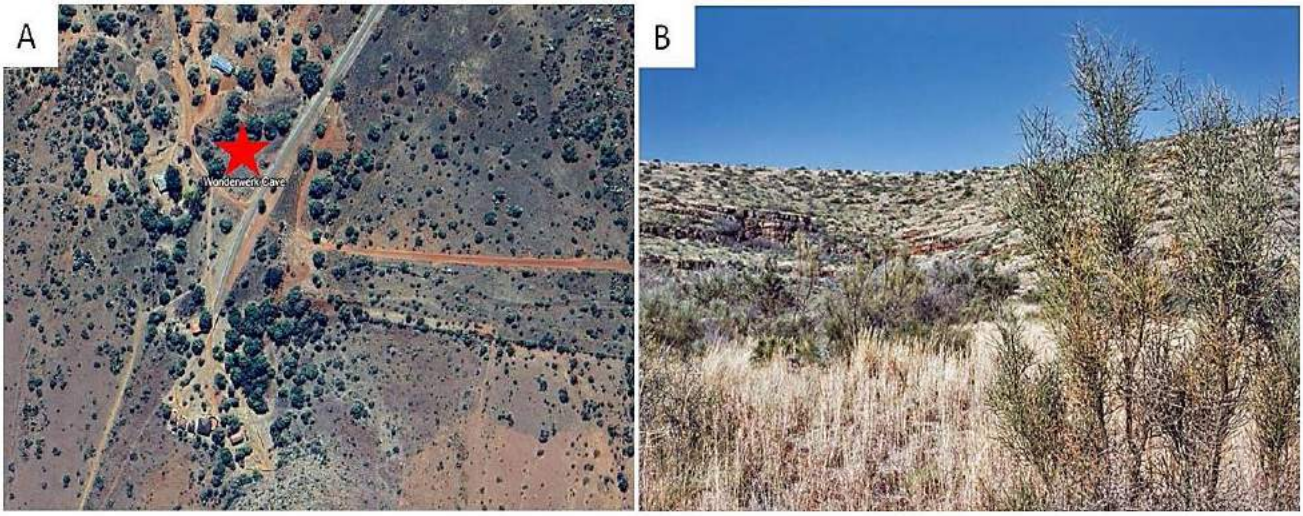


Fig. 3.3: A) Image showing the current environment around the Wonderwerk Cave (indicated by red star) (Source: Google Earth). B) Image showing the open low bushveld vegetation described as the Kuruman Mountain Bushveld (SVk 10) (Source: Rutherford *et al.,* 2006).

Table 3.1: A list of important woody taxa growing near the Wonderwerk Cave (Rutherford *et al.,* 2006).

Plant type	**Plant description**	**Kuruman Mountain Bushveld (SVk 10)**
Small trees	A single-stemmed woody plant shorter than 15 meters in forests and 10 meters in savanna.	*Searsia lancea*
Low shrubs	A multi-stemmed or single-stemmed woody plant that branches from the base and is less than 2 m in height.	*Amphiglossa triflora, Anthospermum rigidum* subsp*. pumilum, Gomphocarpus fruticosus* subsp. *fruticosus, Helichrysum zeyheri, Lantana rugosa, Searsia ciliata, Wahlenbergia nodosa*
Tall shrubs	A multi-stemmed or single-stemmed woody plant that branches from the base and has a height of over 2 m.	*Diospyros austro-africana, Euclea crispa* subsp. *crispa, E. undulata, Olea europaea* subsp*. africana, Searsia pyroides var. pyroides, S. tridactyla, Tarchonanthus camphoratus, Tephrosia longipes*
Grasses	Plants that have long and narrow leaves that grow in tufts.	*Andropogon chinensis, A. schirensis, Anthephora pubescens, Aristida congesta, A. diffusa, Brachiaria nigropedata, Bulbostylis burchellii, Cymbopogon caesius, Digitaria eriantha* subsp. *eriantha, Diheteropogon amplectens, Elionurus muticus, Eragrostis chloromelas, E. nindensis, Eustachys paspaloides, Heteropogon contortus, Melinis repens, Themeda triandra, Trichoneura grandiglumis, Triraphis andropogonoides, Schizachyrium sanguineum*

3.3 Climate

The weather and climate of the southern African subcontinent are spatially heterogeneous with three distinct rainfall seasonality zones (Fig. 3.4). This is mainly due to its location at the subtropical latitude. Hence, the climate is influenced by the interplay between various atmospheric and oceanic circulation systems, including subtropical, tropical, and temperate climate systems, as well as the Atlantic, Indian, and Southern oceans. The Summer Rainfall Zone (SRZ) is a vast South African region that includes the interior and eastern areas. This region receives convective summer rainfall, accounting for over 66% of the average annual precipitation during the summer months (Chase and Meadows, 2007; Roffe *et al.,* 2019; 2021). The interaction between subtropical high-pressure cells and the movements of the easterly winds linked to the Intertropical Convergence Zone (ITCZ) brings moisture to central southern Africa from the western Indian Ocean (Chase and Meadows, 2007; Burrough and Thomas, 2013).

The winter rainfall zone (WRZ) occupies the southern and western coasts, whereby more than 66% of the mean annual precipitation is experienced during the winter months, April- September. This zone receives frontal systems-induced rainfall controlled by westerlies from mid-latitude cyclone cold fronts, which transports moisture from the southwest Atlantic Ocean. The year-round rainfall zone (YRZ) is located along the southern coast and receives rainfall from tropical, subtropical and temperate weather systems of both summer and winter rainfall systems (Roffe *et al.,* 2019; 2021).

South Africa is generally arid, with about two-thirds of its land receiving less than 500 mm of mean annual rainfall (Roffe *et al.,* 2019). The Wonderwerk Cave is situated in the SRZ and experiences mostly summer rainfall, which accounts for about 80% of the total rainfall the area receives. The region has a warm desert climate with low rainfall and a mean annual rainfall of 420 mm. Additionally, the area has a mean annual temperature of 16.8 ºC. The winters in this region are dry,

with frequent frost occurrences (Rutherford *et al.,* 2006; Bamford, 2015b; Brook *et al.,* 2015).

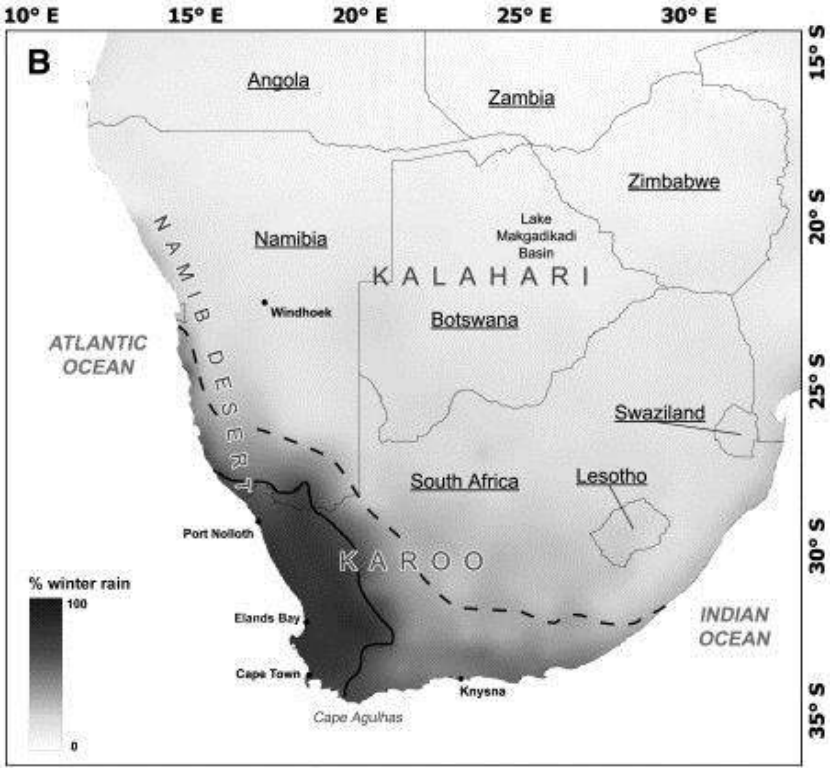


Fig. 3.4: Map showing the mean annual rainfall of Southern Africa (in mm) with winter rainfall increasing towards the left. The rainfall zones are marked by solid and dotted lines: WRZ (on the left-hand side), YRZ (in the middle) and SRZ (on the right-hand side) (Source: Chase and Meadows, 2007).

3.4 Excavation history of the Wonderwerk Cave

The first written descriptions of the cave were by Methuen, who visited it in 1846 (Malan and Cooke, 1941). A farmer and his livestock occupied the cave in the 1990s. They used to harvest bat guano from the cave floors for fertilizer (Beaumont and Vogel, 2006). Archaeologists Malan and Cooke conducted the first formal scientific excavations between 1943 and 1946 in the section behind the stalagmite, now referred to as Excavation 1. The analysis of the excavated materials in 1974-

77 revealed that the cave contained artifacts and faunal remains from the ESA, MSA, and LSA periods (Malan and Cooke, 1941).

Peter Beaumont re-excavated the cave from 1978 to 1996, exploring seven areas, including excavation 1, and uncovered a wealth of lithic, faunal, and botanical findings (Horwitz and Chazan, 2015). Unfortunately, a significant portion of Beaumont's findings have not yet been examined or published (Bamford, 2015a). In Chapter 4, the excavation techniques used by Beaumont are discussed. Unfortunately, these techniques have their drawbacks as they limit the spatial exploration of the artifacts. This is because Beaumont did not plot the artifacts, botanical and faunal remains or divide the excavation squares into subunits, nor provide field notes or photographs.As a result, the distribution of the artifacts can only be analysed using squares, and not the actual deposition position (Horwitz and Chazan, 2015; Ecker *et al.,* 2017).

In 1979, Francis and Anne Thackeray extended Beaumont's excavation with a specific focus on the cultural, faunal and sedimentary record from the LSA sequence of Excavation 1 (Horwitz and Chazan, 2015). In the early 2000s, a multidisciplinary project directed by Michael Chazan and Liora Kolska Horwitz refined Beaumont's excavations through high-resolution mapping and dating techniques (Bamford, 2015b). The project uncovered a long cultural sequence and well-preserved faunal and botanical remains, which provide excellent proxies for paleoenvironmental studies (Horwits and Chazan, 2015). The excavation plots by all the abovementioned authors are illustrated in Fig. 4.1 B and C. In 2018, another team re-excavated a small section of archaeological layers left from Beaumont's 1978 excavation to improve the provenience data of the artifacts and the radiocarbon dates for LSA strata (Rhodes *et al.,* 2022).

Excavation 1 is located about 20 meters inside the cave, behind the stalagmite. The Holocene archaeological strata are represented by approximately one meter of deposits. They are mainly composed of quartz sands of the Kalahari deposits

blown by wind into the cave through the entrance (Rhodes *et al*., 2022) (Fig. 4.1D). Although there is evidence of occasional unoccupancy, the local cultural succession is well documented in the cave sediments. The lithic assemblages and the sands composing the Holocene strata are described below (from the top (youngest) downwards).

Strata 1 and 2a: The top two archaeological layers of the cave represent occupation during the Historic period. Artifacts found in these strata include metal, glass, and porcelain. The layer appears to have been disturbed, as indicated by the presence of sheep and cattle dung, thought to be from the time when the farm owner lived in the cave. As a result, no radiocarbon dating has been done on these strata (Ecker *et al.,* 2017).

Strata 2b and 3a: The matrix of these strata comprises soft dark-brown sands containing plain grit-tempered ceramic body sherds. Thus, it is assigned to the Ceramic LSA (Ecker *et al.,* 2017).

Strata 3b, 4a, 4b and 4c: The strata comprise soft, dark-brown sands and the Wilton culture. These tools are highly concentrated in stratum 4aLH, a small convex section between stratum 4a and 4b. There is a significant shift in the Wilton artifact typology and dominant raw material type. The top, youngest strata (3b, 4a, and 4aLH) contain backed bladelets made from chert, while scrapers made from banded ironstone dominated the bottom, older strata (4b and 4c). Other discoveries include pigments like ochre and specularite, charcoal, stone pendants and rings, and decorated fragments of ostrich eggshells, some of which have been transformed into beads (Ecker *et al.,* 2017).

Faunal remains from stratum 4b include baboon, klipspringer, steenbok, alcelaphine, buffalo, roan, zebra, *Megalotragus*, hare, porcupine, tortoise, and bullfrogs. These remains were likely accumulated by humans (Thackeray, 2015).

Stratum 4d: Composed of red/brown to orange sands, this layer primarily contains the Oakhurst Industries, locally designated as Kuruman Industries. Scrappers made from banded ironstone and dolomite represents the mostly found tools found in this stratum (Ecker *et al.,* 2017).

Stratum 5a: This stratum mainly comprises small pebbles. A significant quantity of damaged chert tools, primarily flakes and cores, were discovered in this stratum. While the lithic assemblage in this stratum was initially classified as belonging to the Robberg Industries, it is now considered an unassigned mixed assemblage from the Pre-Holocene period as scrappers, few retouched adzes made of banded ironstone and dolomite were also found in significant numbers (Lee-Thorp and Ecker, 2015; Ecker *et al.,* 2017). Charcoal deposits recovered by Beaumont in this stratum were analysed by Bamford (2015b).



Fig. 3.5: Image showing Wonderwerk Cave. (A) The outside view of the cave. (B) The inside view with a stalagmite in the centre (note Excavation 1 behind it, where the material of this study comes from). (C) The rock art on the walls. (D) The dark rear part of the cave. (Source: www.zamaniproject.org).

3.5 Dating of the cave strata

The recovery of multiple indicators of palaeoenvironmental conditions in association with a lengthy cultural sequence has enabled the employment of different methods to determine the ages of the cave strata, from comparative lithic technologies to radiometric dating. This, in turn, allows timed palaeoreconstructions, which are rare in most South African cave sites. The ages of ESA strata (12-6) have been determined using palaeomagnetic and cosmogenic burial dating (Horwitz and Chazan, 2015). The lowermost stratum (stratum 12) had Oldowan lithics dated to 1.78-1.96 Ma (Rossouw, 2016). Shaar *et al.* (2021) recently corrected the ages of the stratum using the same method. This study

suggests that the oldest stratum of Wonderwerk Cave was deposited at 1.77–1.93 Ma.

Some of the first radiocarbon dates of the LSA strata (strata 5-1) of the cave were provided by Vogel *et al.* (1986) using charcoal. Anne and Francis Thackeray used radiocarbon dating of equid teeth in 1983 (Bamford, 2015a). The resulting 14C dates in both studies were not calibrated or modelled to strengthen their chronostratigraphic framework. More studies have been conducted since then, and the site has the most ^{14}C dates in the province (Horwitz and Chazan, 2015). However, most of these dates are rejected as they either use material currently not accepted for ^{14}C dating or are coarsely distributed (Ecker *et al.,* 2017). Lee-Thorp and Ecker (2015) and Ecker *et al.* (2017) calibrated the available pre-Holocene and Holocene dates using Bayesian models and ostrich eggshell and charcoal isotopes, respectively (Table 3.2). Ecker *et al.* (2017) provide the latest radiocarbon dates of the pre-Holocene and Holocene strata used in this study.

Table 3.2: The dominant lithic technology, revised ages, and the estimated abundance of charcoal packets and pieces recovered from the Holocene strata of the Wonderwerk Cave.

Archaeological stratigraphic units	Lithics assemblage (Ecker *et al.*, 2017)	Estimated number of excavated charcoal packets and pieces (House *et al.,* 2022)	Lee-Thorp and Ecker (2015) radiocarbon dates (ka cal BP)	Ecker *et al.* (2017) radiocarbon dates (ka cal BP)
1 and 2a	Historic	Not analysed	100	Historic

2b and 3a	Ceramic LSA	45 packets; 1952 pieces	0.29 - 0.19	0.5 - 2.3
3b	Wilton (backed bladelets/chert)	20 packets; <1500 pieces	4.8 - 2.06	2.8 - 4.5
4a	Wilton (backed bladelets/chert)	26 packets; 1450 pieces	5.9 - 4.3	5.3 - 4.6
4b	Wilton (scrapers/ironstone)	24 packets; 1300 pieces	6.5 - 5.5	6.9 - 5.9
4c	Wilton (scrapers/ironstone)	16 packets; 900 pieces	9.8 - 5.9	9.4 - 6.8
4d	Oakhurst/Kuruman (ironstone)	79 packets; 1500 pieces	12.2 - 8.6	11.8 - 10.4
5a	Unassigned mixed assemblage	16 packets; 136 pieces	12.5	12.3 - 11.4

3.6 Summary of the chapter

This chapter focuses on describing the Wonderwerk Cave, including its location, the surrounding vegetation, and climate. Additionally, the chapter provides a detailed account of the cave's excavation history, from its discovery to the excavation process and dating of the sediment layers.

CHAPTER FOUR

Materials and Methods

4.1 Material

The material originates from Peter Beaumont and the Thackeray's 1978-79 excavations. To excavate, the natural stratification of the cave sediments and a 0.92 m square grid were used (Fig. 4.1 A-D). The strata were only subdivided into 5 or 10-cm spits where required. The sediments were trowelled, collected in a bucket and dry-sieved using a 1-mm mesh. The sieved material was sorted into floral, faunal, and lithic categories. The macrocharcoal material was washed, marked, and packaged at the McGregor Museum in Kimberley between 1997 and 2002 (Beaumont and Vogel, 2006). The charcoal packets were labelled based on the archaeological stratum, square numbers, and excavation depth, for example, 4b-T27 or 4b-T21.

The most recent ages for the studied material are from Ecker *et al.* (2017). The study suggests 6.9-5.9 ka cal BP as the age of stratum 4b and the charcoal in this stratum (Table 3.2).

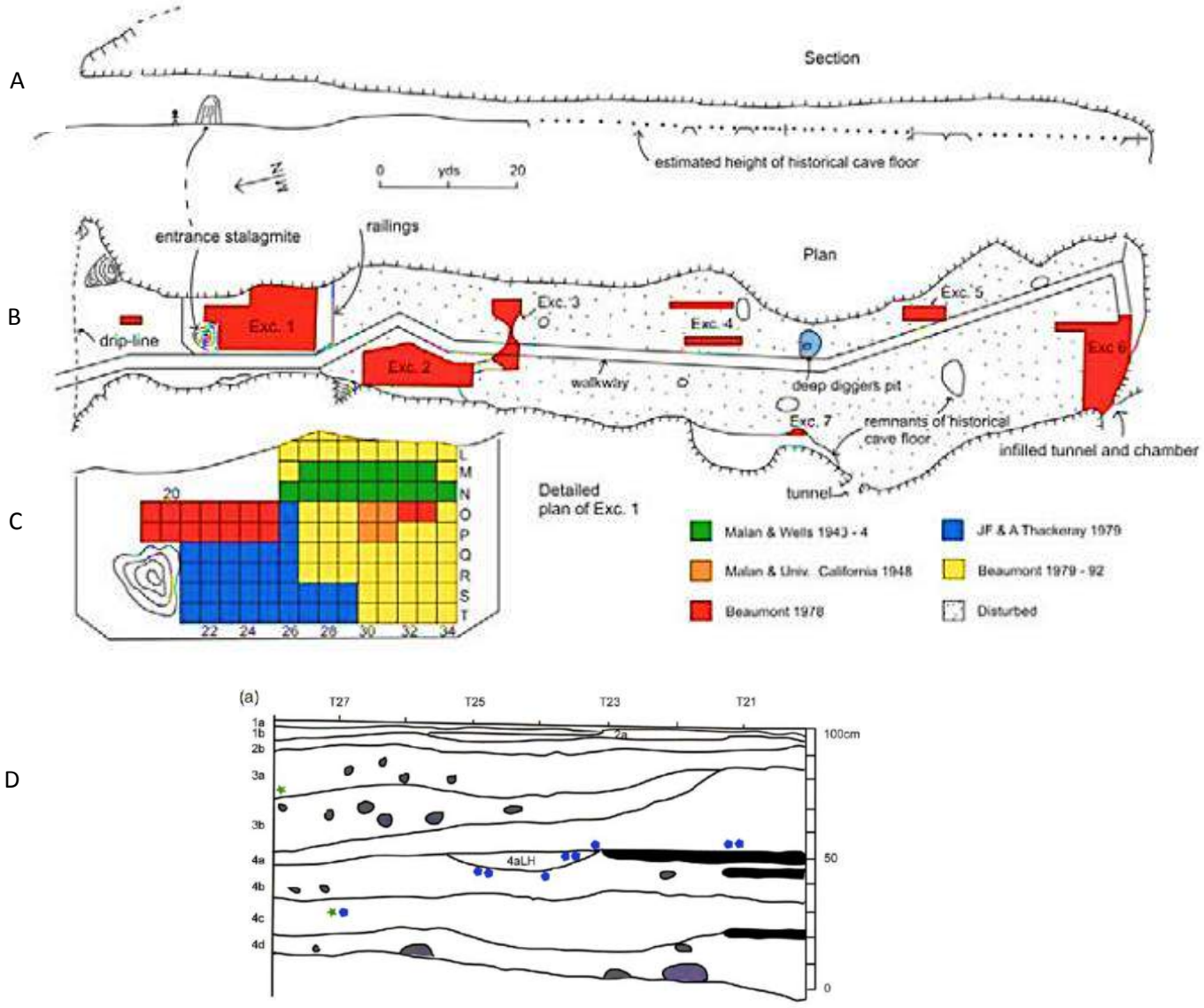


Fig. 4.1: The profiles of the Wonderwerk Cave. A) The side profile of the cave, showing the stalagmite near the entrance and Excavation 1 behind it. B) The seven areas excavated by Beaumont in 1978-79. C) The excavation plan of Excavation 1 and the excavators. D) The side profile of the Holocene strata excavated by Beaumont and the Thackerays. Note the natural stratification of the sediments indicated by the horizontal lines and the squares (T27, T25, T23 and T21) used to excavate. (Source: Beaumont and Vogel, 2006).

4.2 Methods

The standard anthracological procedures were employed to obtain accurate results and an understanding of the vegetation and climate changes in the interior southern Africa. To accomplish this, the study was subdivided into phases:

4.2.1 Phase 1: Charcoal reference database creation

The modern charcoal collection from the Evolutionary Studies Institute (ESI) was used as a reference to identify the archaeological charcoal material. This collection currently comprises more than 1000 samples of modern wood collected from various parts of southern Africa by different collectors. The trees were identified, and then wood and herbarium voucher specimens were collected, preferably the branches. The wood was added to the modern wood collection database and carbonized in a Lenton muffle furnace at the ESI to produce charcoal to be used for comparison. The wood was carbonized at 350 °C for 2 hours 30 minutes while wrapped in aluminium foil to limit the oxygen. This process does not alter the wood's anatomical features.

To create a comparative charcoal collection specific to the Wonderwerk Cave locality, a list of the trees and shrubs growing near the cave was compiled using literature such as Rutherford *et al.* (2006) and Wyk and Wyk (2013) (Table 3.1 & Appendix A). The reference charcoal of the listed woody species was gathered from the ESI modern charcoal collection, and the charcoals' internal anatomy was described, recorded and photographed using an Olympus BX51 microscope (using Dark Field and Bright Field at 50x and 200x magnification), digital camera and software Stream Essentials®. Each woody species has its unique combination of anatomical features that are key to identifying it.

To study the wood anatomy of the species currently unavailable in the modern charcoal collection, literature such as Kromhout (1975), Terrazas (1994), Allott (2005), Bamford (2015b), Lennox and Bamford (2017) and House *et al.* (2022; 2023) and more were used. Descriptions and photographs from InsideWood, an online database, were also utilized.

4.2.2 Phase 2: Taxonomy approach

This approach involves the collection of data and the botanical identification of archaeological charcoal. After identification, the geographic distribution and ecology of the modern analogs were used to infer the environmental conditions of the Mid-Holocene of interior southern Africa. The analyses are strictly qualitative and only based on the overlapping of the taxa, climate tolerance and habitat.

Laboratory procedures

In the laboratory, 13 random charcoal packets were gathered, and due to limited time, 10 to 29 charcoal fragments were sampled from each packet. The fragments were randomly subsampled from the packets. Each fragment was given its unique specimen number based on which packet it was collected and the order in which it was studied. For example, the first fragment analysed from packet 4b-S23 was labelled WW-4b-S23-A, and the second was labelled WW-4b-S23-B.

To prepare the charcoal samples for analysis, each piece of charcoal was fractured to get a clear view of the wood anatomical features from the three wood anatomical planes required for study: transverse section (TS), tangential longitudinal section (TLS), and radial longitudinal section (RLS) (Fig. 4.2 A, B). The fracturing process was done manually by snapping the charcoal using the fingertips. While this method worked for most charcoal pieces, some were harder to break and required extra measures, such as using a thin scalpel or fingernail tips to create a crack along the charcoal piece. This had to be done carefully as the scalpel or fingernails could easily scratch the surface of the charcoal, making it difficult to see the tissues. The fragmented pieces were affixed to microscope slides using Prestick® as a temporary adhesive, allowing easy readjustment during viewing and removal after use (Fig. 4.2 A). Upon completion, the fragments from each sample were placed in small, labelled plastic ziplock bags and will be returned to the McGregor Museum.

The wood anatomy was studied from the three anatomical planes using a reflected light microscope (Olympus BX51) at 50x, 200x and 500x magnification. Photomicrographs and measurements of the wood tissues were taken using an Olympus DP26 camera and an image analysis software called Stream Essentials®. Cell dimensions measured and recorded were vessels and ray lengths and diameters. The maximum diameter was measured for at least 25 vessels from the TS. The lengths of at least 25 vessels were measured from one tail end to the other. The counting of vessels and rays was done on a per square mm and linear mm basis, respectively. Individual vessels were counted from the lowest magnification, 50x, from at least ten different 1 mm x 1 mm fields.

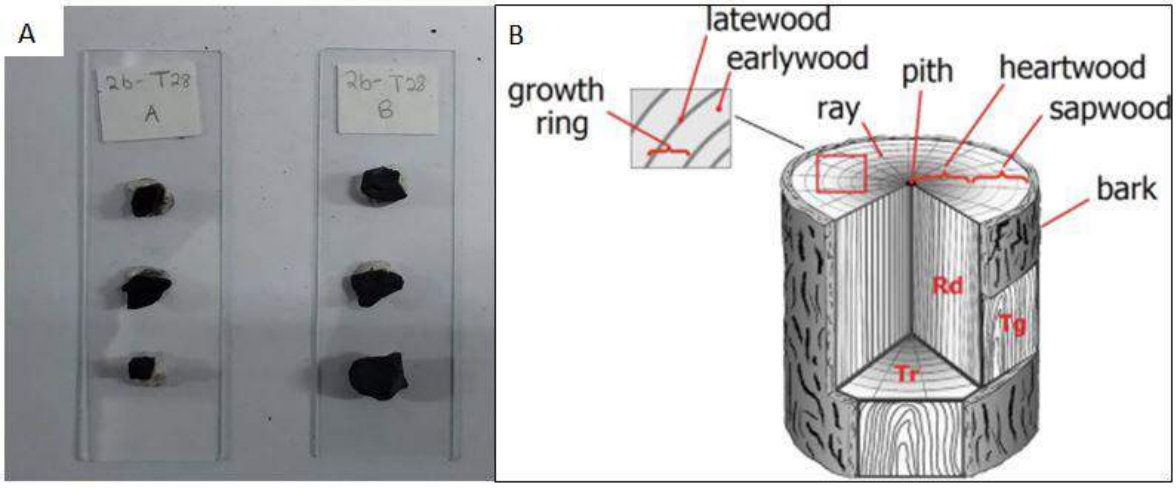


Fig. 4.2: The three anatomical planes of wood charcoal. A) The two charcoal samples, 2b-T28-A and 2b-T28-B, were each fragmented into three pieces, revealing transverse, tangential longitudinal, and radial longitudinal. B) Tr= Transverse section; Rd= Radial longitudinal section; Tg= Tangential longitudinal section. The internal structure of hardwood shows the labeled wood anatomical features and the three anatomical planes: transverse, radial longitudinal, and tangential longitudinal sections (Source: Pournou, (2020)).

Taxonomic identifications

The charcoal was described using the numbered anatomical features from Wheeler *et al.* (1989). The charcoal was grouped into different types based on the common features shared. The types were labelled as type 1, type 2, type 3, and so on. The charcoal types were identified by comparing archaeological charcoal to the modern database of Wonderwerk Cave wood charcoal created during phase 1. To confirm the identifications, anthracological publications were utilized, e.g., Kromhout (1975), Terrazas (1994), Allott (2005), Bamford (2015b), Lennox and Bamford (2017), House *et al.* (2022; 2023), InsideWood and more. To identify the charcoal fragments that did not match any of the charcoal in the Wonderwerk database, InsideWood and the key complied by M. Bamford for the Allott (2005) wood descriptions (unpublished) were used.

Data analysis

The Nearest Living Relative approach was utilized to analyse the data. This approach is based on the close relationship between modern and more recent fossil plants. This approach assumes that the modern and fossil taxa have the exact climatic requirements because there have been minimal evolutionary changes in plant environmental requirements since the beginning of the Quaternary (Utescher *et al.,* 2014). Hence, the distribution and ecological needs of the modern taxa were used to deduce the environmental tolerances of the fossil taxa. To collect data on the contemporary distribution and climate tolerances of the taxa identified, literature such as Palmer and Pitman (1972), Coates Palgrave and Coates Palgrave (1983), Mucina and Rutherford (2006) and van Wyk and van Wyk (2013) were utilized. The overlap between the climatic requirements of the taxa identified was used to provide information about the palaeoclimate.

The analysis in this dissertation was based on the Principle of Least Effort, which proposes that people in the past, much like today, collected firewood closest to their dwelling. The amount of firewood collected was directly proportional to its availability in the immediate surroundings (Shackleton and Prins, 1992). Therefore,

the charcoal found in the assemblage indicates the presence of some of the species that were once present in the immediate environment of the Wonderwerk Cave.

4.2.3 Phase 3: Physiognomic approach

In this approach, the wood's vessel elements are assessed and used as an environmental parameter. Large-diameter vessels have a much larger capacity than small-diameter vessels for water uptake. Woods with numerous small vessels have the same water transport capacity as woods with a few large vessels. However, the blockage of one small vessel has a lesser impact on water uptake efficiency than that of one large-diameter vessel. Therefore, woods with large diameter vessels are more vulnerable to embolisms caused by water deficits.

Because of this relationship between vessels and the environment, it is possible to infer water availability in the environment by analysing the vessel diameter and frequency from a reasonable sample of the plants present in each environment. Several indices have been created that use vessel diameter and frequency to determine the vegetation type and climate in which woody taxa grew. In this dissertation, the vulnerability index, conductivity capacity, and mesomorphy index were calculated using vessel data. The advantage of this method is that it does not depend on the correct identification of the wood.

Wood physiognomy interpretation

Using the vessel measurements acquired in phase 2, the vulnerability index, mesomorphy index and conductivity capacity were calculated using the formulae proposed by Carlquist (1977) and Wolfe and Upchurch (1987).

Vulnerability index (V) = $\frac{diameter\ (d)}{average\ number\ of\ vessels/mm^2 (D)}$

Conductivity capacity (C) = $\frac{r4}{10^6} \times D$

Mesomorphy index (M) = $V\ \times vessel\ length\ (l)$

Carlquist (1977) and Wolfe and Upchurch (1987) were consulted to interpret the results, and the values provided in the publications were used to infer climate and vegetation type. Based on data collected from modern woods in known environments, they provide a number of parameters. Vulnerability indices below 1.0 are a syndrome of shrubs or small xerophytic trees, while values between 1.0-2.5 or larger indicate large mesophytic trees. Conductivity capacity values below 200 were expected in small trees and shrubs, while values larger than 200 are a syndrome of larger mesophytic trees. Mesomorphy indices larger than 200 were expected in mesophytic plants, while values of 75 and below indicated xerophytes.

4.3 Summary of the chapter

A general overview of the methods used for the analysis of the charcoal from layer 4b, Excavation 1 of Wonderwerk Cave, is provided in this chapter. This chapter highlights the location of the archaeological charcoal, the subsampling procedure and the standard anthracological procedure followed to analyse the charcoal samples. The two methods, i.e. taxonomy and physiognomy, used in this study are detailed, including the methods used to interpret the results.

CHAPTER FIVE

Results

5.1 Description of the archaeological charcoal specimens

204 charcoal fragments were large and well-preserved and suitable for analysis. Despite clear anatomical features, 106 could not be determined and remain unidentified. The total charcoal analysed was categorized into 19 wood types based on shared features. These represent various woody species collected from the surroundings, brought into the cave and burnt for different purposes. Of these, only 15 types could be identified at the species level, and one at the genus level and 4 types were unidentifiable. The identifiable charcoal fragments represent the families Anacardiaceae, Asteraceae, Boraginaceae, Burseraceae, Apiaceae, Oleaceae, Oliniaceae, Fabaceae, Rhamnaceae and Scrophulariaceae. The charcoal taxa identified with certainty are described below. “cf.” indicates that the species or genus was not identified with confidence, and “sp.” means the genus was confidently identified, but the species is unknown.

The archaeological wood charcoal types are described and illustrated below in alphabetic order. Descriptions follow the IAWA terminology and guidelines. The summary of these types is given in Table 4.1. The summarized descriptions and photomicrographs of the comparative charcoal are provided in Appendices B-F.

5.2.1 Anacardiaceae

5.2.1.1 *Ozoroa paniculosa* (Sonder) R. & A Fernandes

Common name: Common resin tree

Described sample: Type 1 (WW-4b-R25G)

Illustration: Fig. 5.1

Total number of samples identified: 10

Description: The wood has indistinct growth ring boundaries. The wood is diffuse-porous as the vessels have the same diameter throughout the wood. The vessels are arranged in short radial multiples of up to 4, sometimes more. The perforation plates are simple and oblique, sometimes horizontal. The intervessel pits are alternate and minute to small, usually not more than 5 µm wide. The vessel diameters range from 30-70 µm, and the mean tangential diameter is 48.15 µm. On average, there are 39 vessels per square millimetre. The lengths of the vessel elements range from 100-400 µm, and the mean is 262.01 µm. The fibres are non-septate and thin-walled. The axial parenchyma is paratracheal scanty to vasicentric. The rays are 1-3 seriate and up to 300 µm/20 cells high. The rays are primarily composed of square and upright cells, with some rows of procumbent cells. There are between 4-12 rays per square millimetre. Radial canals or crystals were not observed in this specimen. The wood has radial cracks.

Comparison: Specimen R25G was identified using InsideWood, Allott (2005), Bamford (2015b) and House *et al.* (2022). It has features common to the species of the family Anacardiaceae. These features include a radial arrangement of vessels, a 1-3 cells ray width, and heterocellular but rarely procumbent ray cells. According to the three abovementioned authors, *Ozoroa paniculosa* wood has vessels arranged in short radial multiples, scanty to vasicentric parenchyma, minute alternate intervessel pits, 1-3 seriate rays, upright and square ray cells, a vessel frequency higher than 40 vessels per square millimetre and an average vessel diameter of 50 µm.

O paniculosa (BPI/20/15) from the ESI charcoal reference collection material also has similar features (Appendix D).

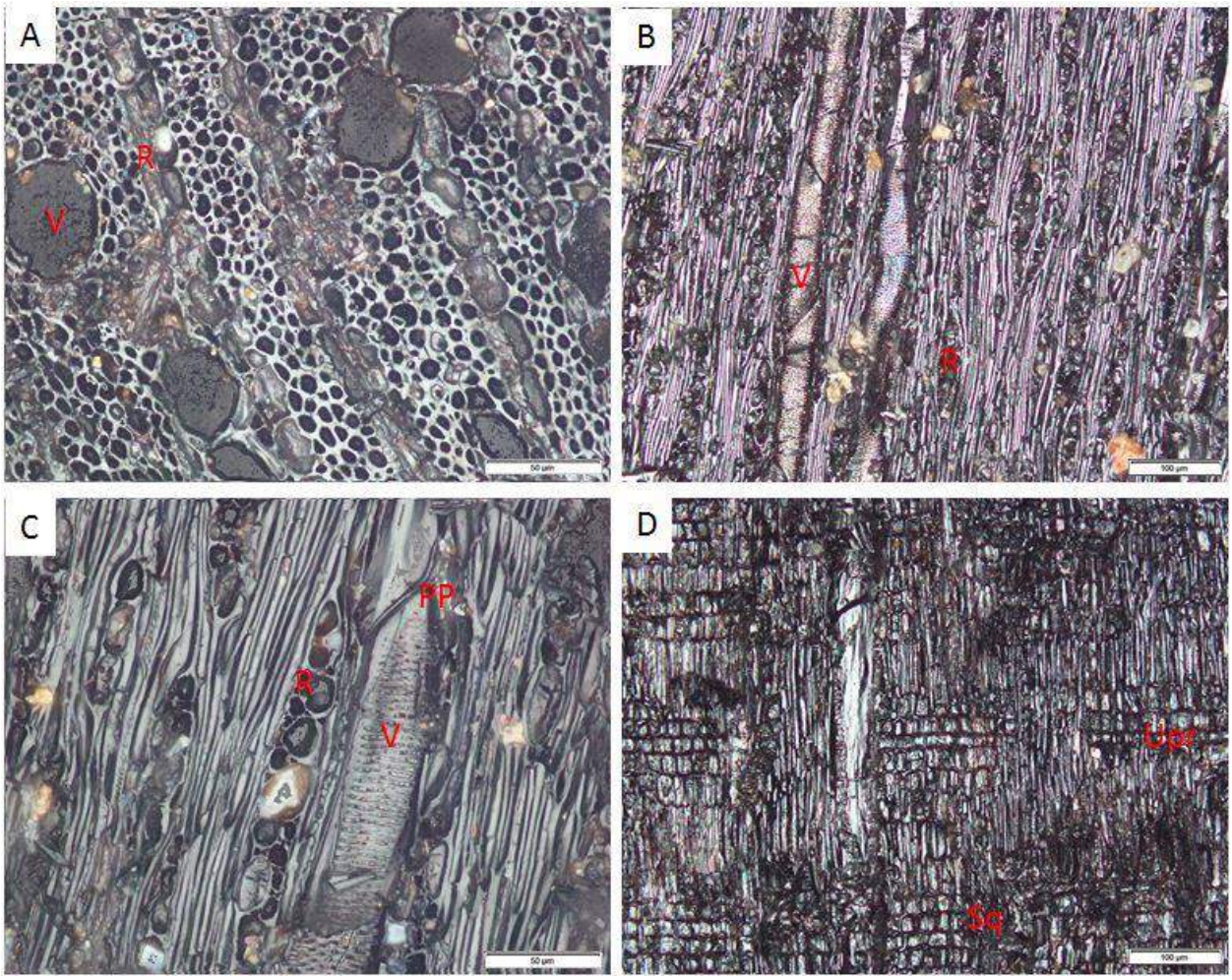


Fig. 5.1: Photomicrographs of *Ozoroa paniculosa* WW-4b-R25G charcoal from stratum 4b of Excavation 1, Wonderwerk Cave. TS= transverse section; TLS= tangential longitudinal section; RLS= radial longitudinal section; V= xylem vessel; R= ray; P= parenchyma; F= fibres; PP= perforation plates; x= crystal. A) TS, vessels shown arranged in short radial multiples of 1-4 and the bi-seriate rays. Scale bar= 50 µm. B) TLS, 1-3 seriate rays and vessels with simple, oblique perforation plates. Scale bar= 100 µm. C) TLS, 1-3 seriate rays mixed with short uniseriate rays. Note the shiny amorphous are not part of the wood. Vessels have small to medium, alternate intervessel pits and oblique perforation plates. Scale bar= 50 µm. D) RLS, Square and upright cells in the rays. Scale bar= 100 µm.

5.2.1.2 *Searsia lancea* L. F.

Common name: Karee (Old name *Rhus lancea*)

Described sample: Type 2 (WW-4b-Q22K)

Illustration: Fig. 5.2

Total number of samples identified: 5

Description: There are no visible growth ring boundaries. The vessels are diffuse and grouped in short radial multiples of 1-3. The perforation plates are simple and oblique. The intervessel pits are alternate and small, 4-7 µm in diameter. Occasionally, the pits are large, wider than 10 µm. On average, the vessel tangential diameter is 58.39 µm wide, and vessel diameters range from 50-80 µm. There are 30 vessels per square millimetre. The average length of the vessel members is 200 µm. The fibres have thin-thick (medium) walls and are non-septate. The axial parenchyma is scanty paratracheal. The rays are 1-3 seriate, and the tri-seriate rays sometimes have radial canals. The ray height ranges from 100-500 µm with up to 27 cells. The body ray cells are procumbent with 2-4 rows of upright and square marginal cells. The rays are abundant, usually more than 12 rays per millimetre. Crystals are poorly preserved in this specimen. The wood has some cracking seen from the transverse and tangential longitudinal sections.

Comparison: The specimen Q22K was identified using modern charcoal reference collection, Terrazas (1994), Allott (2005) and House *et al.* (2022). The specimen Q22K shares many features with species from the family Anacardiaceae (see *Ozoroa paniculosa*). According to Allott (2005), *Searsia lancea* wood has a short radial arrangement of vessels, average vessel diameter below 100 µm, more than 40 vessels per square millimetre, rays are 1-2 cells seriate and mixed with square

and upright ray cells with crystals inside the square and upright ray cells. The only difference is that Q22K has procumbent ray cells mixed with upright and square cells and no crystals. However, other *S. lancea* reference woods, i.e., K152 from Kroumhout (1975), BPI/20/537 (Appendix C) from the reference collection and *S. lancea* in House *et al.* (2022), have a similar RLS, with procumbent body ray cells with square and upright marginal cells. Q22K seems to not have preserved any crystals which were also noted in the ray cells of BPI/20/537, Allott (2005) and House *et al.* (2022).

Other *Searsia/Rhus* species currently growing near the cave are: *S. lancea, S. pyroides* var. pyroides*, S. tridactyla* and *S. ciliata* (Rutherford *et al.,* 2006). *S. pyroides* BPI/20/766 (Appendix F) vessels appear ring to semi-ring porous as they clearly become smaller towards the latewood and the growth rings are shown by flattened fibres at the latewood. This wood also has large intervessel pits and very thin-walled fibres compared to Q22K. *S. tridactyla* and *S. ciliata* are not available in the reference collection or any other reference material. However, the occurence of *S. lancea* in other strata, i.e., 5a, 4d, 4c, 4b, 4a, 3b, 3a and 2b, increases the confidence of this identification (Bamford, 2015; House *et al.,* 2022).

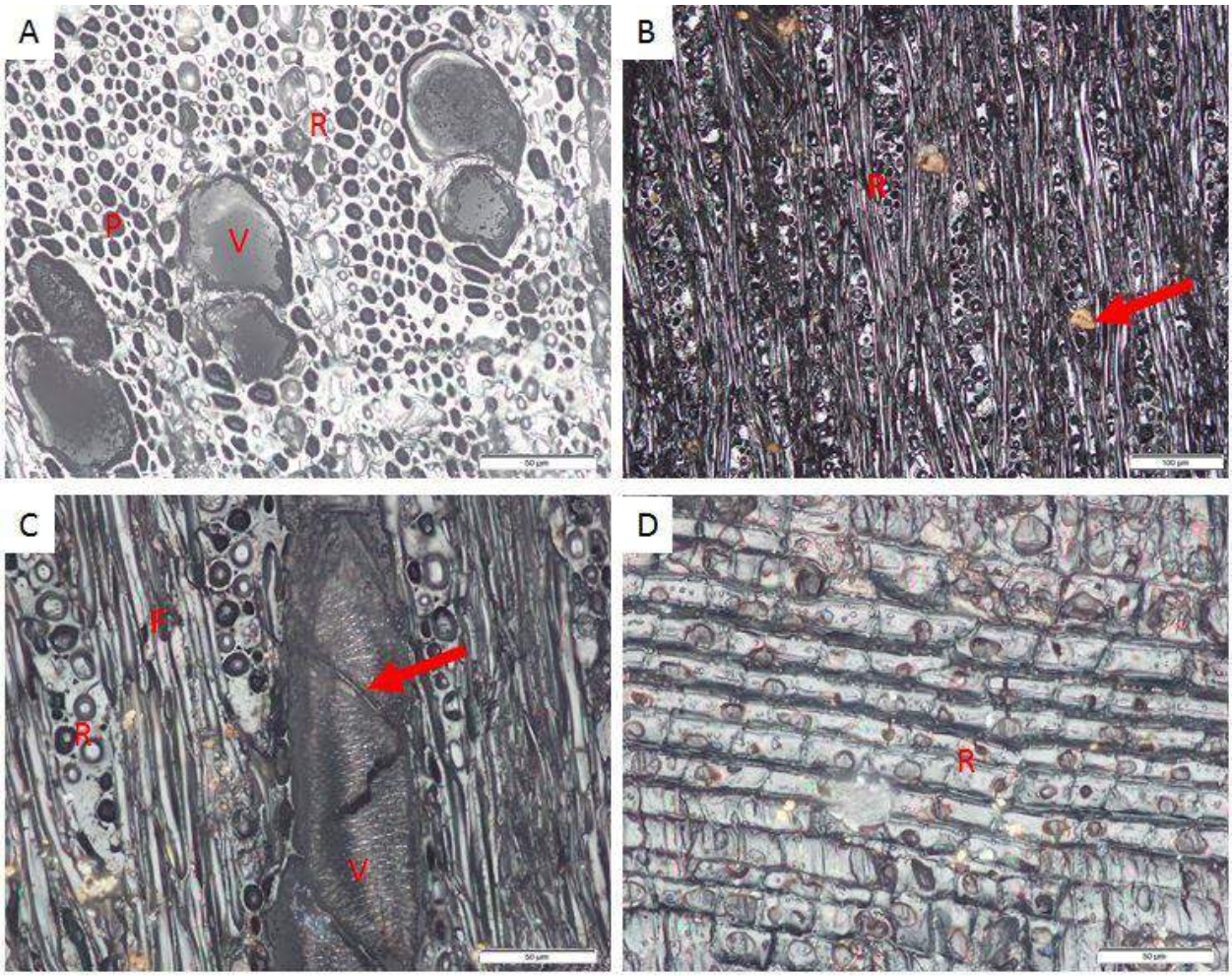


Fig. 5.2: Photomicrographs of *Searsia lancea* WW-4b-Q22K charcoal from stratum 4b of Excavation 1, Wonderwerk Cave. A) TS, vessels arranged in short radial multiples of two and surrounded by thin-thick or medium-walled fibres. Scale bar= 50 µm. B) TLS, long, large 1-3 seriate rays. Amorphous deposits indicated by arrow. Scale bar= 100 µm. C) TLS, 1-2 seriate rays and short wide vessels separated by oblique perforation plates indicated by an arrow. Scale bar= 50 µm. D) RLS, mostly procumbent ray cells are visible with some square cells. Scale bar= 50 µm.

5.2.2. Apiaceae

5.2.2.1. *Heteromorpha arborescens* Cham. & Schltdl.

Common name: Parsley tree

Described sample: Type 3 (WW-4b-S25IA)

Illustration: Fig. 5.3

Total number of samples identified: 28

Description: This specimen has indistinct growth rings. The wood is semi-ring porous as the fibres flatten, and vessels gradually decrease in size across the growth ring. The vessels are arranged in clusters and radial multiples of up to 10. The perforation plates are simple and oblique/horizontal. The intervessel pits are alternate and minute, as the pits mostly have a diameter of less than 4 µm. The mean vessel tangential diameter is 56.94 µm, and the vessels have a diameter range of 50-100 µm. There are approximately 91 vessels per square millimetre. The mean vessel length is 220.14 µm, and the lengths range from 100-350 µm. The fibres are thin- to thick-walled and non-septate. Axial parenchyma is scanty paratracheal. The rays are 1-3 seriate, sometimes up to 5 cells wide. The rays have a height range of 300-500 µm. The body ray cells are procumbent with about 4 rows of upright and square marginal cells. There are 4-12 rays per millimetre. This sample had no tyloses, cracks or crystals.

Comparison: Specimen S25IA was identified using Insidewood, Oskolski and van Wyk (2008) and House *et al.* (2022). Woods of Apiaceae are characterized by small vessels with a radial vessel arrangement of up to 4 vessels, a high vessel frequency, rare parenchyma and 1-4 seriate rays (Allott, 2005). The specimen fits the general description of the woods from this family.

Apiaceae has about 13 tree species indigenous to southern Africa (van Wyk and van Wyk, 2013). The specimen S25IA is identical to the *Heteromorpha arborescens* wood described in Oskolski and van Wyk (2008) and House *et al.* (2022). *H. arborescens* also shares a lot of features with *H. stenophylla*. The

reference collection does not have *H. stenophylla*. However, according to the descriptions and illustrations provided by Oskolski and van Wyk (2008), the difference between these two species is *H. arborescens* vessels are arranged in slightly shorter radial multiples of up to 10 vessels. *H. stenophylla* can have up to 32 vessels. *H. stenophylla* has a very high vessel frequency, with up to 265 vessels per square millimetre compared to 49 in *H. arborescens*. *H. stenophylla* wood usually has 3-5 seriate rays and radial canals, which were not observed in S25IA (Oskolski and van Wyk, 2008). Moreover, *H. arborescens* grows in the Northern Cape today, while *H. stenophylla* and all the other *Heteromorpha* species are mostly found in desserts or dry shrublands like those in Namibia, Malawi, Swaziland, Limpopo and KwaZulu Natal (Coates Palgrave and Coates Palgrave, 1983).

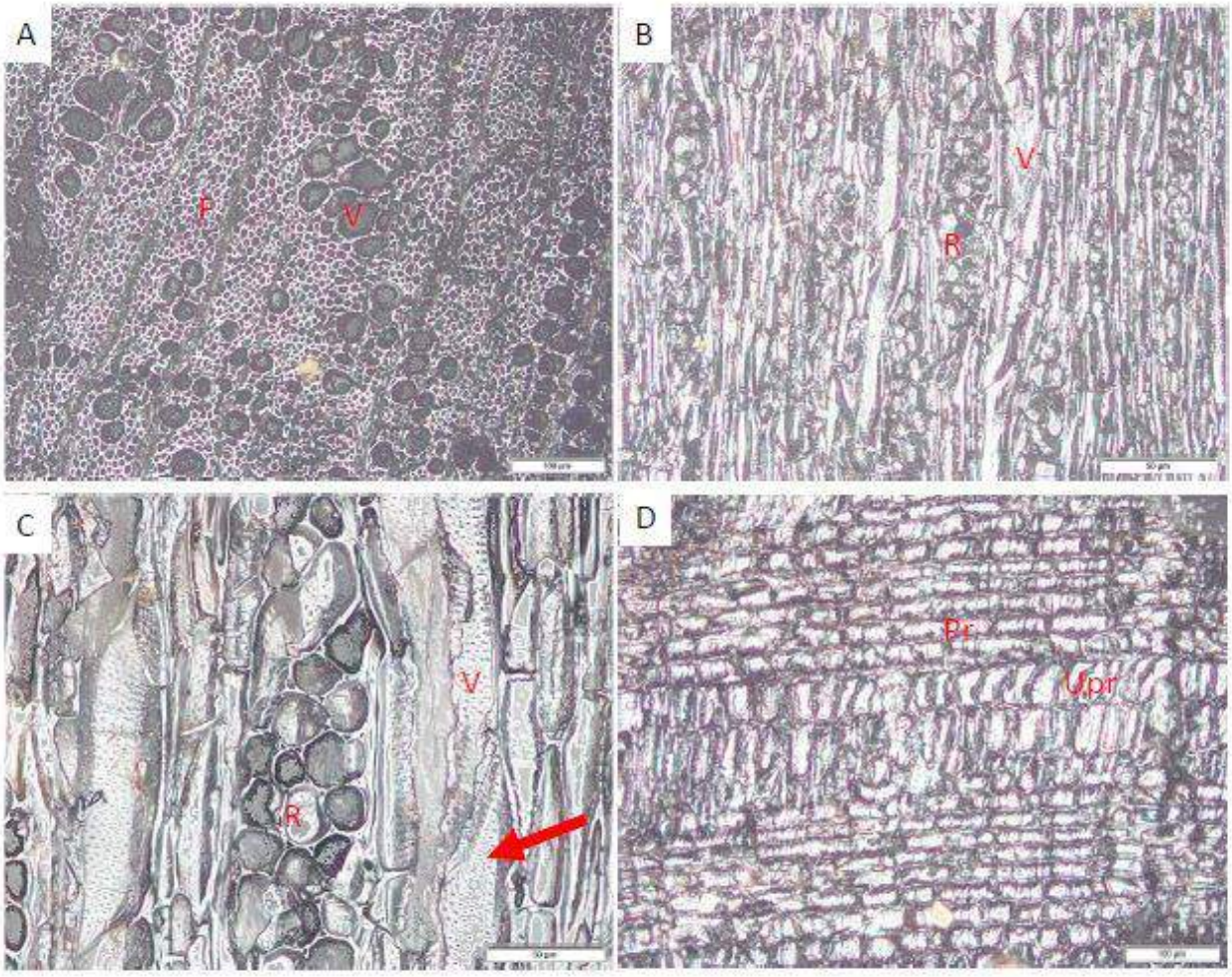


Fig. 5.3: Photomicrographs of *Heteromorpha arborescens* WW-4b-S25IA charcoal from stratum 4b of Excavation 1, Wonderwerk Cave. A) TS, vessels in long radial multiples and clusters. Scale bar= 100 µm. B) TLS, 1-4 seriate rays. Scale bar= 100 µm. C) TLS, 1-3 seriate rays and vessels with alternate and minute intervessel pits, as well as oblique perforation plates. Scale bar= 50 µm. D) RLS, procumbent and upright ray cells. Scale bar= 100 µm.

5.2.3. Asteraceae

5.2.3.1 *Tarchonanthus camphoratus* L.

Common name: Camphor bush

Described sample: Type 4 (WW-4b-Q22B)

Illustration: Fig. 5.4

Total number of samples identified: 16

Description: The wood has indistinct growth rings and diffuse-porous vessels as no significant changes are noted in the vessels diameter. The vessels are arranged in short radial multiples of 1-3 vessels and sometimes clusters. The intervessel pits are alternate and minute, usually less than 4 µm wide. Simple, oblique to horizontal perforation plates are found between the vessels. The vessels have a diameter range of 20-50 µm and a mean of 36.82 µm. The vessel frequency is high, with about 94 vessels per square millimetre. The vessels are angular in outline in the transverse section. The vessels have lengths ranging from 200-300 µm, and the mean vessel length is 256.37 µm. The fibres are non-septate, and the walls are thin- to thick-walled. The axial parenchyma is scanty paratracheal. The rays are 1-2 seriate and narrow and up to 12 cells/250 µm high. The body ray cells are procumbent with 2-4 rows of marginal square cells. There are between 4-12 rays per square millimetre. No crystals were observed in this specimen.

Comparison: The specimen Q22B was identified using modern charcoal reference and confirmed by Lennox and Bamford (2017). The specimen has features typical for most woody Asteraceae species. These features include a radial arrangement of vessels, diffuse and scanty parenchyma, alternate and minute intervessel pits and a heterocellular ray cell composition. This specimen has features common to the genus *Tarchonanthus*. *Tarchonanthus* is closely related to the genus *Brachylaena*, so the two genera have similar features. However, *Tarchonanthus* wood usually has a radial arrangement of vessels, whereas *Brachylaena* wood has clustered vessels. The fibres in *Tarchonanthus* are thin- to thick-walled compared to the very thick walls in *Brachylaena*. The rays in *Tarchonanthus* are 1-3 seriate

and very narrow, compared to the wider 1-6 seriate observed in *Brachylaena.* Rays in *Brachylaena* are often storied (Lennox and Bamford, 2017).

The genus *Tarchonanthus* has five species in southern Africa: *T. camphoratus, T. littoralis, T. minor, T. obovatus* and *T. parvicapitulatu*s. *T. camphoratus* (BPI/20/421, Appendix E) matches Q22B as they both have vessels in short radial multiples of up to 3 vessels, thin- to thick-walled fibres, scanty paratracheal parenchyma, 1-2 seriate rays with mostly rows of procumbent cells and 1 to 2 rows of square cells. Lennox and Bamford (2017) also agree that *T. camphoratus* wood has vessels arranged in short radial multiples, sometimes clustered, 20-40 vessels per square millimetre, paratracheal scanty parenchyma, narrow 1-2 seriate rays with procumbent body cells and sometimes square marginal cells. Thus supporting the classification of Q22B as *T. camphoratus*.

Specimen Q22B is also shares some features with *T. parvicapitulatus* (BPI/20/454, Appendix E), except that Q22B has less numerous vessels (94 per square millimetre), which are arranged in short radial multiples of not more than 3, whereas *T. parvicapitulatus* wood has numerous vessels (average of 120-150 per square millimetre) often arranged in long radial multiples of 1-3-5. Futhermore, *T. caphoratus* still grows in the area (Table 3.1).

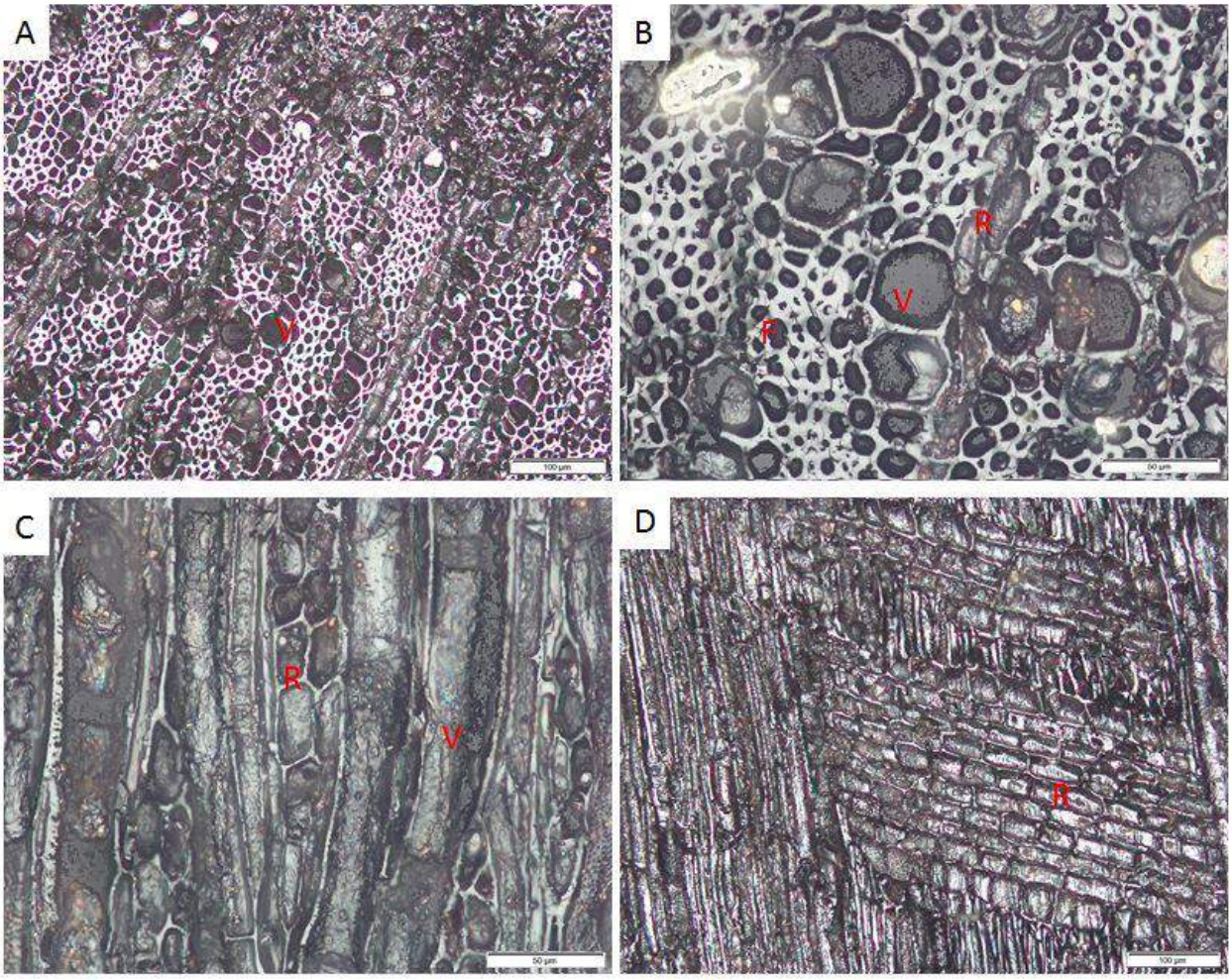


Fig. 5.4: Photomicrographs of *Tarchonanthus camphoratus* WW-4b-Q22B charcoal from stratum 4b of Excavation 1, Wonderwerk Cave. A) TS, short radial arrangement of up to 3 vessels. Note the light reflecting in the vessels, appearing as shiny inclusions inside the vessels. Scale bar= 100 µm. B) TS, vessels arranged in a short radial pattern with up to 3, thin- to thick fibre walls, uniseriate rays and medium-walled fibres. Scale bar= 50 µm. C) TLS, narrow 1-2 seriate rays, and intervessel pits are unclear in this sample. Scale bar= 50 µm. D) RLS, weakly homocellular rays comprising procumbent ray cells with one line of square ray cells on the margins. Scale bar= 100 µm.

5.2.3.2 *Tarchonanthus parvicapitulatus* P.P.J. Herman

Common name: Small-headed camphor bush

Described sample: Type 5 (WW-4b-S23E)

Illustration: Fig. 5.5

Total number of samples identified: 19

Description: Growth ring boundaries are indistinct, and the vessels are diffuse-porous. The vessels are arranged in radial multiples of up to 5 vessels and clusters. The perforation plates are simple and oblique. The intervessel pits are non-vestured, alternate and minute, with a diameter of less than 4 µm. The vessel-ray pits have distinct borders and are the same as the intervessel pits. The vessels have a diameter range from 20-50 µm and a mean tangential diameter of 36.0 µm. The vessels are rounded and very numerous, with 172 vessels per square millimetre. The average vessel length is 210 µm, and the range is 100-300 µm. Fibres are thin- to thick-walled and non-septate. The axial parenchyma is paratracheal scanty. The rays are narrow, 1-2 seriate and short, with about 11 cells high. The ray cells are mostly procumbent, sometimes with about two rows of square marginal cells. There are 4-12 rays per millimetre. There are no deposits or crystals in this specimen.

Comparison: Specimen S23E was identified using *T. parvicapitulatus* (BPI/20/453, Appendix E) from the modern charcoal collection. BPI/20/453 wood vessels are arranged in radial multiples of 1-3 and sometimes five. The fibre walls are thin to thick. The vessels are small and numerous. The rays are 1-2 seriate and thin. The rays are mostly procumbent with a few rows of square cells. This matches S23E, hence it was identified as *T. parvicapitulatus*.

The wood anatomy of *T. parvicapitulatus* is similar to *T. trilobus* (BPI/20/420, Appendix E) and *T. littoralis* (BPI/20/745). However, the vessels in *T. trilobus* are larger (±50 µm) and more rounded, while those in *T. parvicapitulatus* are irregularly shaped and smaller. Most importantly, the procumbent ray cells have crystals in *T.*

trilobus. On the other hand, *T. littoralis* has irregularly shaped vessels and a high vessel frequency like *T. parvicapitulatus*. However, *T. littoralis* has thicker fibre walls, and the rays are usually uni- or tri-seriate and wide, whereas *T. parvicapitulatus* has uniseriate and very narrow biseriate rays.

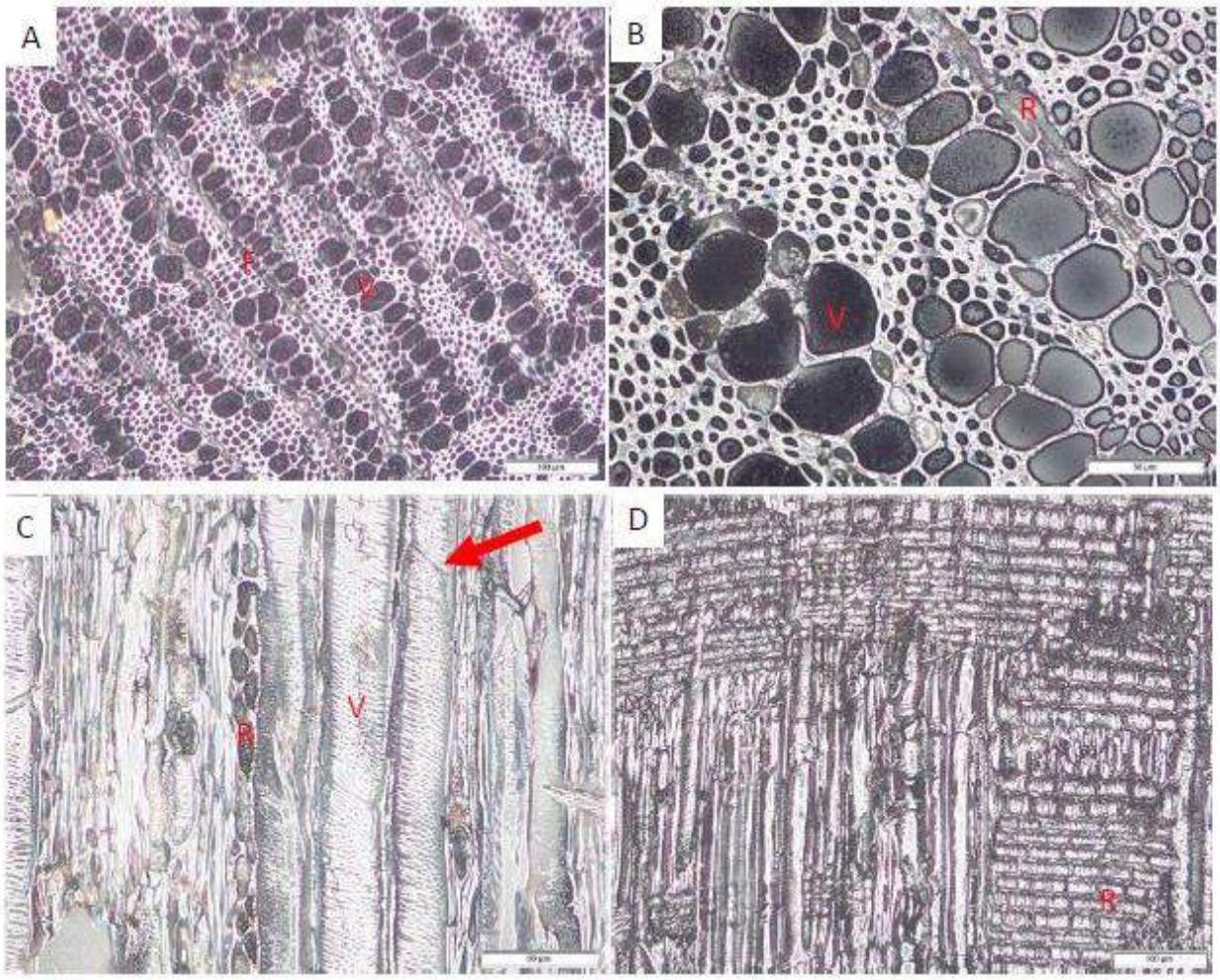


Fig 5.5: Photomicrographs of *Tarchonanthus parvicapitulatus* WW-4b-S23E charcoal from stratum 4b of Excavation 1, Wonderwerk Cave. A) TS, vessels arranged in long radial multiples of up to 5 and clusters. Scale bar= 100 µm. B) TS, scanty paratracheal parenchyma and thick-walled fibres. Scale bar= 50 µm. C) TLS, narrow biseriate rays. Vessels have alternate and minute intervessel pits and oblique perforation plates indicated by an arrow. Scale bar= 50 µm. D) RLS, procumbent ray cells. Scale bar= 50 µm.

5.2.4 Boraginaceae

5.2.4.1 *Ehretia* sp. L.

Described sample: Type 6 (WW-4b-Q22IN)

Illustration: Fig. 5.6

Total number of pieces identified: 1

Description: The growth ring boundaries are not visible. The perforation plates in this specimen are simple. The intervessel pits are non-vestured, alternate and small, 4-7 µm wide. The vessel-ray pits have distinct borders and are similar to the intervessel pits. The wood has diffuse-porous vessels with diameters ranging from 50-100 µm and a mean of 73.14 µm. There are only a few vessels present, arranged in groups of 1-2 multiples, with a frequency of 5-20 vessels per square millimetre. The mean vessel length is below 350 µm. The fibres are non-septate and thick-walled. Parenchyma is aliform and confluent. The parenchyma is also narrowly banded, with up to three bands per mm. There are 2-4 cells per parenchyma strand. The rays are procumbent with 1-2 rows of square marginal cells that are sometimes poorly preserved. The rays are 4-8 cells wide, sometimes aggregate. There are 4-12 rays per millimetre. The rays are 300-600 µm high and abundant. Crystals were not observed in this specimen.

Comparison: The specimen Q22IN was identified using Allott (2005) and Bamford (2015). The description of this specimen mostly matches the description of Boraginaceae wood. Wood from this family usually has a low vessel frequency, a short vessel arrangement of 1-2 vessels, 2-6 seriate rays that are heterocellular and banded parenchyma (Allott, 2005).

Bamford (2015b) identified *Ehretia*-type wood in stratum 5a and described it as wood with short radial multiples vessel arrangement, an average vessel diameter of about 80 µm, aliform to confluent parenchyma which is almost banded, 4-8 cells in parenchyma strands, thick fibres, procumbent body ray cells with 1 row of upright to square marginal cells and 4-8 seriate rays usually wide and abundant. It is identical to Q22IN.

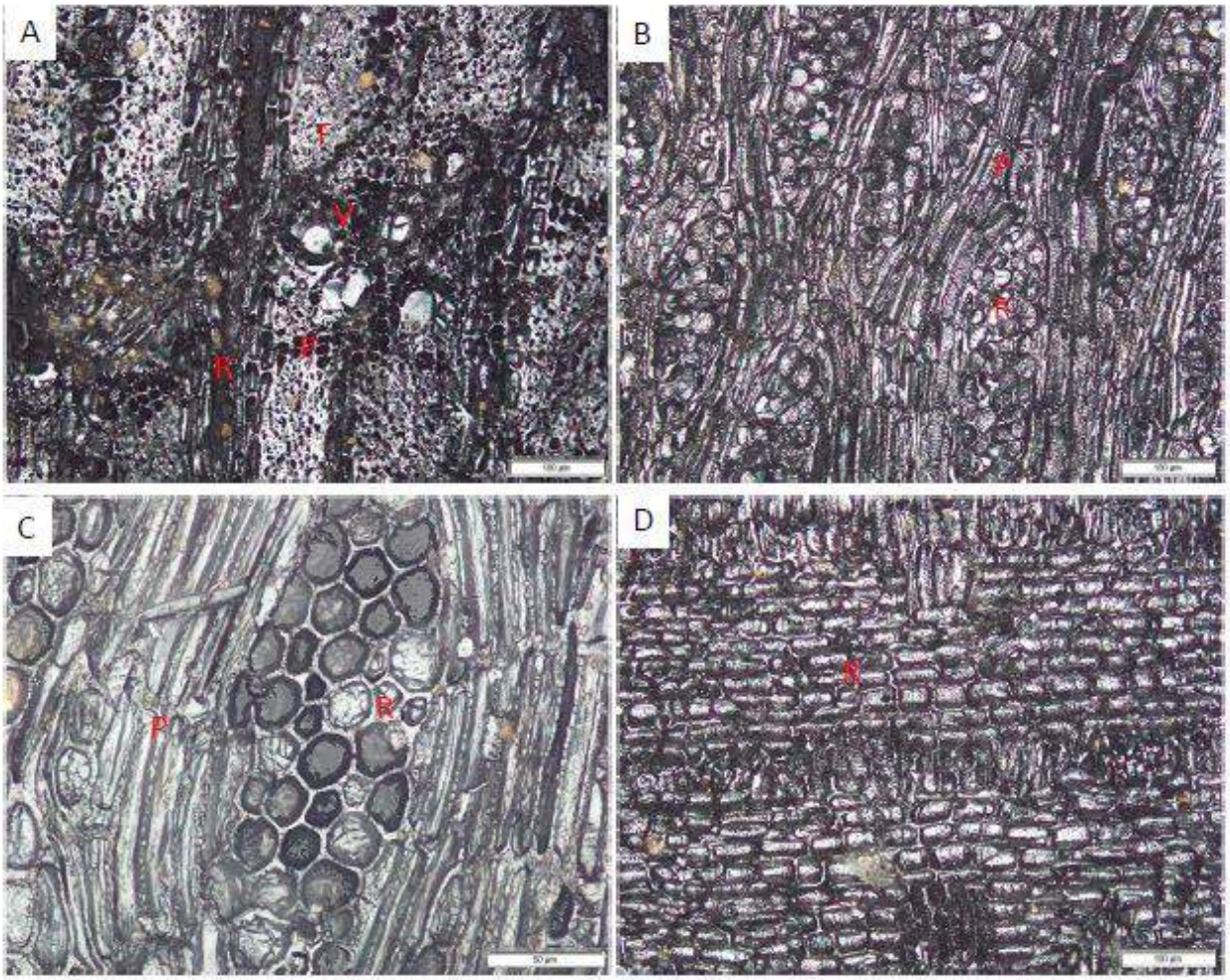


Fig. 5.6: Photomicrographs of *Ehretia* sp. WW-4b-Q22IN charcoal from stratum 4b of Excavation 1, Wonderwerk Cave. A) TS, large solitary vessels mostly obstructed by microscope light reflection. Banded parenchyma, with 3 parenchyma bands. Thick-walled fibres around the vessels. Scale bar= 100 µm. B) TLS, 4-5 seriate, short rays. Scale bar= 100 µm. C) TLS, 6 seriate rays and 2-4 parenchyma strands around the rays. Scale bar= 50 µm. D) RLS, procumbent ray cells. Scale bar= 100 µm.

5.2.5 Burseraceae

5.2.5.1 *Commiphora schimperi* (O.Berg) Engl

Common name: Glossy-leaved corkwood

Described sample: Type 7 (WW-4b-Q22N)

Illustration: Fig. 5.7

Total number of samples identified: 7

Description: Wood is diffuse-porous with undefined growth rings. The vessels are arranged in short radial multiples of 1-2 vessels. The perforation plates are simple and oblique. The intervessel pits are alternate and large, with a more than 10 µm diameter. The vessel-ray pits have distinct borders and are the same as the intervessel pits. The vessels have a tangential diameter range of 20-50 µm and a mean of 39.72 µm. On average, there are about 24 vessels per square millimetre. The mean vessel length is 178.56 µm, and the length of the vessel members ranges from 100-300 µm. The fibres are non-septate and have very thin walls. Paratracheal parenchyma is rare. The rays are 1-3 seriate and 200-400 µm high. Tri-seriate rays have radial canals. The rays are heterocellular, with procumbent, square and upright cells mixed throughout. Square and upright ray cells have prismatic crystals. There are more than 12 rays per millimetre. The wood has radial cracking.

Comparison: The specimen Q22N was identified by comparison with *Commiphora schimperi* (A34) from the Allott collection, Bamford (2015b), House *et al.* (2022) and *C. schimperi* (BPI/20/561, Appendix D) from the modern reference collection. *Commiphora schimperi* woods in Allott (2005), Bamford (2015) and BPI/20/561

have vessels with a diameter range of less than 50 µm, a vessel frequency of more than 40 vessels per square millimetre, a radial vessel arrangement of up to 4 vessels, rare parenchyma and rays with procumbent body cells and upright marginal cells, which have crystals. However, A34 has uniseriate rays, rarely biseriate, whereas BPI/20/561 and Q22N both have 1-3 seriate rays, and the tri-seriate rays bear radial canals.

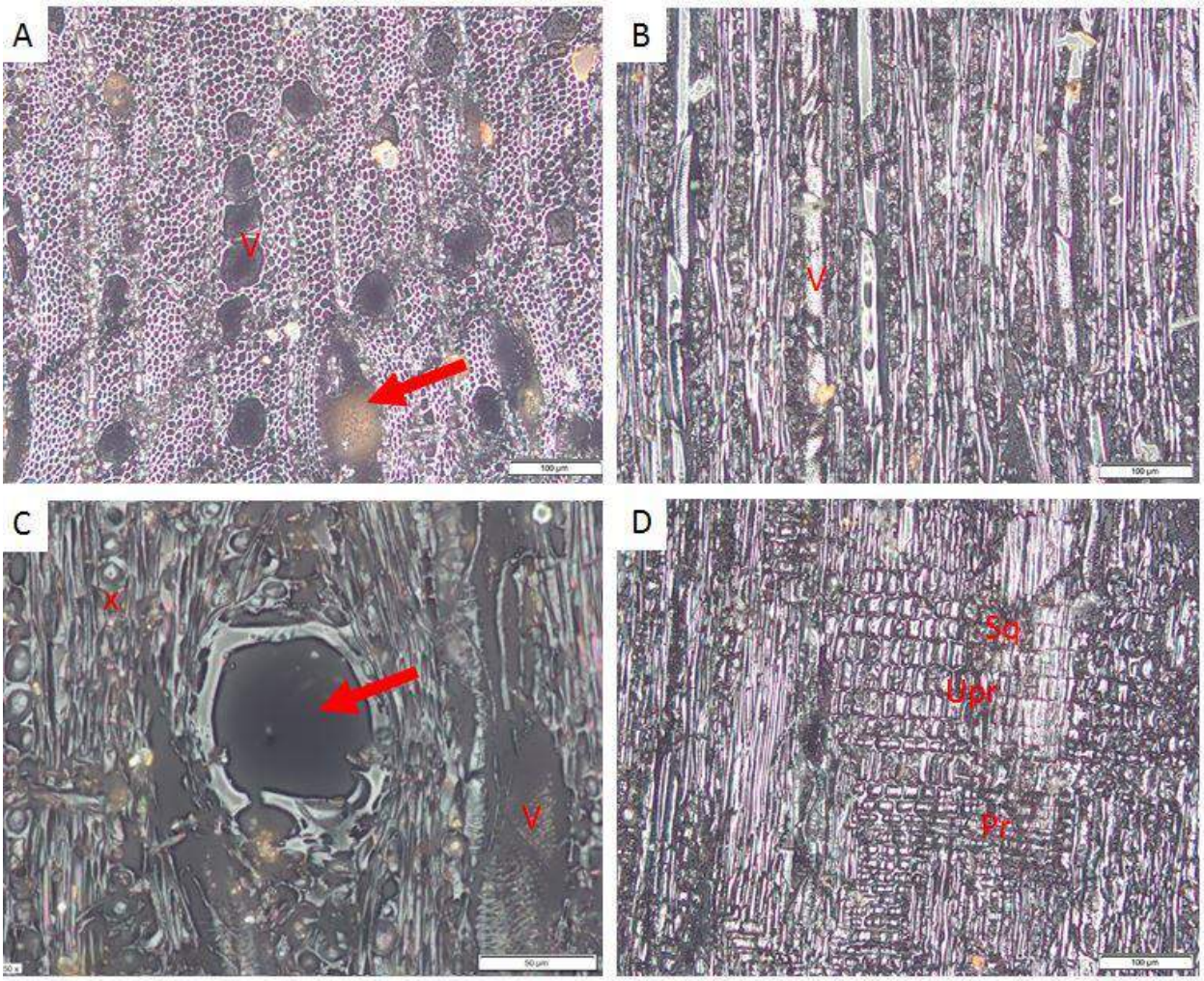


Fig. 5.7: Photomicrographs of *Commiphora schimperi* WW-4b-S23C charcoal from stratum 4b of Excavation 1, Wonderwerk Cave. A) TS, round vessels in multiples of up to 3. Note the radial cracks in this specimen, one indicated by an arrow. Scale bar= 100 µm. B) TS, bi-seriate rays. Scale bar= 100 µm. C) TLS, short uni-seriate rays comprising crystals. Radial canal in the large tri-seriate ray indicated by the arrow. Scale bar= 50 µm. D) RLS, procumbent, square and upright cells mixed throughout the ray. Scale bar= 100 µm.

5.2.6 Oleaceae

5.2.6.1 *Olea europaea* subsp. *africana* (Mill.) P.S.Green

Common name: Wild olive

Described sample: Type 8 (WW-4b-R21B)

Illustration: Fig. 5.8

Type: 8

Total number of samples identified: 10

Description: Vessels are arranged in short radial multiples of 1-3 vessels. The perforation plates are simple and oblique. The intervessel pits are non-vestured, alternate and minute, as they are 4 µm wide. The tangential diameter of the vessels ranges from 30-50 µm. The average vessel diameter is 43.53 µm. The vessel-ray pits are the same as the intervessel pits. There are about 76 vessels per square millimetre. The vessel length ranges between 100- 300 µm, and the mean is 248.58 µm. Growth rings are not visible, and the wood is diffuse porous. The fibres are non-septate and very thick-walled. Axial parenchyma is vasicentric. The rays are 1-2 seriate, narrow and short with heights ranging from 200-300 µm. The ray cells are procumbent with mostly 2- 4 rows of upright cells. There are 4-12 cells per millimetre.

Comparison: The specimen R21B was identified using *O. africana* (BPI/20/931) from the modern charcoal reference, Allott (2005), Bamford (2015) and House *et al.* (2022). The specimen shares a lot of features with the woods of the Oleaceae family. These features include short radial multiples of 1-4 vessels, a small mean

vessel diameter of less than 50 µm, a vessel frequency of more than 40 vessels per square millimetre, scanty or vasicentric parenchyma, 1-5 seriate rays and procumbent ray cells with about 4 rows of upright marginal cells.

In southern Africa, Oleaceae has about 15 woody species (van Wyk and van Wyk, 2013). *O. africana* has wood identical to specimen R21B. *O. africana* (A108) from Allott (2005) and BPI/20/931 (Appendix D) wood has a radial vessel arrangement of 1-3 vessels, minute alternate intervessel pitting, very thick fibre walls, vasicentric parenchyma, mixed procumbent and upright ray cells, and 1-2 seriate rays. The identification was positively confirmed by *O. africana* (K134) from Kroumhout (1975) and another *O. africana* (BPI/20/847) from the reference collection. *O. africana* still grows near the cave (Table 3.1). This species was also identified in strata 3a and 2b by House *et al*. (2022).

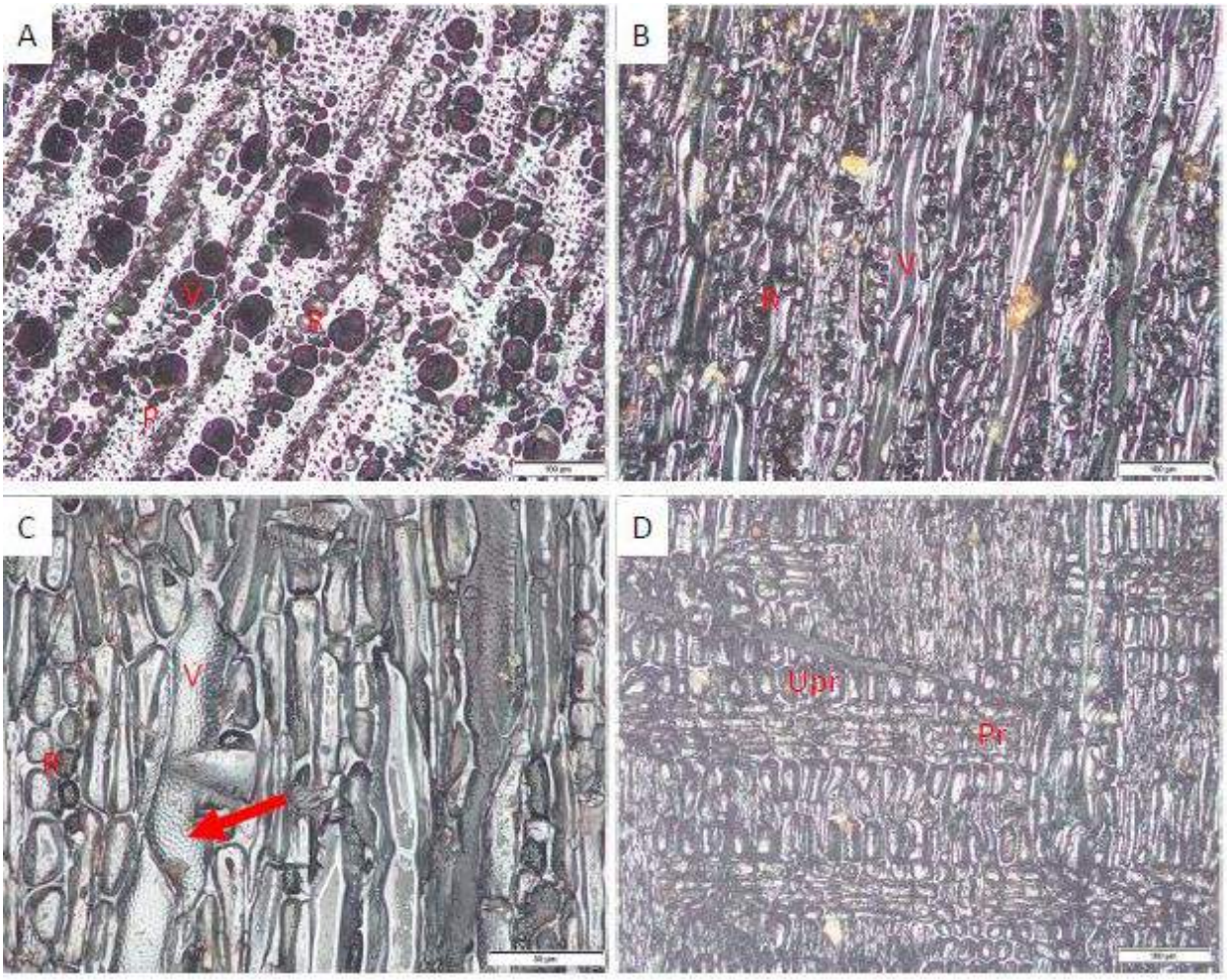


Fig. 5.8: Photomicrographs of *Olea europaea* subsp. *africana* WW-4b-R21B charcoal from stratum 4b of Excavation 1, Wonderwerk Cave. A) TS, vessels in low radial multiples with scanty-vasicentric parenchyma. Scale bar= 100 µm. B) TLS, 1-2 seriate rays. Scale bar= 100 µm. C) TLS, 1-2 seriate rays. Minute intervessel pits. Scale bar= 50 µm. D) RLS, upright and procumbent cells mixed. Scale bar= 100 µm.

5.2.7 Oliniaceae

5.1.7.1 *Olinia ventosa* (L.) Cufod.

Common name: Hard pear (Old name *Olinia cymosa*)

Described sample: Type 9 (WW-4b-Q22IL)

Illustration: Fig. 5.9

Total number of samples identified: 1

Description: The wood is diffuse porous and there are no distinct growth rings. The vessels are arranged in short radial multiples of up to 4 vessels. The perforation plates are simple and alternate between horizontal and oblique. The intervessel pits are alternate and minute, with a diameter below 4 µm. Vessel-ray pits are minutely bordered and similar to the minute, alternate intervessel pits. The vessel diameter ranges from 30-50 µm, and the mean is 39.53 µm. This wood has about 140 vessels per square millimetre. The vessels have lengths up to 350 µm, and the mean length is 268.12 µm. The fibres are septate and have very thick walls. The parenchyma is scanty paratracheal and the apotracheal parenchyma forms narrow, irregular bands. The rays are 200-300 µm tall and 1-3 cells wide. The uniseriate portions are as wide as the bi- and tri-seriate portions. The body ray cells are procumbent with more than 4 rows of upright and square marginal cells. There are 4-12 rays per square millimetre.

Comparison: This specimen was identified using Allott (2005) and Bamford (2015). It shares a lot of anatomical features with the woods of Oliniaceae. These features include a radial or oblique vessel arrangement of 2-3 vessels, paratracheal scanty parenchyma with bands, 1-2 seriate rays and heterocellular ray cells.

Oliniaceae has one genus, *Olinia* and about 10 tree species (van Wyk and van Wyk, 2013). This specimen matches the description of *Olinia cymosa* (A111) in Allott (2005). According to Allott (2005), *O. cymosa* has a vessel diameter range from 20-50 µm, a vessel frequency of more than 40 vessels per square millimetre,

a radial arrangement of vessels, scanty parenchyma and 1-3 seriate rays with the uniseriate portions as wide as the triseriate portions.

The identification was confirmed by the photomicrographs of *O. cymosa* in the Allott photomicrograph collection, *O. ventosa* (BPI/20/308, Appendix C) from the modern charcoal reference collection and *O. cymosa* (K137) from Kromhout (1975). BPI/20/308 wood has 1-3 small vessels arranged in radial multiples, procumbent, upright and square cells mixed, 1-3 seriate rays with the uniseriate portions of the rays as wide as the bi- and tri-seriate portions. *O. ventosa* is very similar to *Olea africana*. However, the presence of narrow parenchyma bands, square ray body cells and the tri-seriate rays in *Olinia ventosa* distinguishes it from *Olea europaea* subsp. *africana*.

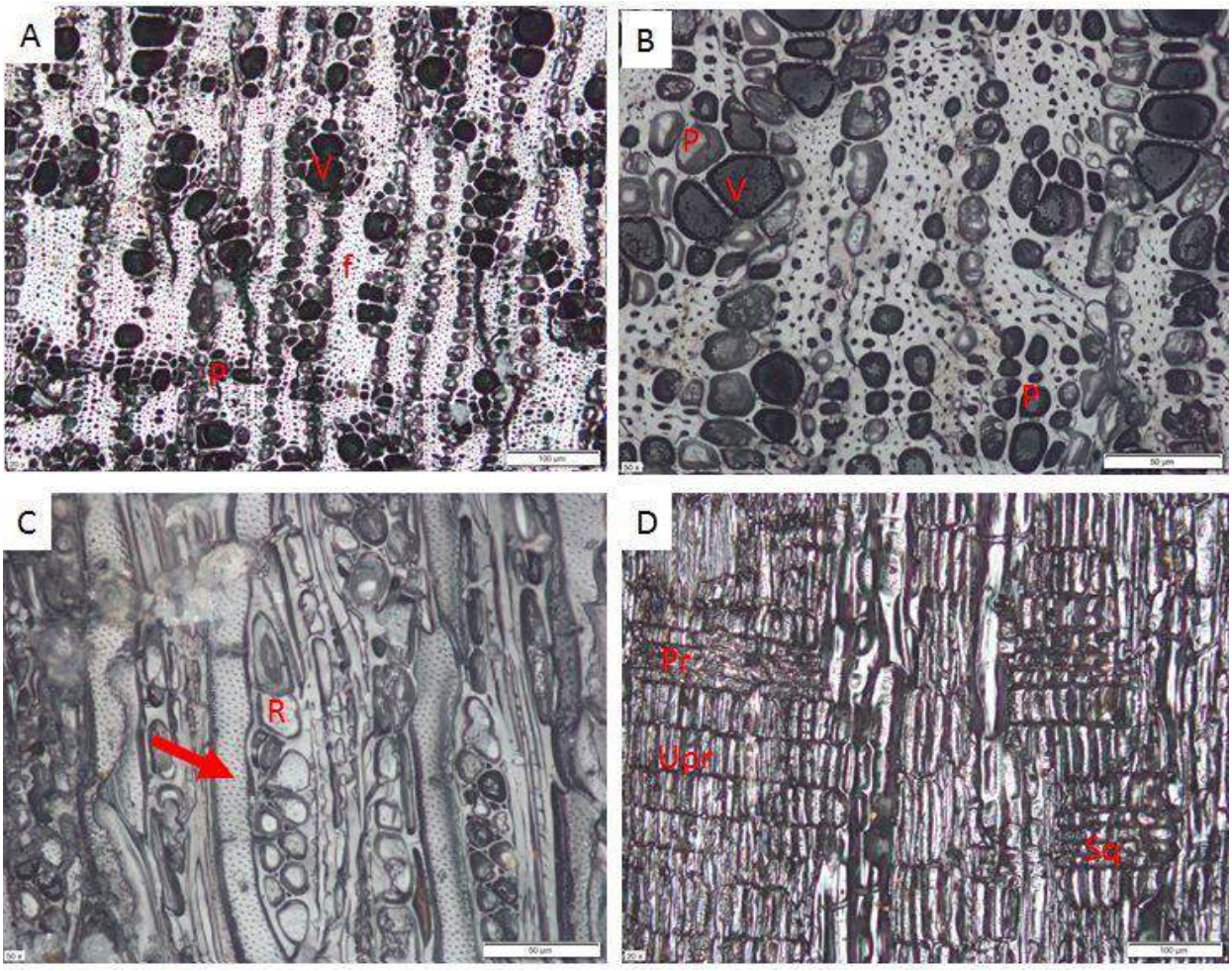


Fig. 5.9: Photomicrographs of *Olinia ventosa* WW-4b-Q22IL charcoal from stratum 4b of Excavation 1, Wonderwerk Cave. A) TS, vessels in low radial multiples with narrow bands of parenchyma indicated by P. Scale bar= 100 µm. B) vessels are arranged radially in multiples of up to four, with the scanty parenchyma around them and some parenchyma clusters. Scale bar= 50 µm. C) TS, narrow biseriate rays with the uniseriate parts of the rays wide as the biseriate parts. The vessels have alternate, minute intervessel pits indicated by the arrows. Scale bar= 50 µm. D) RLS, procumbent, upright and square ray cells mixed throughout. Scale bar= 100 µm.

5.2.8 Fabaceae

5.2.8.1 *Senegalia caffra* (Thunb.) Willd.

Common name: common hook thorn (Old name *Acacia caffra*)

Described sample: Type 10 (WW-4b-S21IIH)

Illustration: Fig. 5.10

Total number of pieces identified: 1

Description: The growth rings in this wood are indistinct, and the wood is diffuse-porous. This wood has simple, horizontal and oblique perforation plates. Vessels are primarily solitary and large, with an average tangential diameter of 169.51 µm and a 100-200 µm range. The mean vessel length ranges between 100-200 µm. The average number of vessels per square millimetre is 7. Intervessel pits are vestured, alternate and small, 4-7 µm wide. Fibres have very thick walls. The parenchyma is vasicentric to aliform. The smaller rays are 1-3 seriate (~42 µm wide) and the larger rays are 4-6 seriate (~87 µm wide). The rays are 300-600 µm tall. The ray cells are all procumbent and very narrow. On average, there are about 4 rays per millimetre.

Comparison: This wood type was identified using the modern reference collection in conjunction with Allott (2005). It has features typically found in Fabaceae and *Acacia* (now divided into *Vachellia*/*Senegalia*) species, such as vessels in 1-2 radial multiples, homocellular procumbent ray cells and vasicentric to aliform/confluent. Most woods from the genus *Vachellia* and *Senegalia* have vessels arranged in radial multiples of 1-3 and wide rays.

Senegalia caffra (BPI/20/716 & A195) and *Vachellia sieberiana* (BPI/20/721) were the only species with features similar to S21IIH. Both species have large, solitary vessels with a tangential diameter greater than 150 µm. However, *V. sieberiana* has wide, large rays that are up to 10 cells wide (~200 µm) and 400-1200 µm tall, whereas *S. caffra* has relatively narrower 1-5 seriate rays (~50 µm wide) and

shorter rays that are 500-700 µm tall. Therefore, S21IIH was identified as *S. caffra*. This species is no longer found in SVk 10 but in SVk 2 on the far east.

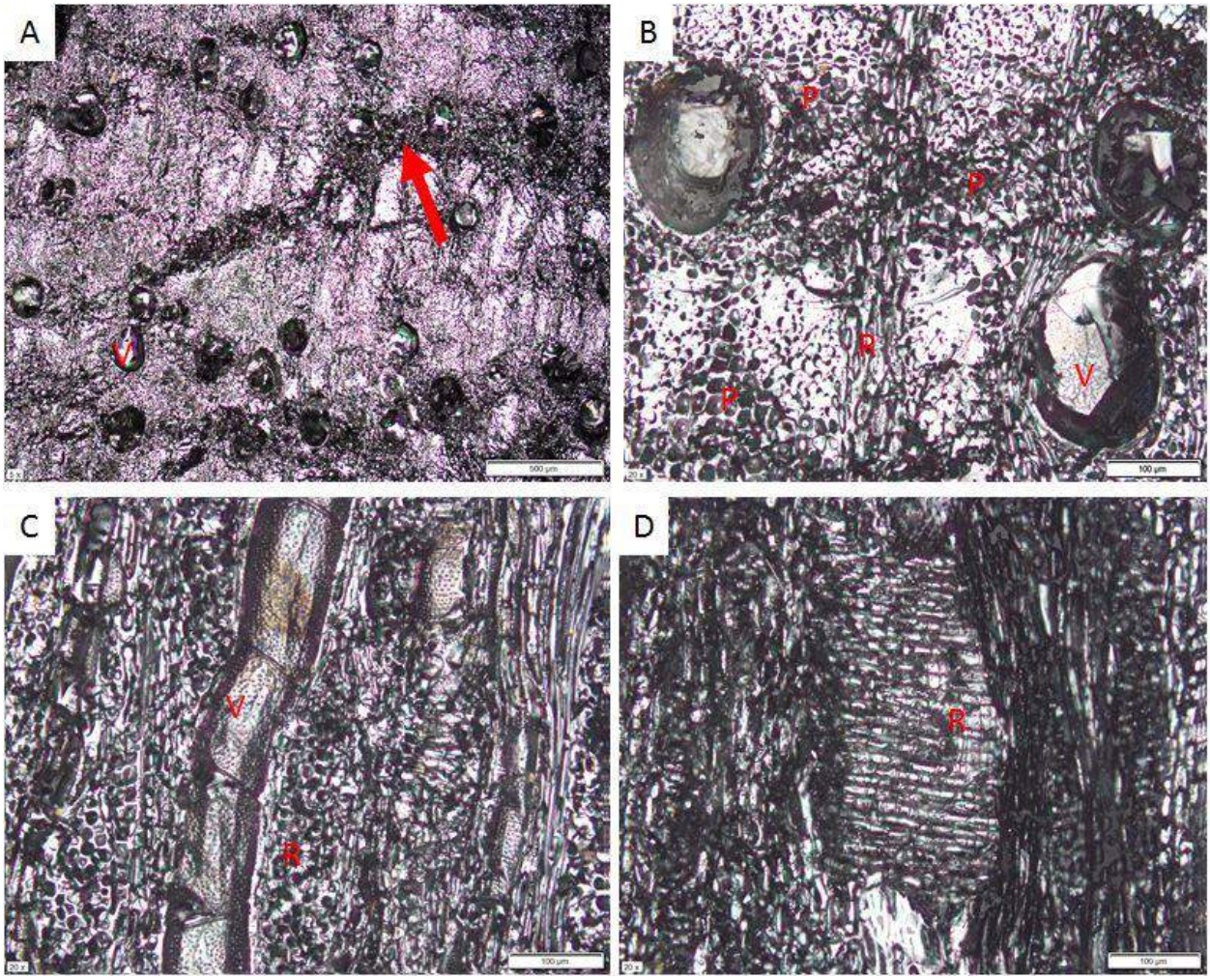


Fig. 5.10: Photomicrographs of *Senegalia caffra* WW-4b-S21IIH charcoal from stratum 4b of Excavation 1, Wonderwerk Cave. A) TS, large solitary vessels and the associated aliform parenchyma indicated by the arrow. Scale bar= 500 µm. B) TS, aliform parenchyma around the vessels. Vessels contain shiny deposits. Scale bar= 100 µm. C) TLS, 1-3 seriate rays and 4-6 seriate rays mixed. Scale bar= 100 µm. D) TS, homocellular procumbent ray cells. Scale bar= 100 µm.

5.2.8.2 *Vachellia* cf. *tortilis* (Forssk.) Hayne

Common name: Umbrella thorn (Old name *Acacia tortilis*)

Described sample: Type 11 (WW-4b-Q24G)

Illustration: Fig. 5.11

Total number of pieces identified: 4

Description: The wood has indistinct growth rings and is diffuse-porous. The vessels are mostly arranged as solitary or in clusters. The wood has simple, horizontal perforation plates. The intervessel pits are alternate, and medium (7-10 µm wide). The intervessel pits are vestured. The vessels have diameters up to 100 µm. There are about 32 vessels per millimetre square. The average vessel length is 214.7 µm. The fibres are non-septate and very thick-walled. The parenchyma is vasicentric, lozenge-aliform and confluent and also banded, with slightly more than 3 bands per mm. Parenchyma is abundant in this wood. There are 2-4 cells per parenchyma strand. The rays are 1-4 seriate and narrow. The rays are 300-400 µm long. The ray cells are procumbent. There are about 6 rays per millimetre, the rays are less frequent. No crystals were noted in the specimen. The wood has radial cracks.

Comparison: This specimen was identified using the modern charcoal reference collection and Allott (2005). The specimen has most of the features typical of woods from the Mimosoideae subfamily of the Fabaceae family. Most species in this subfamily have a radial vessel arrangement of up to 4 vessels, homocellular procumbent rays and aliform to confluent parenchyma (Allott, 2005).

The descriptions of this specimen match with two species species from the genus *Vachellia*: *Vacchellia robusta* and *V. tortilis. V. robusta* (BPI/20/249) wood mostly has solitary vessels, wider 4-6 seriate rays, confluent parenchyma and medium-walled fibres. Whereas, *V. tortilis* (BPI/20/409, Appendix F) has a solitary and

clustered arrangement of vessels, medium intervessel pits, 3-6 seriate rays, aliform and confluent parenchyma and thick-walled fibres. T21E matches *V. tortilis.*

This specimen is also identical to another *V. tortilis* (BPI/20/722) from the ESI reference collection, *A. tortilis* (A196) from Allott (2005) and *A. tortilis* (K47) from Kromhout (1975). *V. tortilis* still grows near the cave in the SVk 10 (Bamford, 2015a). Although not to species level, *Acacia* (*Vachellia/Senegalia*) wood was identified by House *et al.* (2022) in the younger strata 3b, 3a and 2b.

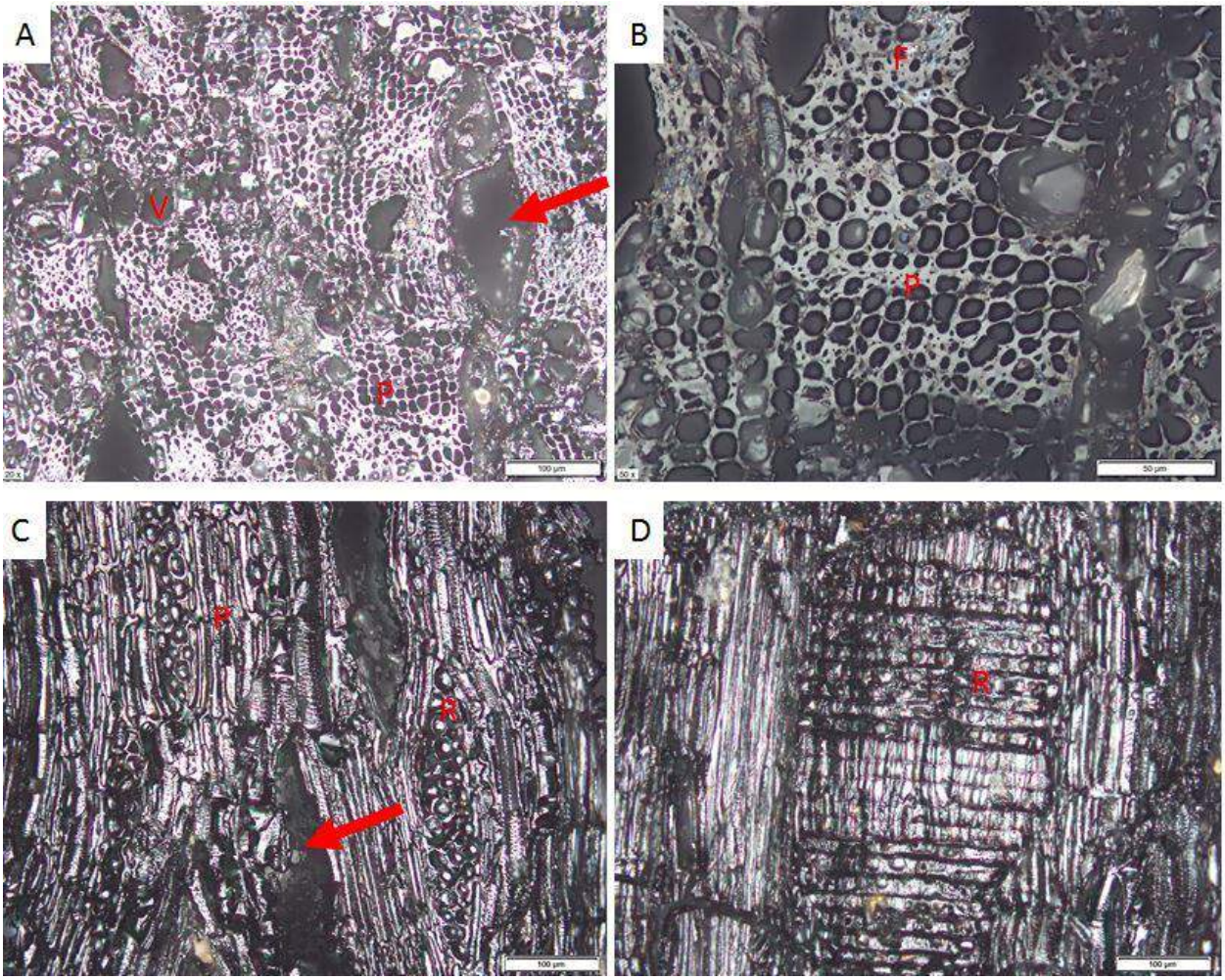


Fig. 5.11: Photomicrographs of *Vachellia* cf. *tortilis* WW-4b-Q24G charcoal from stratum 4b of Excavation 1, Wonderwerk Cave. A) TS, a solitary arrangement of vessels which have light reflecting inside them. Banded parenchyma, more than 4 bands. Note the radial cracks, indicated by arrows. Scale bar= 100 µm. B) TS, vasicentric, lozenge-aliform parenchyma associated with the vessels and parenchyma bands shown as P. Scale bar= 50 µm. C) TLS,

1-4 seriate rays, some with radial cracks indicated by an arrow. Scale bar= 100 µm. D) RLS, procumbent ray cells with rare square cells. Scale bar= 100 µm.

5.2.8.3 *Vachellia* cf. *karroo* Hayne

Common name: Sweet thorn (Old name *Acacia karroo*)

Described sample: Type 12 (WW-4b-S21IIIK)

Illustration: Fig. 5.12

Total number of pieces identified: 1

Description: The wood has indistinct growth ring boundaries and is diffuse-porous. The vessels are primarily solitary. The wood has simple horizontal perforation plates. The intervessel pits are alternate, with some pits small (4-7 µm) and some medium (7-10 µm). The intervessel pits are vestured. The vessels have diameters ±50 µm. There are about 25 vessels per millimetre square. The vessel length is below 350 µm. The fibres are non-septate and thick-walled. The parenchyma is vasicentric or aliform to confluent. The rays are 1-5 seriate and 200-500 µm high. The ray cells are procumbent. There are about 11 rays per millimetre, the rays are abundant in this wood. No crystals were noted in the specimen. The specimen has radial cracks.

Comparison: This specimen was identified using the modern charcoal collection and Allott (2005). The features of S21IIIK match the description of Fabaceae, Mimosoideae and *Vachellia* species (provided in the *V. tortilis* and *S. caffra* comparison sections). According to Allott (2005), *V. karroo* wood has a radial vessel arrangement and a vessel frequency of over 40 vessels per square

millimetre. It also has aliform to confluent parenchyma, 1-2 and 4-10 seriate rays that are not longer than one millimetre.

Around the site, there are several species of *Vachellia*, including *V. mellifera* subsp. *detinens, V. tortilis, V. erioloba*, and *V. karroo* (Bamford, 2015a). When comparing the wood anatomy of these species, it was found that the description and photomicrographs of *Acacia karroo* (BPI/20/01) and *A. karroo* wood in House *et al.* (2023) match the features of S21IIIK. The two references show that the wood of *V. karroo* has a short radial arrangement of 1 or 2 vessels, with a vessel diameter range of approximately 100 µm. The rays are 2-8 cells wide, but mostly 4 cells, and are narrow with procumbent cells. The fibres are thin- to thick-walled. Based on these characteristics, it is most likely that this specimen is *V. karroo*.

The identification was confirmed by *Acacia karroo* (BPI/20/06), which was similar to S21IIIK. The wood of BPI/20/06 shows 1-2 radial vessel patterns, large alternate intervessel pits, aliform to confluent parenchyma, procumbent rays and the shorter rays are 1-3 seriate while the longer rays are 4-10 seriate.

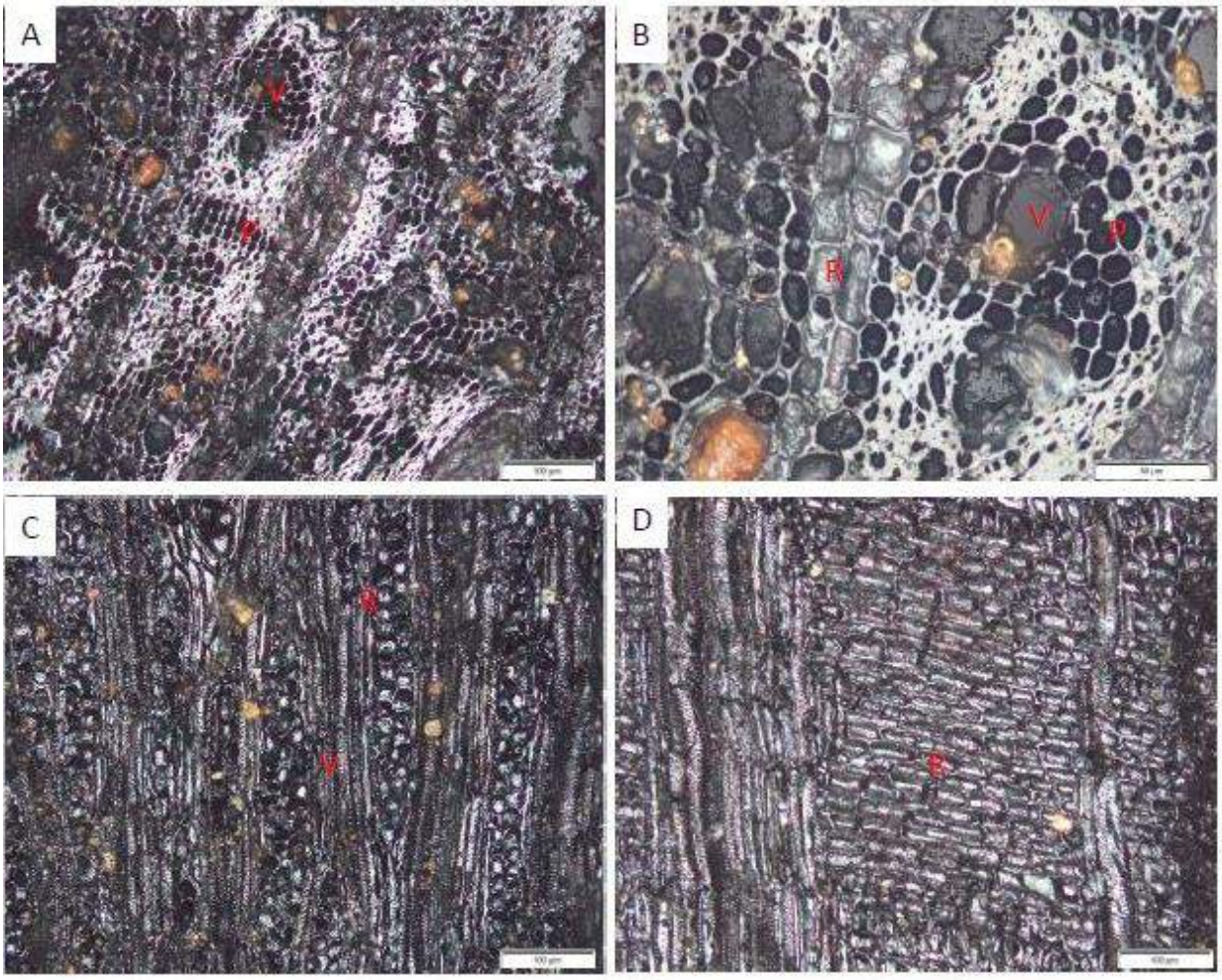


Fig. 5.12: Photomicrographs of *Vachellia* cf. *karroo* WW-4b-S21IIIK charcoal from stratum 4b of Excavation 1, Wonderwerk Cave. A) TS, vessels arranged in 1-2 radial multiples. Banded parenchyma indicated as P. Scale bar= 100 µm. B) TS, solitary vessels with diameters ~50 µm and winged aliform parenchyma around them. Scale bar= 50 µm. C) TLS, 1-3 seriate rays. Scale bar= 100 µm. D) RLS, procumbent ray cells. Scale bar= 100 µm.

5.2.9 Rhamnaceae

5.2.9.1 *Berchemia* cf. *zeyheri* (Sonder) Grubov

Common name: Red ivory (Old name *Phyllogeiton zeyheri/Rhamnus zeyheri*)

Described sample: Type 13 (WW-4b-S25ID)

Illustration: Fig. 5.13

Total number of pieces identified: 1

Description: The growth ring boundaries are indistinct, and the wood is diffuse-porous. The wood has simple, oblique perforation plates. The vessels are arranged in a radial pattern and grouped in radial multiples of 1-3. The intervessel pits are alternate and small. The mean tangential diameter of the vessel lumina is 56.34 µm, and the vessel diameter range between 50-100 µm. On average, there are about 22 vessels per square millimetre. The fibre walls are thin- to thick-walled. The parenchyma is scanty paratracheal. The rays are 1-3 seriate and their heights vary between 200 to 400 µm. The body ray cells are procumbent with about 2-4 rows of upright marginal cells. There are more than 12 rays per millimetre. No crystals, gums or tyloses were observed in this specimen. The tangential longitudinal section of this wood is warped.

Comparison: Specimen S25ID was identified using *B. zeyheri* (BPI/20/252) from the modern charcoal reference. The genus *Berchemia* has only 2 species in southern Africa, *Berchemia discolor* and *B. zeyheri* previously known as *Phyllogeiton discolor* and *P. zeyheri* respectively (van Wyk and van Wyk, 2013). *B. discolor* was identified in strata 5a, 4a and 3b in Bamford (2015) and House *et al.* (2022). *B. zeyheri* charcoal has not been found in any of the layers, nor does it grow near the cave anymore. Both these species woods have a radial arrangement of vessels, intervessel pits alternate and small, the mean vessel diameter from 50-100 µm, scanty paratracheal parenchyma, thin- to thick-walled fibres and procumbent body ray cells with about 2-4 rows of upright marginal cells. However, *B. zeyheri* has only scanty paratracheal parenchyma, whereas *B. discolor* has scanty paratracheal to aliform and narrowly banded parenchyma. S25ID description fits *B. zeyheri* (BPI/20/252).

This identification was confirmed by comparing the specimen to the *B. zeyheri* photomicrographs from Insidewood. The description also matches the description of *P. zeyheri* in Schirarend (1991).

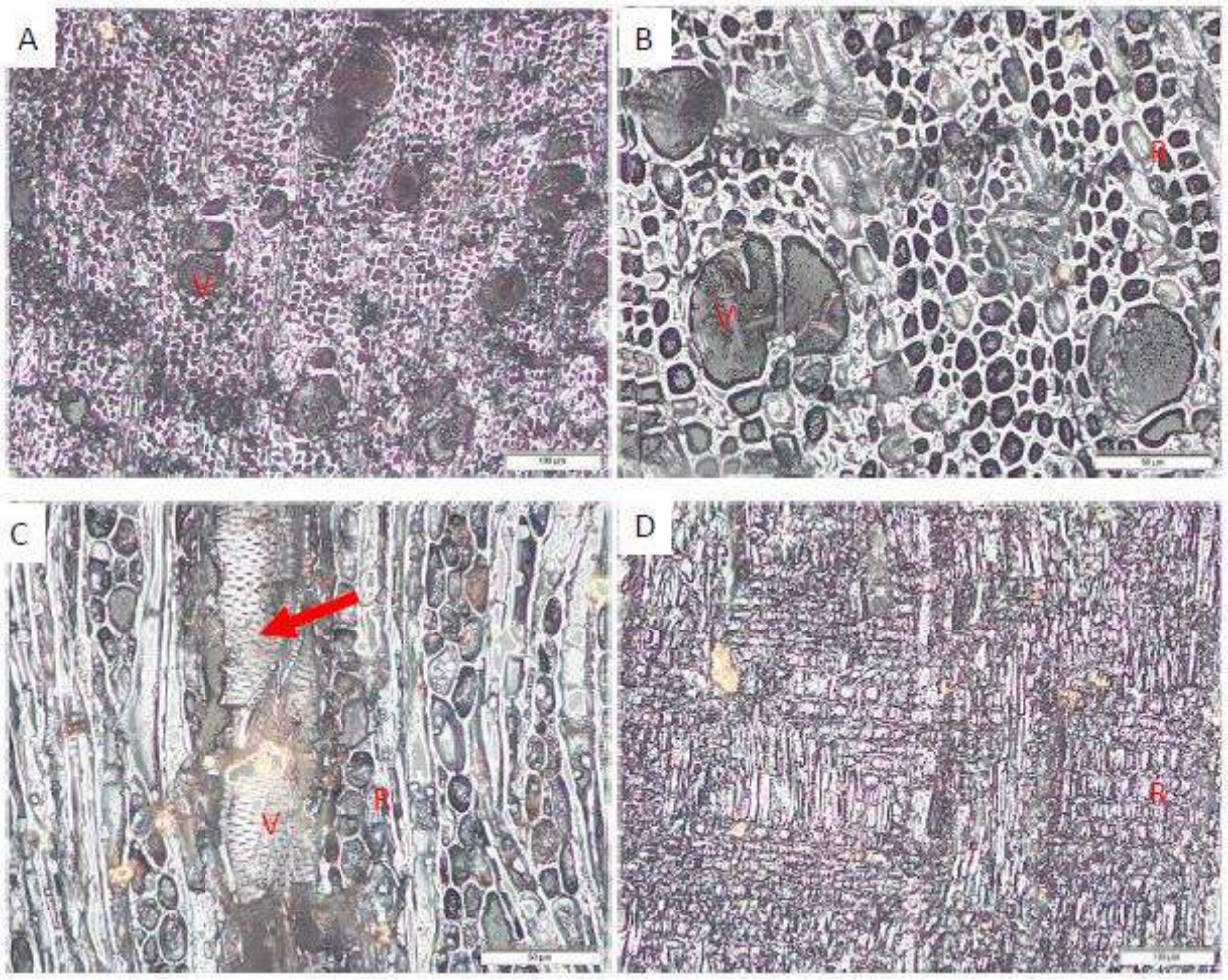


Fig. 5.13: Photomicrographs of *Berchemia* cf. *zeyheri* WW-4b-S25ID charcoal from stratum 4b of Excavation 1, Wonderwerk Cave. A) TS, solitary and paired vessels. Scale bar= 100 µm. B) TS, solitary and paired vessels with scanty paratracheal parenchyma and medium-walled fibres. Scale bar= 50 µm. C) TLS, 1-3 seriate rays. Vessels with small, distinctly bordered alternate intervessel pits indicated by the arrow. Scale bar= 100 µm. D) RLS, procumbent and upright ray cells mixed. Scale bar= 100 µm.

5.2.9.2 *Ziziphus mucronata* Willd.

Common name: Buffalo thorn

Described sample: Type 13 (WW-4b-R24D)

Illustration: Fig.5.14

Total number of pieces identified: 1

Description: The wood has indistinct growth ring boundaries and is diffuse-porous. The vessels are arranged in short radial multiples of 1 or 2 vessels. The wood has simple, oblique perforation plates. The intervessel pits are vestured, alternate and small, 4-7 µm wide. The solitary vessels are round to oval, have a tangential diameter ranging from 50-100 µm, and a mean of 72.85 µm. On average, the wood has about 42 vessels per square millimetre. The vessel length ranges from 200-400 µm, with a mean of 282.89 µm. The fibres are thin to thick-walled. The parenchyma around the vessels is vasicentric. The rays are all uniseriate and 200-300 µm tall. There are more than 12 rays per millimetre. All the ray cells are upright and square. Prismatic crystals square and upright ray cells.

Comparison: The description of specimen R24D fits the description of *Z. mucronata* in Schirarend (1991), Allott (2005) and House *et al.* (2022). According to these publications, the wood of this species has a mean vessel diameter of less than 100 µm, more than 40 vessels per square millimetre, vasicentric and aliform parenchyma, uniseriate rays and mixed upright and square ray cells.

There are 3 species of *Ziziphus* in southern Africa, *Z. abyssinica, Z. mucronata* and *Z. rivularis*. Currently, *Z. abyssinica* and *Z. rivularis* grow far from the cave in Namibia, Botswana, and along the east coast of South Africa. *Z. mucronata* still has a wide distribution, including near the cave (van Wyk and van Wyk, 2013). It

was also identified in the younger strata 3a and 2b (House *et al.*, 2022). R24D matches *Z. mucronata* (BPI/20/647, Appendix C) from the modern reference collection. The wood of BPI/20/647 has a radial arrangement of vessels, thin- to thick-walled parenchyma, vasicentric parenchyma, alternate and small intervessel pits, upright and square marginal ray cells containing crystals and uniseriate rays. The specimen is also identical to *Z. mucronata* in the Allott collection and K172 from Kromhout (1975).

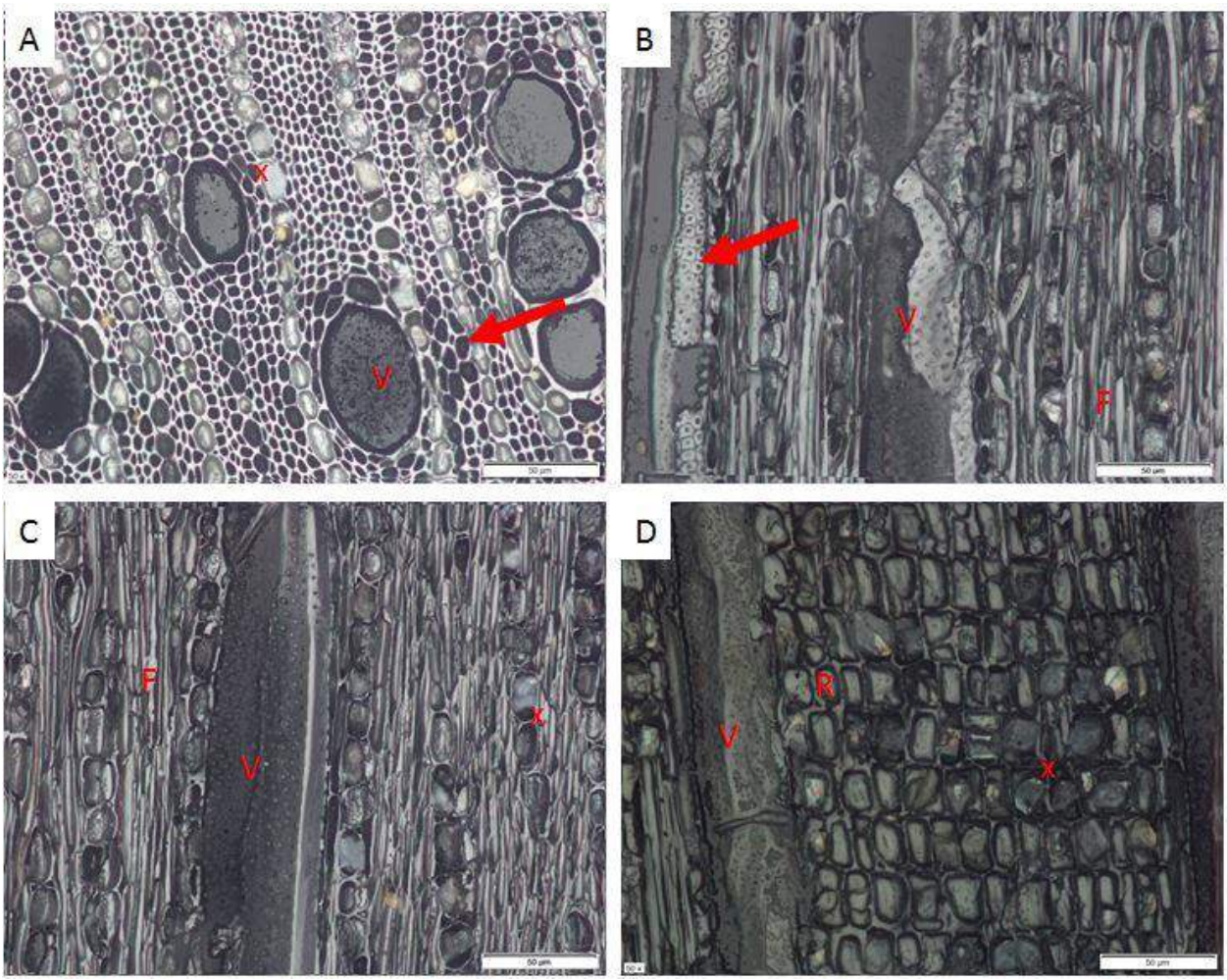


Fig. 5.14: Photomicrographs of *Ziziphus mucronata* WW-4b-R24D charcoal from stratum 4b of Excavation 1, Wonderwerk Cave. A) TS, vessels arranged as solitary or in pairs with the vasicentric and lozenge-aliform around them indicated by an arrow. Crystals can also be seen inside the rows of rays, indicated by x. Scale bar= 50 µm. B) TLS,

vessel element with minute, alternate intervessel pits. The intervessel pits of some vessels are vestured, indicated by the arrow. Scale bar= 50 µm. C) TLS, uniseriate rays with crystals inside them indicated by x. Scale bar= 50 µm. D) RLS, a mixture of upright and procumbent ray cells with crystals inside them indicated by x. Scale bar= 50 µm.

5.2.10 Scrophulariaceae

5.2.10.1 *Halleria lucida* L.

Common name: Tree fuchsia

Described sample: Type 15 (WW-4b-Q22P)

Illustration: Fig. 5.15

Total number of pieces identified: 1

Description: The growth ring boundaries in this wood are indistinct and the vessels are diffuse porous as they have the same size throughout. The vessels are arranged in radial multiples of up to 4 vessels. The perforation plates are simple and oblique. The intervessel pits are alternate and minute sometimes large. The vessels have a tangential diameter range of 50-100 µm and a mean of 91.12 µm. The vessels have a length range of 100-300 µm and a mean of 249.81 µm. There are 53 vessels per square millimetre. The fibres are very thin-walled. The parenchyma is rare. The rays are 1-5 cells wide and 200-700 long. The rays are heterocellular, with procumbent, square and upright cells mixed. There are 4- 12 rays per millimetre.

Comparison: It shares a lot of features with the woods of the Scrophulariaceae family whose woods have a tangential and radial arrangement of 1-4 vessels, rare parenchyma, 3-6 seriate rays and square and upright ray cells (Allott, 2005).

Halleria lucida wood (BPI/20/684) from the modern charcoal reference has a radial arrangement of more than 5 vessels, thin- to thick-walled fibres, 1-5 seriate rays and heterocellular ray cells with procumbent, upright and square ray cells. This wood shares a lot of features with Q22P.

H. lucida was identified in stratum 5a by Bamford (2015b) and was described as wood with indistinct growth ring boundaries, a radial vessel arrangement, alternate and minute intervessel pits, a mean vessel diameter of 80 µm, thick fibres, 30 vessels per square millimetre, 1-5 seriate rays and procumbent, upright and square ray cells mixed. The description of the wood in Bamford (2015) fits Q22P. The species identification was confirmed as *H. lucida* (K109) from Kromhout.

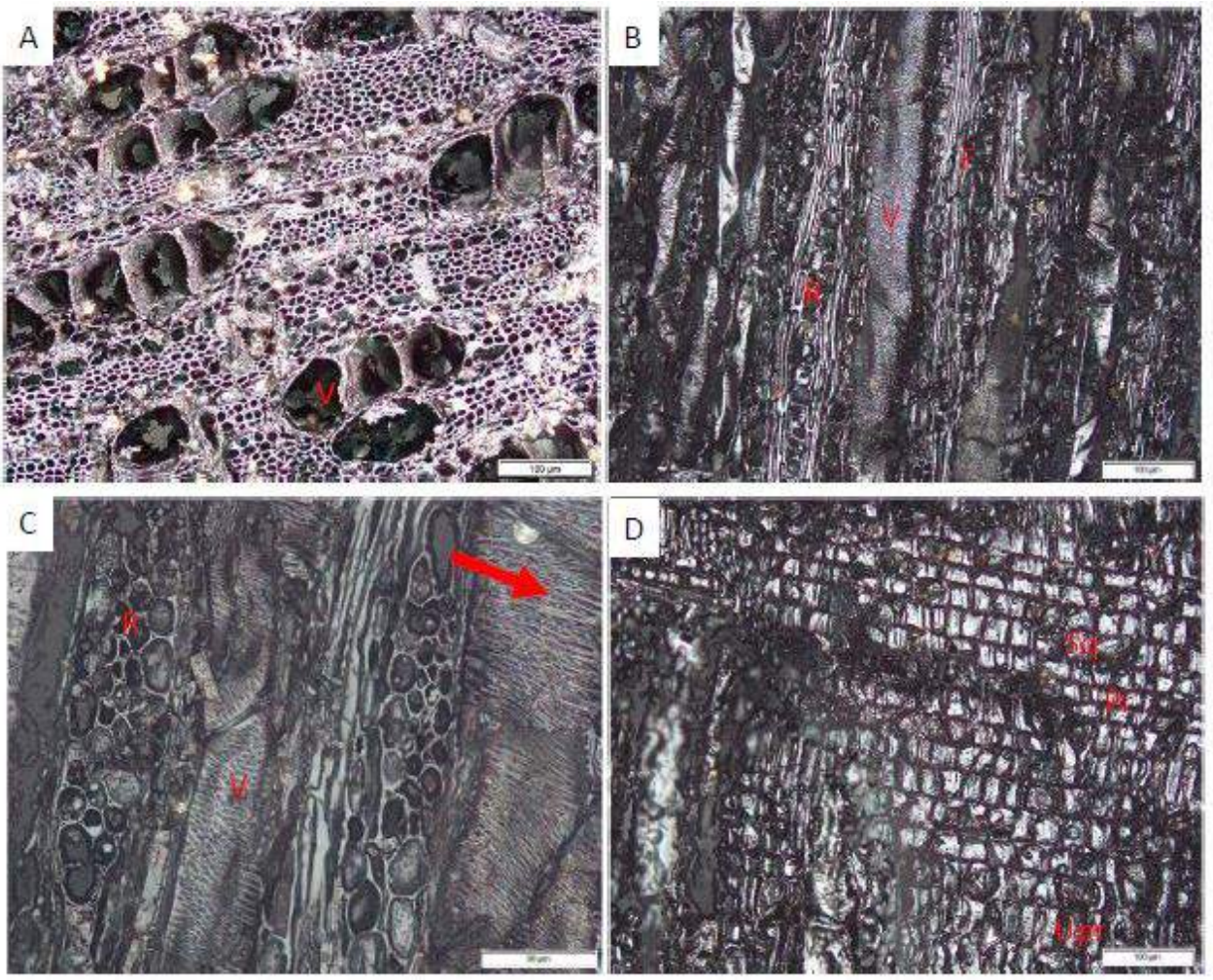


Fig. 5.15: Photomicrographs of *Halleria lucida* WW-4b-Q22P charcoal from stratum 4b of Excavation 1, Wonderwerk Cave. A) TS, vessels arranged in longer radial multiples of up to 5 surrounded by thin-walled fibres and no parenchyma. Scale bar= 100 µm. B) TLS, 1-5 seriate rays. Scale bar= 100 µm. C) 1-5 seriate rays and vessels have oblique perforation plates and the infrequent large intervessel pits indicated by an arrow. Scale bar= 50 µm. D) RLS, heterocellular rays with procumbent, square and upright cells mixed. Scale bar= 100 µm.

5.2.11 Unidentifiable

5.2.11.1 Type 16

Described sample: WW-4b-T21G

Illustration: Fig. 5.16

Total number of pieces identified: 1

Description: Growth rings are indistinct, and the wood is diffuse porous. The vessels are primarily solitary and round to oval with a diameter range of 30- 80 µm and a mean of 57.47 µm. On average, there are about 70 vessels per square millimetre. The vessels have a length range of 200-300 µm. The wood has simple, oblique perforation plates. The fibres in this piece are very thick-walled. The parenchyma is rare to scanty paratracheal and sometimes banded. Intervessel pits are alternate and minute, <4 µm wide. The rays are 1-2 seriate or up to 42 µm wide and 100-300 µm long. This wood has procumbent body ray cells with more than 4 rows of square marginal cells. There are 4-12 rays per square millimetre. This wood has radial cracks and crystals in the square ray cells.

Comparison: Specimen T21G has unique characteristics that set it apart from other charcoals. According to the analysis, the TS of this wood shares some similarities with the *Vachellia* species, such as the presence of large vessels and parenchyma bands. However, the TLS and RLS of the wood show a combination of procumbent and square ray cells, along with narrow 1-2 seriate rays, which are not typically found in *Vachellia* species. T21G does not match any of the woods identified in other strata or SVk 10 and adjacent biozones, so it remains unidentified.

Nonetheless, the well-preserved vessels of the specimen make it possible to make inferences about the vegetation type and climate through wood physiognomy.

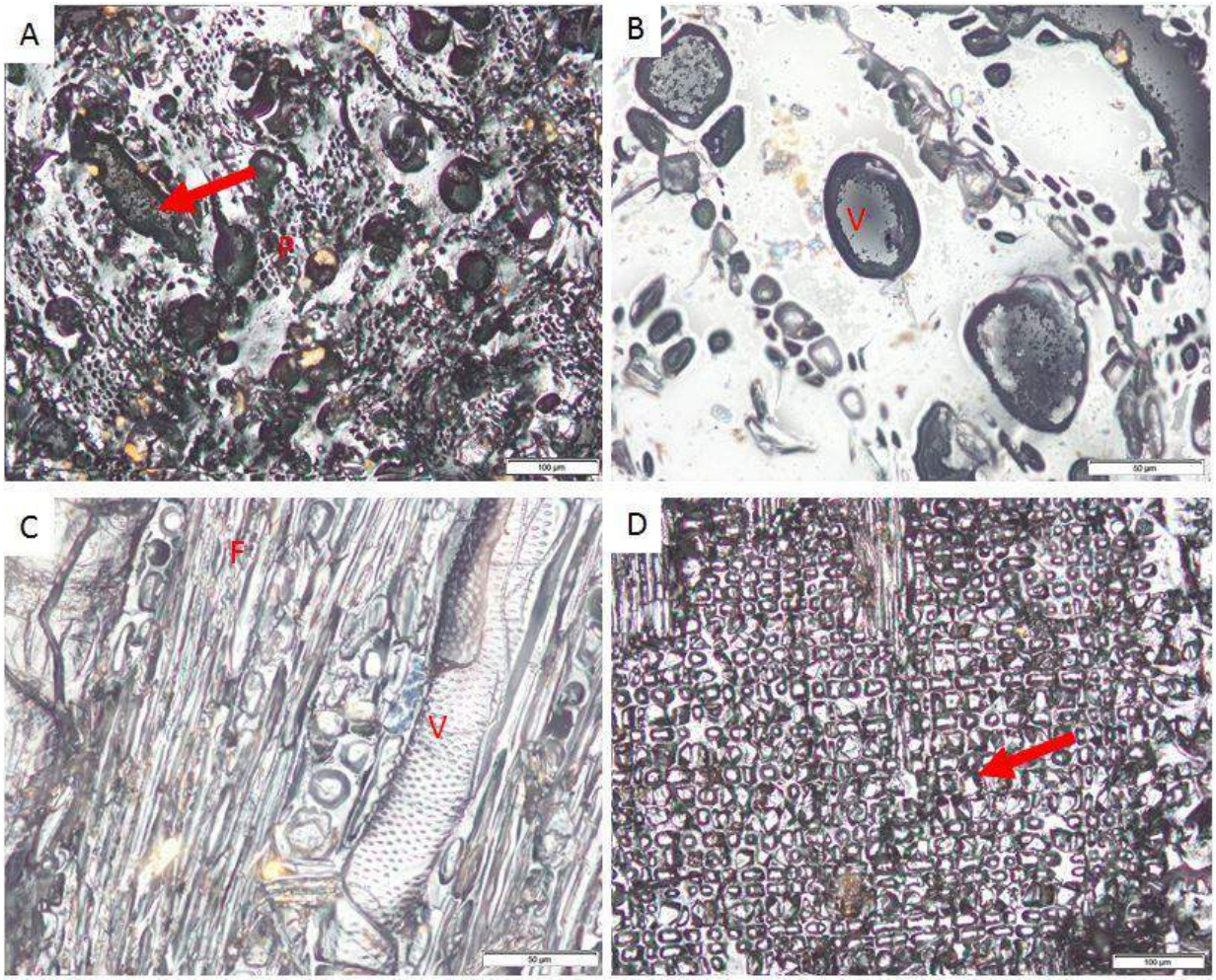


Fig. 5.16: Photomicrographs of Type 16 WW-4b-T21G charcoal from stratum 4b of Excavation 1, Wonderwerk Cave. A) TS, solitary vessels associated with scanty parenchyma. Note the parenchyma bands and radial cracks indicated by P and the arrow, respectively. Scale bar= 100 µm. B) TS, very thick fibre walls around the vessels. Scale bar= 50 µm. C) TLS, 1-2 seriate rays and minute, alternate intervessel pits. Scale bar= 50 µm. D) RLS, procumbent ray cells and square marginal cells containing crystals indicated by the crystals. Scale bar= 100 µm.

5.2.11.2 Type 17

Described sample: WW-4b-S21IIA

Illustration: Fig. 5.17

Total number of pieces identified: 2

Description: This wood is semi-ring porous, with indistinct growth rings. The vessels are solitary to clustered. The perforation plates are simple. The intervessel pits are alternate and medium, 7-10 µm wide. The vessels are narrow, with tangential diameters less than 50 µm (average 39.77 µm). The vessels are numerous, with an average of 108 vessels per square millimetre. The mean vessel length is less than 350 µm. The fibres are very thick-walled with distinctly bordered pits. The axial parenchyma is diffuse and confluent. There are also irregular, narrow parenchyma bands of 1-2 cells occurring 2-3 times per millimetre. The rays are 1-3-5 cells wide (~ 64 µm) with lengths up to 1 mm (average 550 µm). On average, there are 5 rays per axial millimetre. The wood contains procumbent body ray cells and approximately 4 rows of square marginal ray cells.

Comparison: This wood type is represented by two charcoals. These charcoals are similar to each other but different from other wood types studied by Bamford (2015b), House *et al.* (2022), and SVk 8, 9, and 10. Using Allott (2005) and the modern reference collection, *Iboza riparia* (BPI/20/605) and *Protea caffra* (BPI/20/641) woods share some features with S21IIA. For example, they all have narrow (< 50 µm), solitary vessels, sometimes forming clusters or tangential bands, and aliform/confluent parenchyma. Additionally, *Protea caffra* has procumbent and upright ray cells like S21IIA, but with much wider rays of 10± cells (> 100 µm wide). On the other hand, *Iboza riparia* lacks the procumbent ray cells present in S21IIA

and only has upright and square cells. These differences eliminate the two options. Hence, S21IIA remains unidentified.

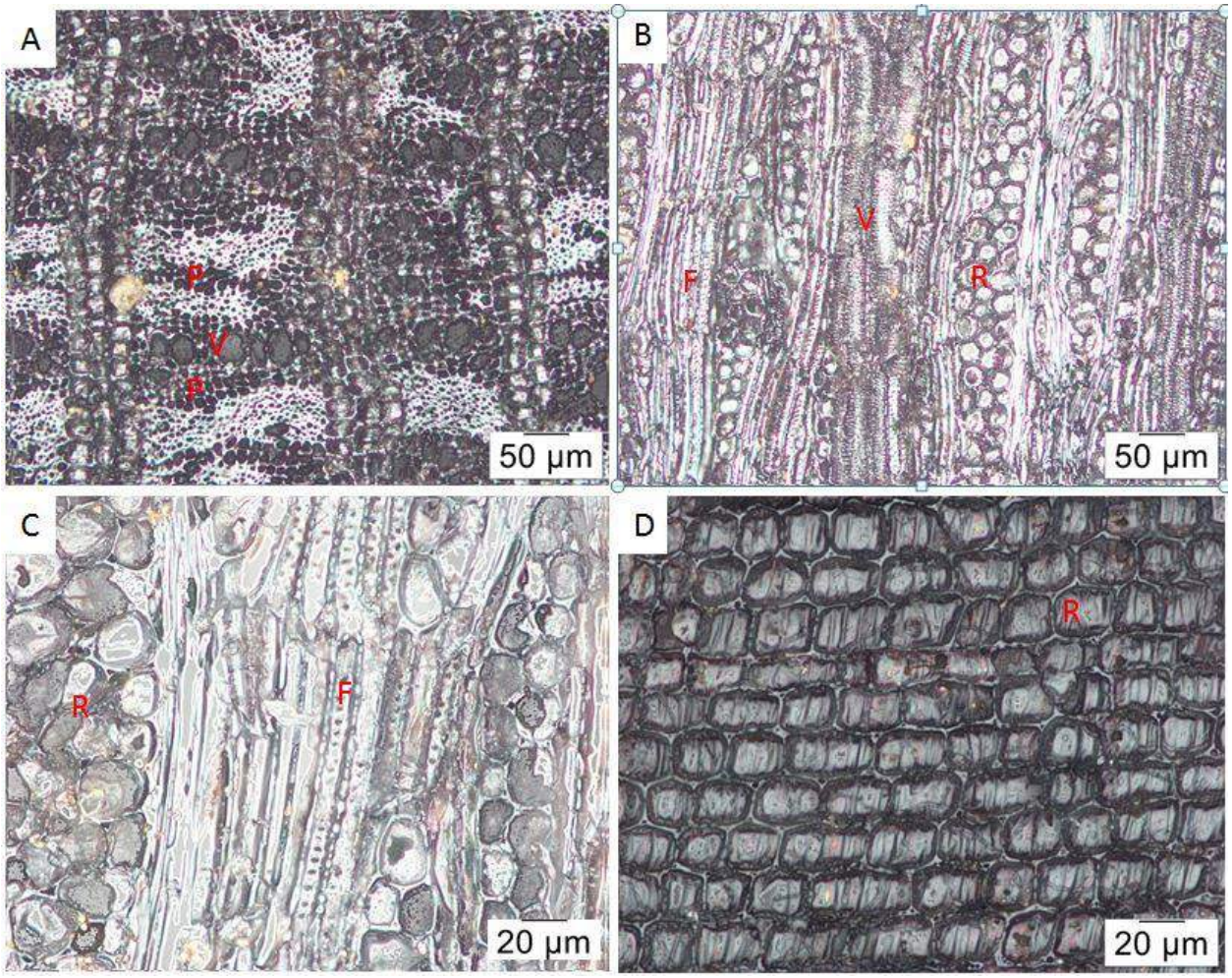


Fig. 5.17: Photomicrographs of Type 17 WW-4b-S21IIA charcoal from stratum 4b of Excavation 1, Wonderwerk Cave. A) TS, confluent parenchyma associated with the vessels, with some parenchyma forming narrow, irregular bands. Scale bar= 50 µm. B) TLS, 1-3 seriate rays. Scale bar= 50 µm. C) TLS, 1-3-5 seriate rays and fibres with bordered pits. Scale bar= 20 µm. D) RLS, procumbent ray cells and some square marginal cells. Scale bar= 20 µm.

5.2.11.3 Type 18

Described sample: WW-4b-Q24C

Illustration: Fig. 5.18

Total number of pieces identified: 27

Description: This wood has no clear growth rings and is diffuse-porous. Vessels have a radial arrangement of 1-3. Perforation plates are simple and oblique. The intervessel pits are alternate and small, 4-7 µm wide and similar to vessel-ray pits. The vessels are small, with a tangential diameter range of 20-50 µm and a mean of 31.63 µm. This wood has a high vessel frequency, about 183 vessels per square millimetre. The average vessel length is 205.02 µm. Fibres have very thick walls. Parenchyma is scanty paratracheal. The rays are narrow and have a width of 1-2 cells. The rays are 120-300 µm tall, mean of 194.8 µm. The rays are heterocellular with procumbent, upright and square cells mixed. On average, there are 5 rays per axial millimetre. The wood has many radial cracks.

Comparison: This wood type is similar to *the Tarchonanthus* wood type as it also has numerous narrow vessels, scanty parenchyma, narrow rays that are 1-2 seriate and small alternate intervessel pits. However, the RLS of the type 17 wood shows it has mixed rays with lots of upright and square ray cells, which are rare in *Tarchonanthus* wood. The features in this wood type do not match any of the woods of species from the SVk 8, 9 and 10 or the woods in Bamford (2015b) and House *et al.* (2022).

The search in the Insidewood database has produced three possible identifications for this wood: *Diospyros abyssinica, Strychnos decussata* and *S. mitis*. However, none of them matched Q24C because *D. abyssinica* has uniseriate rays, prismatic

crystals, and diffuse-in-aggregates parenchyma, while *S. decussata* and *S. mitis* have included phloem and prismatic crystals in the rays. These features are not found in Q24C. Therefore, Q24C cannot be classified as any of these species.

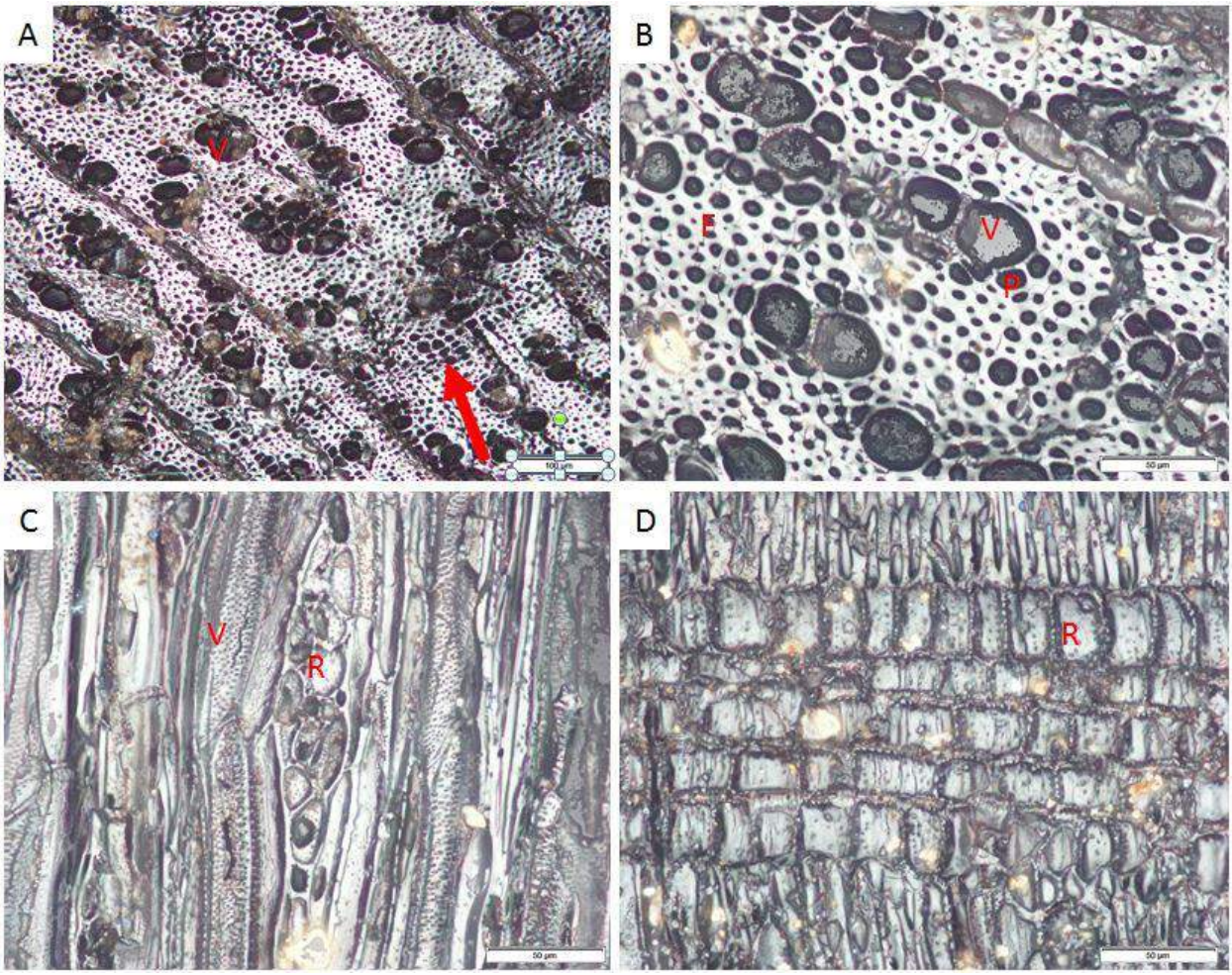


Fig. 5.18: Photomicrographs of Type 18 WW-4b-Q24C charcoal from stratum 4b of Excavation 1, Wonderwerk Cave. A) TS, radially flattened fibres indicated by the arrow, separating the early- and latewood. Scale bar= 100 µm. B) TS, scanty parenchyma associated with the vessels and the thin- to thick fibres. Scale bar= 50 µm. C) TLS, 1-2 seriate rays. Scale bar= 50 µm. D) RLS, procumbent body ray cells with square and upright marginal cells. Scale bar= 50 µm.

5.2.11.4 Type 19

Described sample: WW-4b-S25D

Illustration: Fig. 5.19

Total number of pieces identified: 1

Description: The wood is diffuse-porous, with indistinct growth rings. The vessels are arranged in 1-3 radial multiples, sometimes clusters of up to 4. The solitary vessels are angular. Perforation plates are simple and oblique. Intervessel pits are alternate and medium, about 7- 10 µm wide. The vessel tangential diameters range from 25-50 µm, with a mean of 49.35 µm, with lengths up to 350 µm. The vessels reflect light, which makes it difficult to count the vessels. However, there are more than 100 vessels per square millimetre. Fibres are non-septate and thin-walled. The axial parenchyma is apotracheal diffuse and paratracheal scanty to vasicentric/aliform. The rays are 1-3 cells wide, about 35-90 µm wide (average 60.25 µm). The rays are up to 350 µm tall, averaging 220 µm. The body ray cells are mostly procumbent with 1-3 rows of square marginal cells. On average, there are 7 vessels per square millimetre.

Comparison: This wood type is different from wood types from this assemblage or any of the woods described in Bamford (2015b) and House *et al.* (2022). It is similar to some Asteraceae woods (see *T. camphoratus*), particularly *Brachylaena discolor*. The reference charcoal of this species (BPI/20/721) shows it has thin-thick fibre walls, scanty to vasicentric/aliform parenchyma, 1-3 cells wide rays, predominantly procumbent ray cells with a few rows of square cells as well as small (<50 µm) and numerous vessels (~100) arranged in short radial multiples and clusters. However, this wood has storied rays and the procumbent cells contain crystals, which were not found in this specimen. Because of this, S25D could not be accurately identified as *B. discolor* or any other *Brachylaena* species.

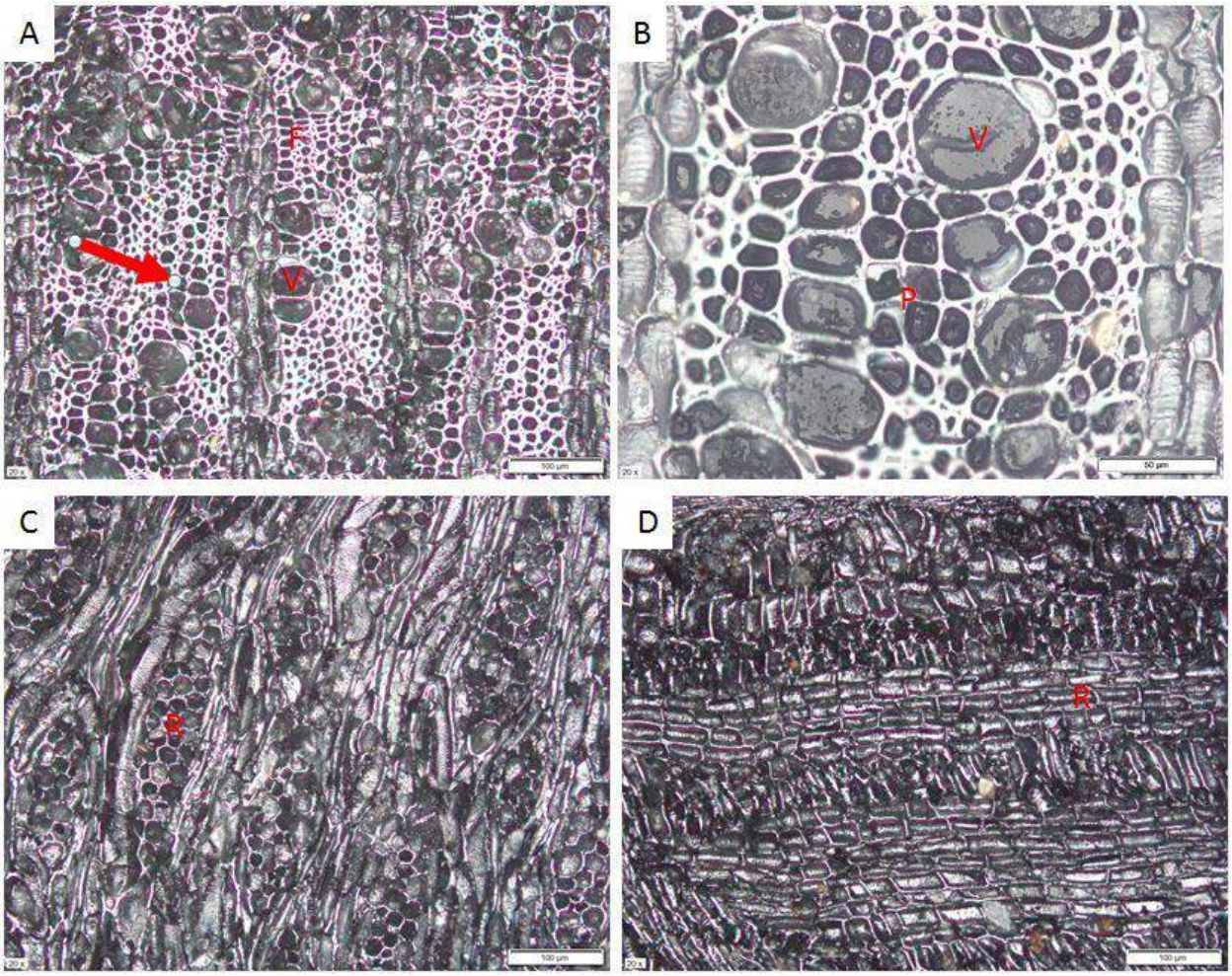


Fig. 5.19: Photomicrographs of Type 19 WW-4b-S21IIH charcoal from stratum 4b of Excavation 1, Wonderwerk Cave. A) TS, parenchyma is scanty, vasicentric and aliform. Scale bar= 100 µm. B) TS, vasicentric and aliform parenchyma shown at higher magnification. Scale bar= 50 µm. C) TLS, 1-3 seriate rays. Scale bar= 100 µm. D) RLS, predominantly procumbent ray cells and the square cells on the margins. Scale bar= 100 µm.

Table 5.1: Summary of the charcoal types from stratum 4b, Excavation 1, Wonderwerk Cave.

Type	Specimen	Taxa	Porosity	Vessels					Parenchyma		Rays				Fibre walls	Other	Illustration
				Average diam (µm)	# /mm^2	Perf. Plates	Arr.	Pits (arr, size in µm)	apotracheal	paratracheal	Width (in cells)	Height (µm)	#/ mm	Cells			
Type 1	WW-4b-R25-G	*Ozoroa paniculosa*	diffuse	48.15	39	simple	1-4 rm	alt, <5	-	scanty-vasicentric	1-3c	100-300	4-12	sq, upr	thin	crystals in sq ray cells	Fig. 5.1
Type 2	WW-4b-Q22K	*Searsia lancea*	diffuse	58.39	30	simple, obl	1-3 rm	alt, 4-7, sometimes >10	-	scanty	1-3c	100-500	>12	pr, upr, sq		radial canals	Fig. 5.2
Type 3	WW-4b-S25IA	*Heteromorpha arborescens*	semi-ring	56.94	91	simple, obl/ hor	<10 rm, clusters	alt, <4	-	scanty	1-3c, sometimes 5c	300-500	4-12	pr, upr, sq	thin-thick		Fig. 5.3
Type 4	WW-4b-Q22B	*Tarchonanthus camphoratus*	diffuse	36.82	94	simple	1-3 rm, clusters	alt, <4	-	scanty	1-2c	100-250	4-12	pr	thin-thick		Fig. 5.4
Type 5	WW-4b-S23E	*Tarchonanthus parvicapitulatus*	diffuse	36.0	172	simple, obl	<5 rm	alt, <4	-	scanty	1-2c	100-300	4-12	pr	thin-thick		Fig. 5.5
Type 6	WW-4b-Q22IN	*Ehretia* sp.	diffuse	73.14	<20	simple	1-2 rm	alt, 4-7	narrow bands	aliform, confluent	4-8c	300-600	4-12	pr, (sq)	thick		Fig. 5.6
Type 7	WW-4b-Q22N	*Commiphora schimperi*	diffuse	39.72	24	simple, obl	1-2 rm	alt, > 10	-	-	1-2c	200-400	>12	pr, upr, sq	thin	crystals in sq & upr ray cells	Fig. 5.7
Type 8	WW-4b-R21B	*Olea europaea* subsp. *africana*	diffuse	43.53	76	simple, obl	1-3 rm	alt, <4	-	vasicentric	1-2c	200-300	4-12	pr, upr	thick		Fig. 5.8
Type 9	WW-4b-Q22IL	*Olinia ventosa*	diffuse	39.53	140	simple, obl, hor	1-4 rm	alt, <4	narrow bands	scanty	1-3c	200-300	4-12	pr, upr, sq	thick	1=2=3	Fig. 5.9
Type 10	WW-4b-S21IIH	*Senegalia caffra*	diffuse	169.51	7	simple, hor & obl	sol	alt, 4-7	-	vasicentric, aliform	1-6c	300-600	4-12	pr	thick	vestured pits	Fig. 5.10
Type 10	WW-4b-Q24G	*Vachellia* cf. *tortilis*	diffuse	<100	32	simple, hor	sol, clusters	alt, 7-10 & vestured	banded	vasicentric, lozenge-aliform & confluent	1-4c	300-400	4-12	pr	thick		Fig. 5. 11
Type 11	WW-4b-S21IIIK	*Vachellia* cf. *karroo*	diffuse	±50	25	simple, hor	sol	alt, 4-10 & vestured	-	vasicentric, aliform& confluent	1-5c	200-500	4-12	pr	thick		Fig. 5. 12
Type 12	WW-4b-S25ID	*Berchemia* cf. *zeyheri*	diffuse	56.34	22	simple, obl	1-3 rm	alt, 4-7	-	scanty	1-3c	200-400	>12	pr, upr	thin-thick		Fig. 5.13
Type 13	WW-4b-R24D	*Ziziphus mucronata*	diffuse	72.85	42	simple, obl	1-2 rm	alt, 4-7	-	vasicentric	1c	200-400	>12	upr, sq	thin-thick	crystals in sq & upr ray cells	Fig. 5.14
Type 14	WW-4b-Q22P	*Halleria lucida*	diffuse	91.12	53	simple, obl	<4 rm	alt, <4, sometimes >10	-	-	1-5c	200	700	pr, upr, sq	thin	crystals in sq & upr cells	Fig. 5.15
Type 15	WW-4b-T21G	Unidentified	diffuse	57.47	70	simple, obl	sol	alt, 4-7	banded	rare-scanty	1-2c	100-400	4-12	pr, sq	thick		Fig. 5.16

Type 16	WW-4b-S21IIA	Unidentified	semi-ring	39.77	108	simple	sol, clusters, tang bands	alt, 7-10	narrow bands	aliform, confluent	1-5c	200-1000	4-12	pr, sq	thick		Fig. 5.17
Type 17	WW-4b-Q24C	Unidentified	diffuse	31.63	183	simple, obl	1-3 rm	alt, 4-7	-	scanty	1-2c	100-300	4-12	pr, upr, sq	thick		Fig. 5.18
Type 19	WW-S25D	Unidentified	diffuse	49.35	>100	simple, obl	1-3 rm	alt, 7-10	diffuse	scanty	1-3c	100-350	4-7	pr, sq	thin		Fig. 5.19

obl= oblique; hor=horizontal; rm= radial multiples; sol= solitary; alt= alternate; c= cells; sq= square; upr= upright; pr= procumbent

5.3 Distribution of the species across the grid squares

The charcoal was scattered on the floor of the cave during the deposition of stratum 4b and this is reflected by the occurrence of charcoal in different packets/squares. A list of the identified charcoal fragments and their frequency across the squares is presented in Table 5.2. The charcoal taxa are arranged alphabetically. A total of 106 charcoals could be identified. Whereas, 98 could not be identified. Some were not distinctive enough to be classified into types and are labelled as “Other” in the table below.

The charcoal analysed in this dissertation originates from several squares, namely Q22, Q23, Q24, R21, R25, S21, S23, S24, S25, T21, T23, and T24. Out of these squares, Q22, S21, Q23, R25, and S25 had the highest number of fragments, listed in order. On the other hand, squares S24, T23, and T24 had the lowest number of charcoals available for analysis, therefore, they had the lowest number of fragments analysed. *Heteromorpha arborescens followed by Tarchonanthus parvicapitutalus and Tarchonanthus camphoratus* were the most frequently identified species, while *Berchemia* cf. *zeyheri, Ehretia* sp., *Halleria lucida, Olinia ventosa, Senegalia caffra, Vachellia* cf. *karroo* and *Ziziphus mucronata* were the least identified species as they are each represented by one charcoal fragment.

Table 5.2: Species distribution in the different grid squares of stratum 4b.

Squares	**Q22**	**Q23**	**Q24**	**R21**	**R24**	**R25**	**S21**	**S23**	**S24**	**S25**	**T21**	**T23**	**T24**	**Total**
***Berchemia* cf. *zeyheri*.**										1				1
Commiphora schimperi	2							1			4			7

***Ehretia* sp.**							1							1
Halleria lucida	1													1
Heteromorpha arborescens		4	1		4	2		2	3	9		2	2	28
Olea europaea* subsp. *africana				1		2	3	2		1	1			10
Olinia ventosa	1													1
Ozoroa paniculosa	2	2	1			1	2				2			10
Searsia lancea	2	1		1			1							5
Senegalia caffra							1							1
Tarchonanthus camphoratus	8	1					4	2			1			16
Tarchonanthus parvicapitutalus	5	3		1			3	4			2		1	19
Vachellia* cf. *tortilis	2		1								1			4
Vachellia* cf. *karroo							1							1
Ziziphus mucronata					1									1
Type 16											1			1
Type 17	1						1							2
Type 18	3	5	3	4			4	3	1	2	2			27
Type 19										3				3
Other	2	4	7	5	8	13	1	0	6	1	0	9	8	64
Total identified	23	11	3	3	5	5	15	11	3	11	11	2	3	106
Unidentifiable	6	9	10	9	8	13	7	3	7	6	3	9	8	98
Total analysed	29	20	13	12	13	18	22	14	10	17	14	11	11	204

5.4 Ecology of the taxa

At present, the identified taxa are found growing in different areas in southern Africa, including all the provinces of South Africa as well as Botswana, Namibia, Lesotho and Swaziland. They are also adapted to different ecoregions structured by rainfall and climate, i.e., bushveld, forest and grassland. Table 5.3 shows the description, geographic distribution and habitat of the modern analogs. The taxa are arranged alphabetically (Palmer and Pitman, 1972; Retief and van Wyk, 2001; Germishuizen and Meyer, 2003; Herman, 2002; van Wyk and van Wyk, 2013).

The different properties of taxa make them important to past and modern human societies. They have medicinal uses, produce edible fruits and gum, and provide strong wood for furniture, utensils, weapons, and fence posts. They also play a vital role in ecology, providing food and shelter for insects, birds, and browsers such as elephants, rhinoceroses, and antelopes. The modern uses of the taxa by humans and animals are presented in Table 5.3, the identified taxa appear alphabetically (Palmer and Pitman, 1972; Retief and van Wyk, 2001; Germishuizen and Meyer, 2003; Herman, 2002; van Wyk and van Wyk, 2013).

Table 5.3: The description, ecoregion and geographical distribution of the modern taxa (Palmer and Pitman, 1972; Coates Palgrave and Coates Palgrave, 1983; Retief and van Wyk, 2001; Germishuizen and Meyer, 2003; Herman, 2002; van Wyk and van Wyk, 2013).

Taxa	**Description**	**Habitat**	**Geographical distribution**	**Uses of modern woods (Coates Palgrave and Coates Palgrave, 1983; van Wyk and van Wyk, 2013)**
Berchemia zeyheri **(Rhamnaceae)**	small or medium-sized deciduous tree	bushveld; rocky soils and stream banks	B, LIM, NW, G, M, S and KZN	Fruits: edible Roots: healing properties Wood: good quality timber Bark: poisonous Leaves: browsed by game and stock
Commiphora schimperi **(Burseraceae)**	shrub or small deciduous tree	hot and arid bushveld; sandy soils	B, LIM, NW, S and KZN	Bark: medicinal uses Twigs: used to start a fire by friction leaves, roots and bark: food for elephants and game.
Ehretia **species (Boraginaceae**)	shrubs or small trees	bushveld, wooded grasslands, forests and savanna; sandy soils, hillsides and rocky soils in the bushveld	N, B, NW, FS, NC, LIM, M, S, KZN, NW and G	Roots of most *Ehretia* species have medicinal properties stock and game often browse the leaves of most *Ehretia* species
Halleria lucida **(Scrophulariaceae)**	shrub or small evergreen tree	forests, forested ravines, grassland and bushveld; along streams or rocky soils in grasslands	N, B, NW, G, M, S, FS, KZN, L, NC, WC and EC	Fruits: edible and have medicinal uses Different parts of this plant are used in different cultural practices. Flowers: provide nectar for birds Flowers: provide nectar for birds
Heteromorpha arborescens **(Apiaceae)**	shrub to small or medium-sized deciduous tree	grassland, bushveld and forests, forest margins and wooded ravines; hillsides and rocky outcrops	B, LIM, NW, G, M, S, FS, KZN, L, NC, WC and EC	Fruits: edible and have aromatic oils used as perfume Various parts have different medicinal properties
Olea europaea **subsp. *africana*** **(Oleaceae)**	small to medium evergreen tree (drought- and frost-tolerant)	wide range of habitats; rocky hillsides and stream banks	N, B, LIM, NW, G, M, S, FS, KZN, L, NC, WC and EC	Wood: used to make furniture and ornaments and produces pleasant-smelling fire Fruits: edible Leaves and bark: medicinal uses and often browsed by

				game and stock
Olinia ventosa **(Oliniaceae)**	medium to tall evergreen tree	forest, coastal scrubs; low altitude areas (15-915 m), rocky hillsides	WC and EC	Wood: tough often used for heavy work such as fencing Fruit: eaten by birds
Ozoroa paniculosa **(Anacardiaceae)**	shrub or small to medium-sized deciduous tree	hot bushveld; rocky hillsides	N, B, LIM, NW, G, M, S, FS and KZN	Fruits: used as a dye for leather Bark and leaves: browsed by rhinos and elephants
Searsia lancea **(Anacardiaceae)**	small to medium-sized evergreen tree (drought- and frost-resistant)	wide range of habitats, open woodlands; along riverbanks, areas with underground water and calcareous soils	N, B, LIM, NW, G, M, FS, L, NC, EC and WC	Fruit: edible, also used for brewing beer and often eaten by birds and poultry Wood: tough used for fence poles, pick handles and wagon parts Branchlets: for making bows and pipe bowls, Bark: tanning
Senegalia caffra	small to medium-sized deciduous tree (drought- and frost-resistant)	bushveld, grassland, coastal scrubs; rocky ridges	B, LIM, NW, G, M, S, FS, KZN, WC and EC	Wood: heavy and used for fencing poles and is good for fires Bark & leaves: medicinal and leaves are often eaten by stock, although poisonous
Tarchonanthus camphoratus **(Asteraceae)**	shrub or small semi-deciduous to evergreen tree (drought-resistant)	semi-deserts, bushvelds, grasslands, savanna; rocky hillsides, riverbanks and sandy soils	N, B, LIM, NW, G, M, FS and NC	Leaves: medicinal uses, used as perfume for hair (camphor scent) and often eaten by game and stock Wood: used for making boats, furniture, musical instruments, ornaments and produces good fire
Tarchonanthus parvicapitutalus **(Asteraceae)**	shrub or small semi-deciduous to evergreen tree	forest and bushveld; forest valleys and bushveld mountain slopes, rocky ridges and riverbanks	N, LIM, NW, G, M, S, KZN and EC	Leaves: medicinal uses, also used as perfume (camphor scent) and often eaten by game and stock Wood: for making ornaments
Vachellia tortilis **(Fabaceae)**	Small or medium-sized tree (drought-resistant)	bushveld and sweet veld; red Kalahari sand, dry soils	N, B, LIM, NW, G, M, S, FS and KZN	Bark: medicinal properties Wood: produces good fire Gum: edible Farmers use the plant as an indicator of sweet veld.

***Vachellia karroo* (Fabaceae)**	shrub or medium tree (frost and drought-resistant)	bushveld and grasslands; along streams banks and near underground water in arid areas	N, B, LIM, NW, G, M, S, FS, KZN, NC, WC and EC	Gum: sweet and edible Wood: making furniture, fire and fence posts Thorns: needles Bark: used for tanning and making medicine and strong ropes. Various parts of the tree: food for game, birds and caterpillars The plant used as an indicator of surface and underground water and sweet veld.
***Ziziphus mucronata* (Rhamnaceae)**	shrub or medium-sized tree (drought-resistant)	open scrub, grassveld, bushveld, open woodland, forest margins; rocky hills, stream banks and near underground water	N, B, LIM, NW, G, M, S, FS, KZN, NC and EC	Fruit: edible Wood: produces good fuel and is used to make bows, tool handles, spoons and kraals Sap: used for bow poison by the San Leaves: browsed by game, stock and butterfly larva The plant has medicinal and cultural uses and is often used as an indicator of underground water.

N= Namibia; B= Botswana; LIM= Limpopo Province; NW= North West Province; G= Gauteng Province; M= Mpumalanga Province; S= Swaziland; FS= Free State Province; KZN= KwaZulu-Natal Province; L= Lesotho; NC= Northern Cape Province; WC= Western Cape Province; EC= Eastern Cape Province

5.5 Wonderwerk charcoal record

The study added 12 species to the previously identified taxa list for stratum 4b of the Wonderwerk Cave (Table 5.4). *Berchemia* cf. *zeyheri, Senegalia caffra, Tarchonanthus camphoratus, Tarchonanthus parvicapitutalus, Vachellia* cf. *karroo* and *Vachellia* cf. *tortilis* were newly identified in Wonderwerk Cave.

Table 5.4: An updated record of the taxa identified from stratum 4b of the Wonderwerk Cave.

Taxa	**Stratum 4b (House *et al.*, 2022)**	**Stratum 4b (This study)**
Berchemia discolor	X	
Berchemia* cf. *zeyheri		X
Commiphora schimperi	X	X
Diospyros austro-africana	X	
***Ehretia* sp.**		X
Halleria lucida		X
Heteromorpha arborescens		X
Olea europaea* subsp. *africana	X	X
Olinia ventosa		X
Ozoroa paniculosa		X
Searsia lancea	X	X
Senegalia caffra		X
Tarchonanthus camphoratus		X
Tarchonanthus parvicapitutalus		X
Vachellia* cf. *karroo		X
Vachellia* cf. *tortilis		X
Vitex mombassae	X	
Ziziphus mucronata		X

5.6 Physiognomy

The wood anatomy, specifically the vessel diameter, frequency and distribution, were used to estimate the hydraulic efficiency of the woody species within the Wonderwerk Cave, layer 4b charcoal assemblage. This allows an estimation of the water availability (high or low water available) and the possible vegetation form (shrubs or trees) growing around the Wonderwerk Cave at 6.9 ka BP.

A total of 115 specimens were unsuitable for this method. These specimens were either too small to enable counting vessels from at least 10 points, or there was difficulty in viewing and measuring the vessels as they were either distorted or the light reflected by the vessels made it challenging to see the vessel walls for measuring. About 43 of the woods had extreme radial cracking, which made it impossible to measure and count the vessels. The anatomy of 88 archaeological wood charcoals was analysed, and the results are provided in Table 5.5 below. The Vulnerability indices (VI) and Conductivity capacity (CC) of all 88 specimens were calculated. However, the Mesomorphy indices were not calculated for all specimens due to the inability to measure vessel lengths in some specimens.

Table 5.5: The physiognomy of the charcoal (Vulnerability index, VI; Conductivity capacity, CC; Mesomorphy index, MI).

Species	**Specimen**	**Diameter (µm)**	**Frequency/ mm^2**	**Length (µm)**	**VI**	**CC**	**MI**
Berchemia* cf. *zeyheri	**S25ID**	56.34	23		2.45	14.48	
Commiphora schimperi	**Q22N**	39.72	24	178.56	1.65	3.73	295.52
Commiphora schimperi	**S23C**	30.21	33		0.92	1.72	
Halleria lucida	**Q22P**	91.12	53	223.59	1.72	228.4	384.4

Heteromorpha arborescens	**Q23F**	44.55	66		0.68	16.25	
Heteromorpha arborescens	**Q23I**	43.67	86		0.51	19.55	
Heteromorpha arborescens	**R24A**	29.84	91	136.04	0.33	4.51	44.61
Heteromorpha arborescens	**R24B**	25	89	183.4	0.28	2.17	51.52
Heteromorpha arborescens	**R24H**	36.12	80		0.45	8.51	
Heteromorpha arborescens	**R24I**	45.37	122		0.37	32.31	
Heteromorpha arborescens	**S23L**	36.09	74	179.86	0.49	7.85	87.72
Heteromorpha arborescens	**S23IIIB**	37.14	65	306.08	0.57	7.73	174.9
Heteromorpha arborescens	**S24B**	51.04	56	244.08	0.91	23.75	222.5
Heteromorpha arborescens	**S24IB**	41.35	63	235.56	0.66	11.51	154.6
Heteromorpha arborescens	**S24IC**	40.78	190		0.22	32.84	
Heteromorpha arborescens	**S25A**	33.7	123		0.27	9.92	
Heteromorpha arborescens	**S25C**	49.16	94		0.52	34.31	
Heteromorpha arborescens	**S25IA**	56.94	91	220.14	0.63	59.78	137.75
Heteromorpha	**S25IB**	42.02	117		0.36	22.8	

arborescens							
Heteromorpha arborescens	**S25IF**	52.02	66		0.79	30.21	
Heteromorpha arborescens	**S25IG**	40.06	89		0.45	14.33	
Heteromorpha arborescens	**T23G**	38.73	260		0.15	36.56	
Heteromorpha arborescens	**T24A**	45.09	107		0.42	27.64	
Heteromorpha arborescens	**T24B**	47.93	100		0.48	32.98	
Olea europaea **subsp. *africana***	**R21B**	43.53	76	258.58	0.57	17.05	148.11
Olea europaea **subsp. *africana***	**S23D**	40.29	94	251.41	0.43	15.48	107.8
Olea europaea **subsp. *africana***	**S23F**	34.42	91	188.76	0.38	7.98	71.4
Olea europaea **subsp. *africana***	**S25IE**	46.92	94	183.18	0.50	28.47	91.43
Ozoroa paniculosa	**Q24E**	42.05	101	226.98	0.42	19.74	94.5
Ozoroa paniculosa	**S21IIIG**	59.98	18	242.79	3.33	14.56	809
Ozoroa paniculosa	**S21IIIM**	40.1	96	190.99	0.43	15.51	79.78
Ozoroa paniculosa	**R25G**	48.15	61	262.01	0.79	20.49	206.8
Ozoroa paniculosa	**Q22IA**	49.58	39		1.27	14.73	

Searsia lancea	**Q22K**	59.39	42		1.97	28.48	
Searsia lancea	**Q22IB**	52.09	18		2.89	8.28	
Tarchonanthus camphoratus	**Q22B**	36.82	94	256.37	0.39	10.79	100.42
Tarchonanthus camphoratus	**S21(RS)A**	37.69	56	148.56	0.67	7.06	99.99
Tarchonanthus camphoratus	**S21IIIN**	44.36	127		0.35	30.74	
Tarchonanthus camphoratus	**T21A**	44.27	129	210.01	0.34	30.97	72.07
Tarchonanthus parvicapitutalus	**Q23III**	35.21	209	192.42	0.17	20.08	32.42
Tarchonanthus parvicapitutalus	**S23G**	39.65	199	225.99	0.20	30.74	45.03
Tarchonanthus parvicapitutalus	**S23I**	38.4	256	259.36	0.15	34.79	38.9
Vachellia* cf. *karroo	**S21IIIK**	44.55	16	139.38	2.78	3.94	388.1
Vachellia* cf. *tortilis	**T21E**	40.33	56		0.72	9.26	
Ziziphus mucronata	**R24D**	72.85	42	282.89	1.73	73.93	490.70
	Q22F	38	232	224.06	0.16	30.23	36.7
	Q22G	26.72	301	148.22	0.09	9.59	13.16
	Q22L	34.34	201		0.09	1.26	
	Q22O	38.43	164	249.81	0.23	22.36	58.54
	Q22Q	35.53	171		0.21	17.03	
	Q23D	45.06	227	246.48	0.20	58.49	48.93
	Q23G	36.85	86		0.43	9.911	

	Q23J	32.5	248	237.83	0.13	17.29	31.17
	Q23K	56.78	91	220.06	0.62	59.12	137.3
	Q23IIA	41.01	265	215.28	0.16	46.85	33.32
	Q23IIC	37.9	169		0.22	21.79	
	Q23IIE	34.47	197		0.18	17.38	
	Q23IIH	31.13	274	158.56	0.11	16.08	18.01
	Q24A	31.92	213		0.15	13.82	
	Q24C	31.63	183	205.02	0.17	11.45	35.44
	Q24D	37.96	190	212.35	0.2	24.66	42.43
	Q24F	56.27	42		1.34	26.32	
	R21D	37.7	124	254.64	0.30	15.66	77.42
	R21O	34.94	131	176.2	0.27	12.2	47
	R21(23)D	32.51	190		0.17	13.26	
	R21(23)E	40.69	159		0.26	27.24	
	R21(23)F	43.75	174	173	0.25	39.84	43.5
	R21(RS)B	32.8	246	194.93	0.13	17.8	25.99
	R21(RS)D	28.77	170	197.39	0.17	7.279	33.41
	S21(RS)B	42.59	131	226.8	0.33	26.94	73.74
	S21(RS)E	32.49	228	257.22	0.14	15.88	36.65
	S21IIA	39.77	108		0.368	16.89	
	S21IIE	69.43	57		1.22	82.78	
	S21IIF	32.49	114	214.7	0.285	7.94	61.19
	S21IIG	38.25	89	185.47	0.43	11.91	79.71
	S21IIIA	57.55	54	207.59	1.07	37.02	221.2
	S21IIIF	60.54	13		4.66	10.91	
	S23B	36.19	321	285.42	0.11	34.41	32.18
	S24C	33.91	138	224.19	0.25	11.4	55.09
	T21C	35.13	162	168.88	0.22	15.42	36.62
	T21F	37.3	185	231.5	0.20	22.38	46.68

	T21G	57.47	70		0.82	47.72	
	T23A	33.11	105	248.44	0.07	36.13	17.1
	T24C	49.7	56		0.89	21.35	
	R25A	50.06	91	223.86	0.55	35.72	123.1
	R25C	47.88	145	223.97	0.33	47.63	73.96
	R25D	42.25	174	198.9	0.243	34.65	48.3
	R25F	49.42	122		0.41	45.48	
Average		42.40	117.65	215.81	0.64	24.45	118.59

The vessel diameters in this sample ranged from 25 µm (unidentified species) to 92.12 µm (*Halleria lucida*). The average vessel diameter was 42.40 µm, and the average length was 215.81 µm. The average vessel frequency per square millimetre was 117.65 µm, with a range of 13-260 vessels. The average vulnerability index, conductivity capacity, and mesomorphy index were 0.64, 24.45, and 118.59, respectively. The ranges for the: vulnerability index is 0.09-3.33, conductivity capacity is 1.26-228.4 and mesomorphy index is 17.1-809.

5.7 Summary of the chapter

This chapter details the taxonomy of the charcoals of stratum 4b and the diagnostic features used for identification. Samples were compared to different publications and modern charcoal for identification. The geographical distribution, appearance, habitat and uses of the modern analogs are detailed. Vessels were used to calculate conductivity capacity, mesomorphy, and vulnerability indices, and the results were provided. Additionally, an updated list of layer 4b charcoal species is included.

CHAPTER SIX

Discussion

6.1 Taxonomic implication of Mid-Holocene Wonderwerk Cave environment

The lower stratum of Excavation 1 revealed evidence of burnt plant and bone material, indicating that humans have been using fire in the cave for over a million years (Berna *et al.,* 2012). Hence, charcoal remains discovered in the Wonderwerk Cave, Excavation 1, stratum 4b are the remnants of wood that were collected and burnt to be used as fuel by humans who inhabited the cave around 6.9 to 5.9 ka. The principle of least effort suggests that people tend to minimize the effort put into collecting firewood by choosing to collect from nearby woodlands (Shackleton and Prins, 1992). This practice is true for modern people in Bushbuckridge today, where individuals prefer to collect firewood from nearby woodlands and travel further only when necessary (Matsika *et al.,* 2013; Finlay and Twine, 2018). Therefore, the archaeological charcoal from Wonderwerk Cave offer valuable insights into the vegetation that was growing in the immediate environment during the Holocene.

It is suggested by the principle of least effort that taxa were collected in proportions similar to their abundance in the environment (Shackleton and Prins, 1992; Braadbaart and Poole, 2008). However, this may not be accurate due to the fact that in the past, humans heavily relied on burning wood as a source of fuel and had acquired knowledge about the properties of different types of woody plants in their surroundings (Lennox *et al.,* 2015). This led to the collection of specific species of wood for tasks such as cooking, lighting, medicine, and cultural practices. Additionally, the availability of wood in the immediate environment is influenced by factors such as seasonality, deadwood abundance, and occurrence of wood along daily routes (Gelabert *et al.,* 2011), which further challenges the accuracy of the principle of least effort in reflecting species abundance.

Moreover, taphonomical influences occurring between combustion and laboratory analysis can also impact the representativeness of the collection (Braadbaart and Poole, 2008). Therefore, the frequency of the species listed in Table 5.2 cannot be used to determine their abundance in the immediate environment, but it can provide a good representation of the taxa occurring in the immediate environment. The charcoal deposits from Wonderwerk Cave are considered "synthetic deposits," scattered across an archaeological layer (Table 5.2), and result from the long-term deposition and mixing of charcoal from domestic fires and specialized fires. Thus, this assemblage is suitable for environmental reconstruction as it contains wood charcoal from domestic and specific fires and collection trips from various species (Chabal, 1997; Théry-Parisot *et al.,* 2010).

The assemblage had at least 19 types of charcoal, out of which only 15 could be identified to their respective genus and species, as shown in Table 5.1. The identified charcoal include *Berchemia* cf. *zeyheri, Commiphora schimperi, Halleria lucida, Heteromorpha arborescens, Olea europaea subsp. africana, Olinia ventosa, Ozoroa paniculosa, Searsia lancea, Senegalia caffra, Tarchonanthus camphoratus, Tarchonanthus parvicapitulatus, Vachellia* cf. *karroo, Vachellia* cf. *tortilis, Ziziphus mucronata,* and a *Ehretia*-type species. Four charcoal types were well-preserved and distinct enough to be classified as separate types but not identifiable. This is because their anatomy did not match any of the woody vegetation found in the Eastern Kalahari Bushveld (SVk) biozones, Bamford (2015b) and House *et al.* (2022). Some did not preserve enough features to make a positive identification. Insidewood was also not very helpful for identifying as this website is poorly developed for South African plant taxa.

Some of the taxa identified in this collection were also identified in previous studies conducted at the Wonderwerk Cave and nearby archaeological sites. For instance, House *et al.* (2022) identified *Commiphora schimperi, Olea europaea* subsp. *africana,* and *Searsia* l*ancea* from charcoal in stratum 4b (Table 5.4). Brook *et al.* (2015) study, which includes prior palynological analyses of the Wonderwerk Cave

from Brook *et al.* (2010) and Van Zinderen Bakker's 1982 studies, as well as new pollen samples from the cave's Holocene sediments, also identified pollen from *Olea, Rhus/Searsia, Acacia*, and *Tarchonanthus*. Pollen preserved in hyena coprolites indicated that *Olea, Rhus/Searsia, Acacia, Tarchonanthus,* and *Rhamnaceae* have grown near the Equus Cave, northeast of the Wonderwerk Cave, since 7.5 ka BP (Scott, 1987).

Berchemia zeyheri, Commiphora schimperi, Olinia ventosa, Ozoroa paniculosa, Senegalia caffra, Tarchonanthus parvicapitulatus, and *Vachellia tortilis* no longer grow near the cave or anywhere in the Northern Cape Province, as stated in Table 5.3 (Germishuizen and Meyer, 2003). This suggests that these species may have had a wider distribution in the past compared to their current distribution (Bamford, 2015b: 170; House *et al*., 2022: 9). The disappearance of these species in the area could also be attributed to past environmental conditions that were more favorable for their growth in the area, or they could have been imported from other regions for medicinal, tool manufacturing, or other reasons. Anthropogenic factors, such as the clearing of natural vegetation for subsistence crops, or overexploitation by modern farmers who lived in the area and in the cave during the 1990s, may also have contributed to their disappearance in the area.

It appears that some of the taxa have migrated towards the wetter savanna vegetation units, futher east: Ghaap Plateau Vaalbosveld (SVk 7) (n=7), Marikana Thornveld (SVcb 6) (n=6), Postmasburg Thornveld (SVk 14) (n=6), and Eastern Valley Bushveld (SVs 6) (n=5) (Rutherford *et al.,* 2006). This suggests that there may have been slight changes in rainfall patterns in the Wonderwerk area, leading to the vegetation shift towards the slightly wetter bioregions in the east.

On the other hand, *Halleria lucida, Heteromorpha arborescens, Olea europaea* subsp. *africana, Searsia lancea, Tarchonanthus camphoratus, Vachellia karroo, Ziziphus mucronata*, and *Ehretia* species (*Ehretia rigida* subsp. *rigida*) still grow

near the cave or in the Northern Cape (Table 5.3), indicating that some taxa have persisted in the area since 6.9 ka.

The occurrence of both deciduous (n=6) and evergreen (n=5) taxa (Appendix G) as well as shrubs and small to medium-sized trees in this assemblage seems to imply that the vegetation community around the cave was open and a mosaic with evergreen and deciduous trees and shrubs that tolerate warm, dry conditions growing on the warm hillsides, termite mounds and rocky outcrops, while the riverine vegetation possibly grew along rivers and streams like Kuruman river and Boesmansgat sinkhole found close to the cave (Fig. 3.1 C).

Climate, particularly temperature and rainfall, has a significant impact on the structure of biomes in southern Africa. Bushveld taxa are very prevalent in this assemblage, n=13 (Appendix I). Three of these taxa, i.e., *Berchemia zeyheri, Commiphora schimperi*, and *Ozoroa paniculosa* are exclusively limited to hot and arid bushveld in the eastern regions of South Africa, Botswana, Namibia and Swaziland (van Wyk and van Wyk, 2013). Grassland woody taxa are also conspicuous in this assemblage (n=10) (Appendix I). However, nine of the ten grassland taxa can also be found in savanna ecosystems. Only one taxon, *Halleria lucida* is restricted to grasslands, forests, and forested ravines (van Wyk and van Wyk, 2013). This implies bushveld vegetation existed around the cave at 6.9-5.9 ka. In the bushveld, the woody component often forms an irregular series of interlocking canopies with openings and little distinction between shrubs and trees (Rutherford *et al.,* 2006). Most of the taxa identified in this study are mostly found in the Eastern Kalahari Bushveld bioregion vegetation units of the savanna, i.e., SVk 7, 10 and 14, thus indicating vegetation and climate similar to the modern Eastern Kalahari Bushveld (Fig. 3.3 A, B) (Rutherford *et al.,* 2006). *Halleria lucida* might have persisted from the wetter environment that existed around 12.3 ka (stratum 5a, Bamford, 2015b) before its disappearance around 6.9-5.9 ka.

The species identified mostly thrive in strictly warm arid environments (n=7), suggesting relatively warm and dry climate conditions (Appendix J). The occurrence of hot, dry woodland species, *Commiphora schimperi* and *Ozoroa paniculosa*, indicate conditions slightly warmer and drier than today persisted in the vicinity of the cave from 8.4-5.9 ka (strata 4c and 4b). However, the occurrence of mesic to moist environment taxa (n=2; *Halleria lucida* and *Olinia ventosa*) suggest that dry climate conditions did not last long, as there may have been fluctuations in moisture availability. The analysis of charcoal from stratum 4a by House *et al.* (2022) shows that wetter climatic conditions began around 6.2 ka cal BP.

This study identified 15 taxa that mostly fall under the summer rainfall zone (Fig. 3.4, Appendix J). Of these, five are also found in the all-year-round and winter rainfall zones. This suggests that the Wonderwerk area mostly experienced environmental conditions associated with the summer rainfall zone seasonality. It is likely that there was an increase in summer rainfall during this period, as indicated by data on herbivore tooth enamel isotopes (Ecker *et al.,* 2018). This shift in rainfall seasonality in the cave locality is important for shaping the strong summer rainfall regime in the area today.

Overall, the composition of charcoal taxa indicates that the landscape surrounding Wonderwerk Cave was occupied by shrubs and small to medium-sized trees such as *Berchemia zeyheri, Commiphora schimperi, Halleria lucida, Heteromorpha arborescens, Olea europaea* subsp. *africana, Olinia ventosa, Ozoroa paniculosa, Searsia lancea, Senegalia caffra, Tarchonanthus camphoratus, Tarchonanthus parvicapitulatus, Vachellia karroo, Vachellia tortilis, Ziziphus mucronata*, and *Ehretia* species. The area had a mix of bushveld and grassland, as well as deciduous and evergreen vegetation communities, suggesting vegetation similar to the modern bushveld around the cave. The climate was initially dry, but it became slightly wetter later, with a summer rainfall zone seasonality experienced in the area.

6. 2 Interpretations of the wood physiognomy

The wood internal anatomy or physiognomy can provide crucial information about past moisture availability and by inference climate and rainfall patterns (Wheeler *et al.,* 2007). This is because plants have water-related adaptations that ensure their survival in areas with low or high moisture availability (Wolfe and Upchurch, 1987; Zwane and Bamford, 2021). The analysis of these adaptations can be informative. Vessel size, frequency, vulnerability index, conductivity capacity and mesomorphy index were analysed to determine if the wood was adapted for water stress or abundance.

Mean vessel diameter and frequency are related to the habitat, as plants tend to have a trade-off between efficient water conduction and safety from cavitation associated with extreme climate conditions (Wheeler, 2007). Large, few vessels enable efficient water conduction, and can function well for trees in high moisture availability environments. Whereas numerous, narrow vessels provide greater safety against air embolisms and cavitation associated with droughts and thawing caused by frost (Wolfe and Upchurch, 1987).

The analysed charcoal wood assemblage has a high proportion of wood with numerous (~117.65 vessels/mm^2), narrow vessels (~42.40 µm) (Table 5.5). This suggests that these plants were adapted to an environment with extreme climatic conditions like droughts and freezing, where prolonged periods of low water availability frequently occurred. The small vessel diameter and high vessel frequency also support the taxonomic identifications that most of the plants identified are shrubs or small trees (Wheeler *et al.,* 2007).

According to Carlquist (1977) and Wolfe and Upchurch (1987), vulnerability indices below 1 suggest vessel redundancy and greater safety during water stress periods, while values over 1 suggest mesomorphy. About 84.09% (n=74) of the woods mostly have vulnerability indices below 1 (Table 5.5). This indicates a huge proportion of the woody vegetation were mostly shrubs or small trees adapted to low moisture environments that are subjected to droughts and freezing conditions. Taxonomic data also shows 7 of the taxa identified can tolerate drought and frost (Appendix J). Only 15.91% (n=14) of the vegetation have indices above 1, which is typical in large mesophytic trees or trees vulnerable during extreme conditions. Small trees/shrubs with deep roots that penetrate underground water supply can also have vulnerability indices over 1 as they are not subjected to seasonal droughts (Carlquist, 1977). An example of this would be *V. karroo*, which has long taproots that allow it to use underground water and nutrients (https://pza.sanbi.org)

Conductivity capacity values above 200 are typical in large trees, while values above 500 are typical in large trees both in water abundant environments (Wolfe and Upchurch, 1987). About 98.86% (n=87) of the woods have conductivity capacity values below 200 (Table 5.5). This indicates small trees and shrubs adapted to xeric/dry soils (Wolfe and Upchurch, 1987). Only 1.14%, one specimen, identified as *H. lucida,* has a conductivity capacity of more than 200, indicating adaptation to high moisture containing soils. Interestingly, *H. lucida* is typically found in moist to mesic environments or along water sources in arid environments

(Coates Palgrave and Coates Palgrave, 1983). This supports that physiognomy can reveal information on water availability and climate.

Mesomorphy indices around 200 are typical in mesophytic woody plants, and indices below 75 are typical in xerophytes. About 52.83% (n=28) have mesomorphy indices below 75, which suggests xerophytic/ dry environment plants (Table 5.5). A small proportion, 15.09% (n=8) of the woods analysed, suggest mesophytic/wet environment plants as they have indices above 200 (Wolfe and Upchurch, 1987).

The wood anatomy overall signals the charcoal assemblage is dominated by shrubs and small trees adapted to a predominantly dry environment that existed around the Wonderwerk Cave between 6.9 and 5.9 ka cal BP. This is in agreement with the taxonomic implications. Differences in the physiognomy data may be due to the tendency of drought and frost-resistant small trees and shrubs not to follow the trend as they have deep roots that can penetrate into underground water sources, hence they are not subjected to drought (Wolfe and Upchurch, 1987). The physiognomic method is most effective when combined with the taxonomic method to interpret climate signals because it lacks specific quantitative ranges for interpreting fossil plant indices.

6.3 Comparison with other southern African records

The field of anthracology continues to grow and has become more accepted as a viable method to reconstruct past environmental conditions in southern Africa since the study by Deacon *et al.* (1984). The findings of this dissertation are in accord with the implication of semi-arid, modern bushveld-like conditions suggested by pollen, macrofauna, macrocharcoal as well as tooth enamel and ostrich eggshell isotopes from Wonderwerk Cave stratum 4b (Brook *et al.,* 2010; 2015; Scott and

Thackeray, 2015; Thackeray, 2015; Lee-Thorp and Ecker, 2015; Ecker *et al.,* 2018; House *et al.,* 2022).

The analysis of the Wonderwerk Cave charcoal from the Holocene strata by Bamford (2015b), House *et al.* (2022) and in this dissertation indicates that dry conditions dominated the Holocene. The key taxa identified in stratum 5a suggest that a dry, but slightly wetter than today's climate conditions existed between 12.3-11.4 ka cal BP and persisted until 10.4 ka cal BP (stratum 4d). From 9.4-5.9 ka cal BP (strata 4c and b), the environment was predominantly dry. These dry conditions were interrupted by a wet interval that occurred between 6.2-4.6 ka cal BP (stratum 4a), indicated by the presence of wet environment taxa such as *Berchemia discolor, Cordia caffra, Heteromorpha arborescens, Heteropyxis natalensis* and *Ochna serrulata*. Subsequently, dry conditions prevailed until the present, as indicated by the presence of dry environment taxa in the strata 3b, 3a, and 2b (Bamford, 2015b; House *et al.,* 2022).

The results of this study are supported by other proxies found in Wonderwerk Cave. The stalagmite shows no growth between 13-3.5 ka, indicating dry conditions/low moisture availability until the Late Holocene (Brook *et al.,* 2015). The pollen, macrofauna abundance, stable isotopes from ostrich eggshells and tooth enamel also indicate that from 11.8 ka cal BP, the environment near the cave was a dry bushveld and dominated by Asteraceae. However, this dry phase was interrupted by a wet phase, coinciding with strata 4aLH and 4a, which occurred between 6.2-4.6 ka cal BP. This phase was marked by an increase in grass pollen, indicating a transition to grassland which caused an increase in grassland herbivores (Lee-Thorp and Ecker, 2015; Scott and Thackeray, 2015; Ecker *et al.,* 2018). In the cave, stratum 4aLH has the highest amount of charcoal, charred stones, artifacts, and faunal remains (Ecker *et al.,* 2017).

The findings of this study are also in accordance with studies from sites in the Eastern Kalahari Bushveld bioregion. Pollen data from Equus Cave (Scott, 1987)

shows a dry environment with modern savanna vegetation existed in the area from 7.5 ka till recent. The Wonderkrater, which is also part of the savanna, located on the far east of the cave, also shows dry, grassy woodland vegetation dominated the area from 9.5-6 ka cal BP (Scott *et al.,* 2003). Lake Eteza, situated along the coastal savanna, also shows that dry climate conditions existed till 6.8 ka, before transitioning to humid forest (Neumann *et al.,* 2010).

The findings are also consistent with palynological analyses from some Dry Highveld Grassland bioregion of the grassland, i.e., Florisband spring and Blydefontein, which both suggests vegetation associated with dry climate occured in the interior of southern Africa from 7 ka cal BP till 6.5 ka cal BP in Florisband Spring and 5.4 ka cal BP in Blydefontein respectively (Scott *et al.,* 2015; 2022).

Similar conditions were noted northwest Botswana in the Okavango Panhandle, which is part of the savanna, as the Mid-Holocene between 7.0-4.0 ka BP was mostly dry, with a short, wet phase consistent with strata 4aLH and 4a of the Wonderwerk Cave was noted around 6.0 ka BP (Nash *et al.,* 2006). High water levels were noted slightly earlier at 6.6±0.8 to 5.2±0.6 ka in the Mababe depression and around 6.8±1.1 ka in Parakarungu beach ridge (in Botswana) (Burrough and Thomas, 2008; 2013). This is consistent with the macrocharcoal, pollen and macrofauna data (Scott and Thackeray, 2015; Lee-Thorp, 2015; Ecker *et al.,* 2018; House *et al.,* 2022).

6.4 Implications on human subsistence and activities in the combustion features

Understanding the uses and distribution of taxa in combustion features can provide valuable insights into how hearths/combustion features and the woody vegetation were used by the LSA hunterer-gatherers. Table 5.3 summarizes the possible uses of the woods, which include kindling for starting fires, fuel, medicine, food, cultural uses and timber for building tools and artifacts. Upon analysing charcoal from 13

squares, it appears that the taxa are scattered across the floor (Appendix D), indicating that none of the squares had a designated use. The scattering may also be due to sweeping or cleaning of combustion areas.

Wood collection in the past could have been either unsystematic, with wood randomly collected from the vicinity of the cave as stated by the principle of least effort, or it could have been systematic, with wood collected based on their firewood properties. Studies have shown that people already had complex interactions with plants around them more than 200 ka. By 200 ka, people in southern Africa were using stacked grass as bedding in South African caves like Sibudu Border Cave (Wadley *et al.*, 2020).

Generally, most of the woody vegetation identified can be used as tinder as they are mostly shrubs, and shrubs shorter than 3 m make good tinder (Lennox *et al.,* 2015). *Commiphora schimperi* wood in particular is known to make good tinder. *Olea europaea* subsp. *africana, Senegalia caffra, Tarchonanthus camphoratus, Tarchonanthus parvicapitulatus, Vachellia karroo, Vachellia tortilis, Ziziphus mucronata* are known for their good fire making properties (van Wyk and van Wyk, 2013). For example, *Acacia* (*Vachellia/Senegalia*) produces dry, dense firewood that can ignite easily and produce less ash and more heat, thus making it a source of good firewood (Lennox *et al.,* 2015). These good firewood producing taxa are found scattered in the different squares (Appendix G), suggesting there was no specific area used to make fires or that there had been a succession of fires in the cave floor which were subsequently swept or cleared, thus scattering the charcoal all over the floor, which also indicated frequent occupation in the cave.

About 21.18% (n=43) of the charcoals displayed radial cracking, potentially indicating the use of wet or fresh wood rather than the preferred dry wood, which is lightweight, easy to carry, and quick to burn. It's possible that the wet wood was gathered from live trees for smudge fires or mixed with dry wood for longer-lasting fires (Théry-Parisot and Henry, 2012). For instance, species such as

Tarchonanthus camphoratus, yield good firewood that can be burned even when wet (Coates Palgrave and Coates Palgrave, 1983). Nonetheless, it's worth noting that dry wood charcoal can also exhibit radial cracking, although not as frequently as in wet wood, so this may not consistently signify wet wood (Théry-Parisot and Henry, 2012).

Out of the 15 identified taxa, 11 have healing properties, some of which are scientifically proven (Table 5.3). For instance, in the past, people living in southern Africa would harvest various parts of *Ziziphus mucronata*, commonly known as buffalo thorn, to treat toothaches, chest complaints, coughs, boils, tubercular gland-swelling, dysentery and lower back pains (Palmer and Pitman, 1972; Coates Palgrave and Coates Palgrave, 1983). Recent scientific evaluations of the medicinal properties of this tree have shown that its antioxidants can treat most body pains, including toothaches, coughs, and respiratory infections when infused. Moreover, the roots and leaves of this tree can heal boils, sores, and glandular swelling when applied externally (Olajuyigbe and Afolayan, 2011).

Tarchonanthus camphoratus and *Heteromorpha arborescens* are known to produce smoke that can alleviate blocked sinuses and headaches when inhaled (Coates Palgrave and Coates Palgrave, 1983). These two taxa are found scattered across the squares (Appendix G), with no indication that there was a square/area in the cave specifically used for burning wood for medicinal purposes.

A few of these trees and shrubs such as *Halleria lucida, Heteromorpha arborescens,* and *Tarchonanthus camphoratus* are often used or burnt for magical and cultural purposes. For example, *Berchemia zeyheri* is known as a royal tree amongst Zulu people and their royals often carry knobkerries carved from its wood. *Ziziphus mucronata* is known as *Umlahlankosi* by the Zulu people and is usually planted on a deceased chief’s grave as a reminder or indication of where they were buried. The branches of this tree are normally harvested and used to guide the spirits of the deceased from where they died to a new site. This tree is also

believed to ward off evil spirits and lightning, so often southern Africans would drag its branches around the village or seek shelter under the tree in case of lightning. Twigs of *Halleria lucida* are burnt as part of ritual offerings to ancestral spirits. Moreover, the ashes of this plant are collected and mixed with fat, then smeared into cuttings of *Rhamnus prinoides*. These cuttings are then dragged across the village to protect the people from evil (Coates Palgrave and Coates Palgrave, 1983).

Some are used for cosmetics and aesthetics. For example, *Tarchonanthus* leaves are aromatic as they contain volatile and essential oils and were used by Zulu women in the past as perfume for hair. They still continue to be infused with cosmetics for fragrant body and hair products. *Searsia lancea* and *Vachellia karroo* bark produces tannin, which were previously used to tan leather (Coates Palgrave andCoates Palgrave, 1983).

It appears that there are various types of taxa, such as *Berchemia zeyheri, Searsia lancea, Olinia ventosa, Ozoroa paniculosa* and *Ehretia* wood-type, that do not produce good firewood, but make excellent timber wood for making pick handles, wagon parts, bows and furniture. It is possible that they were randomly collected and used as firewood since they are small and easy to collect, or that they are remnants of wood collected and used for tool construction and building then later discarded into the fire.

These are some of the modern uses of these taxa but it is important to note that they might not all necessarily apply to past human societies. However, some uses we know now, might date back to before 6.9 ka and were passed on down to generations as indigenous knowledge. This shows that trees have had a very significant and enduring role in our culture and history as humans and they still continue to be an important part of many societies around the world. The taxa are found sparsley distributed across the cave floor, indicating that there were no specific uses of the combustion features or that the cave floor was swept, which

indicates continuous use of the cave. Fire has played a significant role in the intellectual and social complexity of humans. As humans learned to associate different types of wood with varying fire properties, they were able to carry out diverse social activities or transfer crucial knowledge around the hearths.

6.5 Limitations and future research

The research was restricted by time, so only 204 charcoal fragments could be sampled and analysed. In the future, now that more experience on the field has been gained, more charcoal could be analysed, maybe about 300 for each stratum as recommended by Scheel-Ybert (2002) for the tropics. The identification of the analysed fragments was limited by preservation and the non-availability of all taxa currently growing in the vicinity of the cave in the modern charcoal reference collection. To combat this, it would be better that before analysis, the study area is visited and the woody plants that grow in a walking distance are collected. However, anthropogenic influences might have disturbed the taxa, hence causing the disappearance of some taxa. But overall visiting the area will not only assist with the identifications, but it will also allow the analysis of the physiognomy of the plants today so that we can compare changes in moisture availability since 6.9 ka.

In the future, other methods, such as carbon isotope analysis can inform about past temperatures, rainfall and humidity when used cautiously on young charcoal specimens (Hall *et al.,* 2008). Although the accuracy of physiognomy method has been debated for a long time, this study has shown the effectiveness of this method when used alongside the taxonomy method.

6.6 Summary of the chapter

Although there are many debates around the use of charcoal analysis and wood physiognomy as a climate analysis tool, this study has shown that when used in conjunction with taxonomic identifications these can be a very powerful tool. This study has successfully shown that the interior of southern Africa during the Mid-Holocene at 6.9-5.9 ka cal BP was dry through the identification of taxa like *Berchemia* cf. *zeyheri, Commiphora schimperi, Heteromorpha arborescens*, *Olea europaea* subsp. *africana, Ozoroa paniculosa, Searsia lancea, Senegalia caffra, Tarchonanthus camphoratus, Tarchonanthus parvicapitulatus, Vachellia* cf. *karroo, Vachellia* cf. *tortilis, Ziziphus mucronata* and *Ehretia*-type species. Although not clear when, the data seems to also suggest there was a period of slightly increased moisture, which other studies suggest to be around 6.5/6.2 ka cal BP. The data shows the environment around the cave was an open bushveld, similar to today's and dominated by a mosaic of evergreen and deciduous small trees and shrubs growing in microhabitats such as the warm rocky hillsides and water sources possibly like the Kuruman River or Boesmansgat.

Physiognomy of the charcoal also shows that the plants in this assemblage were small trees and shrubs adapted to dry environments and can withstand frost and drought. Inferences made from this charcoal study are consistent with other studies from the Wonderwerk Cave and other sites using various proxies such as pollen and faunal remains. The trees and shrubs have numerous uses we know now, such as magical, medicinal, food source, construction and fuel which may have been already known by the people inhabiting the cave at 6.9 ka. Fires have been instrumental in shaping our social and intellectual development.

CHAPTER SEVEN

Conclusion

This research has effectively demonstrated that anthracological analyses continue to be a valuable source of paleoclimate information, particularly in the interior regions of southern Africa where dry climatic conditions prevail. These conditions have made it difficult to preserve commonly used paleoenvironment proxies like pollen and phytoliths, which are often found in lakes and swamps and commonly used in palaeoreconstruction studies. Additionally, these analyses were utilized to explore how people could have utilized the cave and vegetation around them.

The taxonomic composition of the charcoal from stratum 4b of Excavation 1, Wonderwerk Cave indicated that dry, bushveld/ grassland conditions dominated the Mid-Holocene (6.9-5.9 ka), particularly the occurrence of dry bushveld taxa like *Commiphora schimperi* and *Ozoroa paniculosa.* However, the occurrence of mesic-moist environment tolerant taxa, i.e., *Olinia ventosa* and *Halleria lucida*, suggests climate fluctuations occurred. Pollen and faunal composition data from Wonderwerk Cave stratum 4b suggest that a shift to a wetter climate occurred at 6.5/6.2 ka. The charcoal data also indicates that the landscape then was similar to the modern Eastern Kalahari Bushveld around the cave, with patches of evergreen and deciduous trees and shrubs such as *Berchemia zeyheri, Commiphora schimperi, Halleria lucida, Heteromorpha arborescens, Olea europaea subsp. africana, Olinia ventosa, Ozoroa paniculosa, Searsia lancea, Senegalia caffra, Tarchonanthus camphoratus, Tarchonanthus parvicapitulatus, Vachellia karroo, Vachellia tortilis, Ziziphus mucronata,* and *Ehretia*-type species. Taxa tolerating warm, dry conditions possibly grew on the warm hillsides, termite mounds and rocky outcrops while the riverine taxa grew along rivers and streams. The

taxonomic composition of this assemblage also suggests that conditions associated with summer rainfall seasonality dominated the landscape.

The internal anatomy of most charcoals from the analysed assemblage suggests most of the woody plants that occurred near the cave were adapted to dry climate as the wood shows adaptations to safety against cavitation or air embolisms that occur during periods of low moisture availability.

The identified plants have various uses such as fuel, food source, medicine, construction, and cultural practices. It is highly likely that people were already familiar with the uses of these plants by 6.9 ka and they were often harvested for any of the given reasons. The charcoal found in different squares suggests that there were no specific features for burning plants for medicine or cultural purposes.

References

Akkemik, U., Toprak, Ö., Mantzouka, D. and Çelik, H. (2023). A Mediterranean woody species composition from Late Miocene-Early Pliocene deposits of northeastern Turkey with newly described fossil-taxa palaeoclimatically evaluated. *Review of Palaeobotany and Palynology,* **316**. https://doi.org/10.1016/j.revpalbo.2023.104916.

Allott, L.F. (2005). Palaeoenvironments of the Middle Stone Age at Sibudu Cave, Kwazulu-Natal, South Africa: An Analysis of Archaeological Charcoal, Unpublished PhD Thesis. University of the Witwatersrand, Johannesburg.

Asouti, E. and Austin, P. (2005). Reconstructing woodland vegetation and its exploitation by past societies, based on the analysis and interpretation of archaeological wood charcoal macro-remains. *Environmental Archaeology,* **10**, 1-18. https://doi.org/10.1179/146141005790083867.

Baas, P., Werker, E., and Fahn, A. (1983). Some Ecological Trends in Vessel Characters. *IAWA Journal*, **4**(2-3), 141-159. https://doi.org/10.1163/22941932-90000407.

Bailey, I.W. and Sinnott, E.W. (1915). A botanical index of Cretaceous and Tertiary climates. *Science*, **41**, 831-834. https://doi.org/10.1126/science.41.1066.831.

Balout, L. (1952). A propos des charbons de bois préhistoriques. B.S.H.N. de l'Afrique du nord, **43**, 160–163.

Bamford, M.K. (2015a). Macrobotanical remains from Wonderwerk Cave (Excavation 1), Oldowan to Late Pleistocene (2 Ma to 14 ka bp), South Africa. *African Archaeological Review*, **32**(4), 813-838. https://doi.org/10.1007/s10437-015-9200-0.

Bamford, M.K. (2015b). Charcoal from Pre-Holocene Stratum 5, Wonderwerk Cave, South Africa. *Palaeoecology of Africa*, **33**, 153–174.

Bamford, M.K. (2017). Pleistocene fossil woods from the Okote Member, site FwJj 14 in the Ileret region, Koobi Fora Formation, northern Kenya. *Journal of Human Evolution*, **112,** 134-147. http://dx.doi.org/10.1016/j.jhevol.2017.08.003.

Beaumont, P.B. and Vogel, J.C. (2006). On a timescale for the past million years of human history in central South Africa. *South African Journal of Science*, **102**, 217–228. https://doi.org/10.10520/EJC96546.

Berna, F., Goldberg, P., Horwitz, L.K., Brink, J., Holt, S., Bamford, M. and Chazan, M. (2012). Microstratigraphic evidence of in situ fire in the Acheulean strata of Wonderwerk Cave, Northern Cape province, South Africa. *Proceedings of the National Academy of Sciences*, **109,** 1215-1220. https://doi.org/10.1073/pnas.1117620109.

Braadbaart, F. and Poole, I. (2008). Morphological, chemical and physical changes during charcoalification of wood and its relevance to archaeological contexts. *Journal of Archaeological Science*, **35**(9), 2434-2445. https://doi.org/10.1016/j.jas.2008.03.016.

Brook, G.A., Scott, L., Railsback, L.B. and Goddard, E.A. (2010). A 35 ka pollen and isotope record of environmental change along the southern margin of the Kalahari from a stalagmite and animal dung deposits in Wonderwerk Cave, South Africa. *Journal of Arid Environments*, **74**(7), 870-884. https://doi.org/10.1016/j.jaridenv.2009.11.006.

Brook, G.A., Liang, F., Railsback, B., Scott, L. and Voarintsoa, N.R.G. (2015). Late Holocene Stalagmite and Tufa Climate Records for Wonderwerk Cave: Relationships between Archaeology and Climate in Southern Africa. *African Archaeological Reviews,* **32**, 669–700.

Burrough, S. and Thomas, D. (2008). Late Quaternary lake-level fluctuations in the Mababe Depression: Middle Kalahari palaeolakes and the role of Zambezi inflows. *Quaternary Research*, **69**(3), 388-403. https:doi.org/10.1016/j.yqres.2008.02.003.

Burrough, S.L. and Thomas, D.S.G. (2013). Central southern Africa at the time of the African Humid Period: a new analysis of Holocene palaeoenvironmental and palaeoclimate data. *Quaternary Science Reviews*, **80**, 29-46. https://doi.org/10.1016/j.quascirev.2013.08.001.

Carlquist, S. (1977). Ecological factors in wood evolution: a floristic approach. *American Journal of Botany*, **64**(7), 887-896.

Cartwright, C.R. (2013). Identifying the woody resources of Diepkloof Rock Shelter (South Africa) using scanning electron microscopy of the MSA wood charcoal assemblages. *Journal of Archaeological Science*, **40**(9), 3463-3474. https://doi.org/10.1016/j.jas.2012.12.031.

Cartwright, C.R., Porraz, G. and Parkington, J. (2016). The wood charcoal evidence from renewed excavations at Elands Bay Cave, South Africa. *Southern African Humanities*, **29**, 249-258.

Caruso Fermé, L. and Théry-Parisot, I. (2011). Experimentation and combustion properties of Patagonian Andean forest (Argentina). *SAGVNTVM EXTRA*, **11**, 39-40.

Chabal, L. (1990). L'étude paléo-écologique de sites protohistoriques à partir des charbons de bois: la question de l'unité de mesure. Dénombrement de fragments ou pesées. In T. Hackens, A. Munaut and C. Till (eds), *Wood and Archaeology. Bois et Archéologie. First European Conference, Louvain-la-Neuve*, 189–205. PACT, 22. Conseil de l'Europe, Strasbourg.

Chabal, L. (1997). Forêts et sociétés en Languedoc (Néolihique final, Antiquité tardive). L'anthracologie, méthode et paléoécologie. Documents d'archéologie française 63, Éditions de la Maison des sciences de l'homme, Paris.

Chase, B.M. and Meadows, M.E. (2007). Late Quaternary dynamics of southern Africa's winter rainfall zone. *Earth-Science Reviews*, **84**(3-4), 103-138. https://10.1016/j.earscirev.2007.06.002.

Chase, B., Marais, E., Meadows, M., Reimer, P., Scott, L., Sealy, J. and Reimer, P. (2009). A record of rapid Holocene climate change preserved in hyrax middens from southwestern Africa. *Geology*, **37**, 703-706. https://doi.org/10.1130/g30053a.1.

Chazan, M., Avery, M., Goldberg, P., Horwitz, L.K., Matmon, A., Porat, N., Ron, H., Sumner, A. and Yates, R. (2008). Radiometric dating of the Earlier Stone Age sequence in Excavation I at Wonderwerk Cave, South Africa: Preliminary results. *Journal of Human Evolution*, **55**(1), 1-11. https://doi.org/10.1016/j.jhevol.2008.01.004.

Chikumbirike, J. and Bamford, M.K. (2021). A Southern African perspective on the contribution of charcoal analyses to archeology. *Oxford Research Encyclopedia of Anthropology.* https://doi.org/10.1093/acrefore/9780190854584.013.257.

Chikumbirike, J., Bamford, M.K. and Esterhuysen, A. (2016). A study of archaeological charcoal from Great Zimbabwe. *The South African Archaeological Bulletin,* **71**, 107-118.

Chrzazvez, J., Fiorucci, G., Théry-Parisot, I. and Terral, J.F. (2014). Impact of post-depositional processes on charcoal fragmentation and archaeobotanical implications: experimental approach combining charcoal analysis and biomechanics. *Journal of Archaeological Science*, **44**, 30-42. https://doi.org/10.1016/j.jas.2014.01.006.

Coates Palgrave, K. and Coates Palgrave, M. (1983). *Palgrave's Trees of Southern Africa.* 2nd ed. Cape Town: Struik Publishers.

Conran, J.G., Bannister, J.M., Lee, D.E. and Reichgelt, T. (2016). Epiphyllous fungi and leaf physiognomy indicate an ever-wet humid mesothermal subtropical climate in the Late Eocene of southern New Zealand. *Palaeogeography, Palaeoclimatology, Palaeoecology,* **452**, 1-10. https://doi.org/10.1016/j.palaeo.2016.03.032.

Cowling, R.M., Allsopp, J.C., Cartwright, C.R. and Parkington, J.E. (1999). Fossil wood charcoal assemblages from Elands Bay Cave, South Africa: Implications for Late Quaternary vegetation and climates in the winter-rainfall fynbos biome. *Journal of Biogeography,* 367–378. https://doi.org/10.1046/j.1365-2699.1999.00275.x.

Dadswell, H.E. and Ingle, H.D. (1954). The wood anatomy of the New Guinea *Nothofagus* Bl. *Australian Journal of Botany*. **2**, 141-153.

Deacon, H.J., Deacon, J., Scholtz, A., Thackeray, F., Brink, J. and Vogel, J.C. (1984). Correlation of palaeoenvironmental data from the Late Pleistocene and Holocene deposits at Boomplaas Cave, southern Cape. *Late Cainozoic palaeoclimates of the Southern Hemisphere*, *Proc. SASQUA symposium, Swaziland, 1983.* 339-351.

Delhon, C. (2018). Is Choice Acceptable? How the Anthracological Paradigm May Hinder the Consideration of Fuel Gathering as a Cultural Behaviour. *Environmental Archaeology*, **26**(2), 159-167. https://doi.org/10.1080/14614103.2018.1522783.

Depreux, B., Berger, J.F., Boudad, L., Degeai, J.P., El Harradji, A., Lefèvre, D., Limondin-Lozouet, N., and Segaoui, F. (2021). Alluvial records of the African Humid Period from the NW African highlands (Moulouya basin, NE Morocco). *Quaternary Science Reviews*, **255**. https://doi.org/10.1016/j.quascirev.2021.106807.

Dotte-Sarout, E., Byrne, C. and Carah, X. (2015). Not just carbon: assessment and prospects for the application of anthracology in Oceania. *Archaeology in Oceania*, **50,** 1–22. https://doi.org/10.1002/arco.5041.

Ecker, M., Brink, J., Chazan, M., Horwitz, L.K. and Lee-Thorp, J.A. (2017). Radiocarbon Dates Constrain the Timing of Environmental and Cultural Shifts in the Holocene Strata of Wonderwerk Cave, South Africa. *Radiocarbon,* **59**(4), 1067–1086. https://doi.org/10.1017/RDC.2017.55.

Ecker, M., Brink, J., Horwitz, L.K., Lee-Thorp, J.A. and Scott, L. (2018). A 12,000 year record of changes in herbivore niche separation and palaeoclimate (Wonderwerk Cave, South Africa). *Quaternary Science Reviews*, **180**, 132–144. https://doi.org/10.1016/j.quascirev.2017.11.025.

Fauquette, S., Guiot, J. and Suc, J.P. (1998). A method for climatic reconstruction of the Mediterranean Pliocene using pollen data. *Palaeogeography, Palaeoclimatology, Palaeoecology,* **144**, 183-201.

Findlay, S.J. and Twine, W.C. (2018). Chiefs in a democracy: A case study of the 'new' systems of regulating firewood harvesting in post-apartheid South Africa. *Land*, **7**(35), 1-21. https://doi.org/10.3390/land7010035.

Gelabert, L.P., Asouti, E. and Marti, E.A. (2011). The ethnoarchaeology of firewood management in the Fang villages of Equatorila Guinea, central Africa: Implications for the interpretation of wood fuel remains from arhaeological sites. *Journal of Anthropological Archaeology*, **30**, 375-384. https://doi.org/10.1016/j.aa.2011.05.002.

Germishuizen, G. and Meyer, N.L. (eds) 2003. *Plants of Southern Africa: An annotated Checklist,* Strelitzia 14. Pretoria: South African National Biodiversity Institute.

Godwin, H. and Tansley, A.G. (1941). Prehistoric Charcoals as Evidence of Former Vegetation, Soil and Climate, *Journal of Ecology*, **29(1)**, 117–126. https://doi.org/10.2307/2256222.

Gonçalves, T.A., Marcati, C.R., and Scheel-Ybert, R. (2012). The Effect of Carbonization on wood Structure of Dalbergia Violacea, Stryphnodendron Polyphyllum, Tapirira Guianensis, Vochysia Tucanorum, and Pouteria Torta from the Brazilian Cerrado. *IAWA Journal* 33, **1**, 73-90. https://doi.org/10.1163/22941932-90000081.

Guiot, J., Harrison, S.P. and Prentice, I. (1993). Reconstruction of Holocene precipitaion patterns in Europe using pollen and lake-level data. *Quaternary*

Research, **40**(2), 139-149.Hall, G., Scholes, M. and Woodborne, S. (2008). Stable carbon isotope ratios from archaeological charcoal as palaeoenvironmental indicators. *Chemical Geology*, **247**, 384-400. https://doi.org/10.1016/j.chemgeo.2007.11.001.

Herman, P.P.J. (2002). Revision of the *Tarchonanthus camphoratus* complex (Asteraceae-Tarchonantheae) in southern Africa. *Bothalia,* **32**(1), 21-28. https://doi.org/10.4102/abc.v32i1.458.

Hoffman, K., Gavin, D., Lertzman, K., Smith, D. and Starzomski, B. (2016). 13,000 years of fire history derived from soil charcoal in a British Columbia coastal temperate rain forest. *Ecosphere*, **7**. https://doi.org/e01415.10.1002/ecs2.1415.

Horwitz, L. and Chazan, M. (2015). Past and Present at Wonderwerk Cave (Northern Cape Province, South Africa). *African Archaeological Review*, **32**, 595–612. https://doi.org/10.1007/s10437-015-9208-5.

House, A., Bamford, M.K. and Chikumbirike, J. (2022). Charcoal from Holocene deposits at Wonderwerk Cave, South Africa: A source of palaeoclimate information. *Quaternary International*, **614**, 1-11. https://doi.org/10.1016/j.quaint.2020.10.039.

House, A., Bamford, M.K., Greenfield, H.J. and van Schalkwyk, L.O. (2023). Furnaces, hearths, rituals, and construction: investigating the utilisation of woody plant species at the Early Iron Age site of Ndondondwane by means of identifying archaeological charcoal*. Archaeological and Anthropological Sciences*, **15**, 130. https://doi.org/10.1007/s12520-023-01825-1.

Hubau, W., Beeckman, H., Kitin, P., Mees, F., van den Bulcke, J. and van Acker, J. (2012). Charcoal identification in species-rich biomes: A protocol for Central Africa optimised for the Mayumbe forest. *Review of Palaeobotany and Palynology*, **171**, 164-178. https://doi.org/10.1016/j.revpalbo.2011.11.002.

Kabukcu, C. and Chabal, L. (2021). Sampling and quantitative analysis methods in anthracology from archaeological contexts: Achievements and prospects. *Quaternary International*, **593-594,** 6-18. https://doi.org/10.1016/j.quaint.2021.05.013.

Karkanas, P., Ayalon, A., Bar-Matthews, M., Barkai, R., Gopher, A., Shahack-Gross, R., and Stiner, M. (2007). Evidence for habitual use of fire at the end of the Lower Paleolithic: Site-formation processes at Qesem Cave, Israel. *Journal of Human Evolution*, **53**(2), 197-212. https://doi.org/10.1016/j.jhevol.2007.04.002.

Kromhout, C. (1975). n Sleutel vir die mikroskopiese uitkenning van die vernaamste in- heemse houtsoorte van Suid-Afrika. Unpublished PhD Thesis, University of Stellenbosch, Stellenbosch.

Kühl, N., Gebhardt, C., Hense, A., and Litt, T. (2002). Probability density functions as botanical climatological transfer functions for climate reconstruction. *Quaternary Research*, **58**, 381-392.

Lee-Thorp, J. A. and Ecker, M. (2015). Holocene climate and environmental changes from stable isotopes in ostrich egg shell at Wonderwerk Cave, South Africa. *African Archaeological Reviews*, **32**(4), 793-811. https://doi.org/10.1007/s10437-015-9202-y.

Leney, L. and Casteel, R. (1975). Simplified procedure for examining charcoal specimens for identification. *Journal of Archaeological Science*, **2**, 153–159. https://doi.org/10.1016/0305-4403(75)90035-7.

Lennox, S., Bamford, M. and Wadley, L. (2015). Charcoal analysis from 49 000-year-old hearths at Sibudu: Implications for wood uses and the Kwazulu-Natal environment. *The South African Archaeological Bulletin*, **70**(201), 36–52.

Lennox, S.J. and Bamford, M.K. (2017). Identifying Asteraceae, particularly *Tarchonanthus parvicapitulatus* in archaeological charcoal from the Middle Stone

Age. *Quaternary International*, **457**, 155-171. http://dx.doi.org/10.1016/j.quaint.2017.03.074.

Lennox, S., Backwell, L., d'Errico, F. and Wadley, L. (2022). A vegetation record based on charcoal analysis from Border Cave, KwaZulu-Natal, South Africa, ~227 000 to ~44 000 years ago. *Quaternary Science Reviews*. **293.** https://doi.org/10.1016/j.quascirev.2022.107676.

Leonardi, M., Beyer, R., Hallett, E. Krapp, M. and Manica, A. (2023). Pastclim 1.2: an R package to easily access and use paleoclimatic reconstructions. *Ecography,* **2023**(3). https://doi.org/10.1111/ecog.06481.

Malan, B.D. and Cooke, H.B.S. (1941). A preliminary account of the Wonderwerk Cave, Kuruman District. *South African Journal Of Science*, **37**, 300-312.

Matsika, R., Erasmus, B.F.N. and Twine, W.C. (2013). Double jeopardy: The dichotomy of fuelwood use in rural South Africa. *Energy Policy,* **52,** 716-725. https://doi.org/10.1016/j.enpol.2012.10.030.

Martínez-Cabrera, H.I. and Estrada-Ruiz, E. (2014) Wood Anatomy Reveals High Theoretical Hydraulic Conductivity and Low Resistance to Vessel Implosion in a Cretaceous Fossil Forest from Northern Mexico. *PLoS ONE*, **9**(10): e108866. https://doi.org/10.1371/journal.pone.0108866.

Mauri, A., Collins, P.M., Davis, B.A.S. and Kaplan, J.O. (2015). The climate of Europe during the Holocene: a gridded pollen-based reconstruction and its multi-proxy evaluation. *Quaternary Science Reviews*, **112**, 109-127. https://doi.org/10.1016/j.quascirev.2015.01.013.

Metwally, A.A., Bamford, M., Neumann, F., Scott, L. and Oberhänsli, H. (2014). Holocene palynology and palaeoenvironments in the Savanna Biome at Tswaing Crater, central South Africa. *Palaeogeography Palaeoclimatology Palaeoecology*. **402**, 125-135. https://doi.org/10.1016/j.palaeo.2014.03.019.

Miller, C., Finch, J., Hill, T., Humphries, M., Peterse, F., Schefuß, E. and Zabel, M. (2019) Late Quaternary climate variability at Mfabeni peatland, eastern South Africa. *Climate of the Past*, **15**, 1153–1170. https://doi.org/10.5194/cp-15-1153-2019.

Mosbrugger, V. and Utescher, T. (1997). The coexistence approach — a method for quantitative reconstructions of Tertiary terrestrial palaeoclimate data using plant fossils. *Palaeogeography, Palaeoclimatology, Palaeoecology*, **134**, 61 86.

Mucina, L. and Rutherford, M.C. (eds) 2006. *The Vegetation of South Africa, Lesotho and*

Swaziland. Strelitzia 19. Pretoria: South African National Biodiversity Institute.

Mucina, L., Hoare, D.B., Lötter, M.C., du Preez, P.J., Rutherford, M.C., Scott-Shaw, C.R., Bredenkamp, G.J., Powrie, L.W., Scott, L., Camp, K.G.T., Cilliers, S.S., Bezuidenhout, H., Mostert, T.H., Siebert, S.J., Winter, P.J.D, Burrows, J.E., Dobson, L., Ward, R.A., Stalmans, M., Oliver, E.G.H., Siebert, F., Schmidt, E., Kobisi, K., and Kose, L. (2006). Grassland Biome in Mucina, L. and Rutherford, M.C. (eds). *The Vegetation of South Africa, Lesotho and Swaziland.* Strelitzia 19. Pretoria: South African National Biodiversity Institute, 349-437.

Nash, D.J., Gulliver, V.L. and Meadows, M.E. (2006). Holocene environmental change in the Okavango Panhandle, northwest Botswana. *Quaternary Science Reviews*, **25**(11-12), 1302-1322. https://doi.org/10.1016/j.quascirev.2005.11.00.

Neumann, F.H., Bousman, C.B., Scott, L., and van As, L. (2010). A Holocene sequence of vegetation change at Lake Eteza, coastal KwaZulu-Natal, South Africa. *Review of Palaeobotany and Palynology*, **162**(1), 39-53. https://doi.org/10.1016/j.revpalbo.2010.05.001.

Norström, E., Holmgren, K., Partridge, T.C., Risberg, J. and Scott, L. (2009). Reconstruction of environmental and climate changes at Braamhoek wetland, eastern escarpment South Africa, during the last 16,000 years with emphasis on

the Pleistocene–Holocene transition. *Palaeogeography, Palaeoclimatology, Palaeoecology,* **271**(3-4), 240-258. https://doi.org/10.1016/j.palaeo.2008.10.018.

Norström, E., Bamford, M., Holmstrand, H., Lundqvist, S., Neumann, F., Scott, L., Smittenberg, R., Snowball, I., Sundqvist, H. and Risberg, J. (2014). Late Quaternary vegetation dynamics and hydro-climate in the Drakensberg, South Africa. Quaternary *Science Reviews*, **105**. 48–65. https://doi.org/10.1016/j.quascirev.2014.09.016.

Olajuyigbe, O.O. and Afolayan, A.J. (2013). Evaluation of combination effects of ethanolic extract of *Ziziphus mucronata* Willd. subsp. *mucronata* and antibiotics against clinically important bacteria. *The Scientific World Journal*, **2013**. Article ID: 769594. https://doi.org/10.1155/2013/769594.

Oskolski, A.A. and Van Wyk, B.E. (2008). Systematic and phylogenetic value of wood anatomy in Heteromorpheae (Apiaceae, Apioideae). *Botanical Journal of the Linnean Society*, **158**(4), 569–583. https://doi.org/10.1111/j.1095-8339.2008.00928.x.

Palmer, E. and Pitman, N. (1972) *Trees of Southern Africa, Covering All Known Indigenous Species in the Republic of South Africa, South-West Africa, Botswana, Lesotho and Swaziland*. Cape Town: Balkema.

Parkington, J., Baxter, A., Cartwright, C. and Cowling, R.M. (2000). Palaeovegetation at the last glacial maximum in the Western Cape, South Africa: Wood charcoal and pollen evidence from Elands Bay Cave. *South African Journal of Science,* **96**.

Pournou, A. (2020). Wood Anatomy, Chemistry and Physical Properties. In: Biodeterioration of Wooden Cultural Heritage. Springer, Cham. https://doi.org/10.1007/978-3-030-46504-9_1.

Prior, J., and Alvin, K.L. (1986). Structural Changes on Charring Woods of Dichrostachys and Salix from Southern Africa: The Effect of Moisture

Content. *IAWA Journal*, **7(3)**, 243-250. https://doi.org/10.1163/22941932-90000993.

Prior, J. and Gasson, P. (1993). Anatomical changes on charring six African hardwoods. *IAWA Journal*, **14**, 77-86.

Puech, E., Bamford, M., Porraz, G., Théry-Parisot, I. and Val, A. (2021). Evaluating Sampling Methods in Charcoal-Rich Layers and High Diversity Environment: A Case Study from the Later Stone Age of Bushman Rock Shelter, South Africa. *Quaternary International*, **593–594**, 36-49. https://doi.org/10.1016/j.quaint.2020.11.018.

Red Cross Climate Centre, (2021). Climate Profiles of Countries in Southern Africa: South Africa. The Hague: RCRC. https://www.climatecentre.org/publications/6006/climate-factsheet-south-africa/ (Accessed 23 July 2023).

Renssen, H., Brovkin, V., Fichefet, T. and Goosse, H. (2006). Simulation of the Holocene climate evolution in Northern Africa: The termination of the African Humid Period. *Quaternary International*, **150**(1), 95-102. https://doi.org/10.1016/j.quaint.2005.01.001.

Rhodes, S.E., Boarette, E., Chazan, M., Ecker, M., Goldberg, P. and Horwitz, L.K. (2022). Exploring the Later Stone Age at a Micro-Scale: New High-Resolution Excavations at Wonderwerk Cave. *Quaternary International*, **614**, 136-145. https://doi.org/10.1016/J.Quaint.2021.10.004.

Roffe, S.J., Curtis, C.J. and Fitchett, J.M. (2019). Classifying and mapping rainfall seasonality in South Africa: A review. *South African Geographical Journal,* **101**(2), 158-174. https://doi.org/10.1080/03736245.2019.1573151.

Roffe, S.J., Curtis, C.J. and Fitchett, J.M. (2021). Quantifying rainfall seasonality across South Africa on the basis of the relationship between rainfall and

temperature. *Climate Dynamics,* **56**, 2431–2450. https://doi.org/ 10.1007/s00382-020-05597-5.

Rossouw, L. (2016). An Early Pleistocene Record from Wonderwerk Cave, South Africa. *African Archaeological Review*, **33**, 251-263. https://doi.org/10.1007/s10437-016-9227-x.

Rutherford, M.C., Mucina, L., Lötter, M.C., Bredenkamp, G.J., Smit, J.H.L., Scott-Shaw, C.R., Hoare, D.B., Goodman, P.S., Bezuidenhout, H., Scott, L., Ellis, F., Powrie, L.W., Siebert, F., Mostert, T.H., Henning, B.J., Venter, C.E., Camp, K.G.T., Siebert, S.J., Matthews, W.S., Burrows, J.E., Dobson, L., van Rooyen, N., Schmidt, E., Winter, P.J.D., du Preez, P.J., Ward, R.A., Williamson S. and Hurter, P.J.H. (2006). Savaanna Biome in Mucina, L. and Rutherford, M.C. (eds). *The Vegetation of South Africa, Lesotho and Swaziland.* Strelitzia 19. Pretoria: South African National Biodiversity Institute, 439-538.
SANBI (2023). SANBI Biodiversity for life, Plantzafrica.com. Pza.sanbi.org/vachellia-karroo (Accessed 11 August 2023).

Salisbury, E. J. and Jane, F. W. (1940). Charcoals from Maiden Castle and their Significance in Relation to the Vegetation and Climatic Conditions in Prehistoric Times, *Journal of Ecology*, **28(2)**, 310–325. https://doi.org/10.2307/2256232.

Scheel-Ybert, R. (2002). Evaluation of sample reliability in extant

and fossil assemblages. In S. Thiébault (ed.), *Charcoal Analysis: Methodological Approaches, Palaeoecological Results and Wood Uses. Proceedings of the Second International Meeting in Anthracology, Paris, September 2000*, 9–16. BAR International Series 1063. Archaeopress, Oxford.Schirarend, C. (1991). The Systematic Wood Anatomy of the Rhamnaceae Juss. (Rhamnales). I. Tribe Zizipheae. *IAWA Journal*, **12**(4), 359-388. https://doi.org/10.1163/22941932-90000540.

Scott, L. (1987). Pollen analysis of hyena coprolites and sediments from Equus Cave, Taung, southern Kalahari (South Africa). *Quaternary Research,* **28**(1), 144-156. https://doi.org/10.1016/0033-5894(87)90039-1.

Scott, L., Holmgren, K., Talma, S., Vogel, J.C. and Woodborne, S. (2003). Age interpretation of the Wonderkrater spring sediments and vegetation change in the Savanna Biome, Limpopo province, South Africa. *South African Journal of Science*, **93**(9), 484-488.

Scott, L., Bousman, C.B. and Nyakale, M. (2005). Holocene pollen from swamp, cave and hyrax dung deposits at Blydefontein (Kikvorsberge), Karoo, South Africa. *Quaternary International*, **129**(1), 49-59. https://doi.org.10.1016/j.quaint.2004.04.006.

Scott, L. and Thackeray, J.F. (2015). Palynology of Holocene Deposits in Excavation 1 at Wonderwerk Cave, Northern Cape (South Africa). *African Archaeological Reviews,* **32 (**4), 1–17. https://doi.org/10.1007/s10437-015-9204-9.

Scott, L., Horwitz, L., Fernandez Jalvo, Y., Gil-Romera, G., Neumann, F., Sobol, M. and van Aardt, A. (2022). Late Quaternary palaeoenvironments in the central semi-arid region of South Africa from pollen in cave, pan, spring, stream and dung deposits. *Quaternary International*, **614**, 84-97. https://doi.org10.1016/j.quaint.2020.10.065.

Shaar, R., Arnold, M., Aumaître, G., Bourlès, D., Chazan, M., Ebert, Y., Horwitz, L.K., Keddadouche, K. and Matmon, A. (2021). Magnetostratigraphy and cosmogenic dating of Wonderwerk Cave: New constraints for the chronology of the South African Earlier Stone Age*. Quaternary Science Reviews*, **259**. https://doi.org/10.1016/j.quascirev.2021.106907.

Shackleton, C.M. and Prins, F. (1992). Charcoal analysis and the “Principle of least effort”- A conceptual model. *Journal of Archaeological Science*, **19**(6), 631-637. https://doi.org/10.1016/0305-4403(92)90033-Y.

Shanahan, T., McKay, N.P., Hughen, K.A., Overpeck, J.T., Otto-Bliesner, B., Heil, C.W., King, J., Scholz, C. A. and Peck, J. (2015). The time-transgressive termination of the African Humid Period. *Nature Geoscience,* **8**, 140–144. https://doi.org/10.1038/ngeo2329.

Smit, P.J. (1978). Groundwater Recharge in the Dolomite of the Ghaap Plateau near Kuruman in the Northern Cape, Republic of South Africa. *Water SA*, **4**(2), 81-92.

Sonsin, J.O., Gasson, P.E., Barros, C.F. and Marcati, C.R. (2012). A comparison of the wood anatomy of 11 species from two cerrado habitats (cerrado s.s. and adjacent gallery forest). *Botanical Journal of the Linnean Society*, **170**(2), 257–276. https://doi.org/10.1111/j.1095-8339.2012.01282.x.

Terrazas, T. (1999). Wood anatomy of Anacardiaceae with emphasis on American. *Botanical Sciences*, **64**, 103-109. https://doi.org/10.17129/botsci.1587.

Thackeray, J.F. (2015). Faunal Remains from Holocene Deposits, Excavation 1, Wonderwerk Cave, South Africa. *African Archaeological Review*, **32**, 729-750. https://doi.org/10.1007/s10437-015-9201-z.

Théry-Parisot, I., Chabal, L. and Chrzavzez, J. (2010). Anthracology and taphonomy, from wood gathering to charcoal analysis. A review of the taphonomic processes modifying charcoal assemblages. *Palaeogeography, Palaeoclimatology, Palaeoecology*, **291**(1-2), 142-153. https://doi.org/10.1016/j.palaeo.2009.09.016.

Théry-Parisot, I. and Henry, A. (2012). Seasoned or green? Radial cracks analysis as a method for identifying the use of green wood as fuel in archaeological charcoal. *Journal of Archaeological Science*, **39**(2), 381-388. https://doi.org/10.1016/j.jas.2011.09.024.

Utescher, T., Bruch, A.A., Erdei, B., Francois, L., Jacques, F.M.B., Kern, A.K., Liu, Y.S.C., Mosbrugger, V. and Spicer, R.A. (2014). The Co-Existence Approach-Theoretical Background and Practical Considerations of Using Plant Fossils for

Climate Quantification. *Palaeogeography, Palaeoclimatology, Palaeoecology,* **410**, 58-73. https://doi.org/10.1016/j.palaeo.2014.05.031.

van Wyk, B. and van Wyk, P. (2013). *Field guide to trees of southern Africa*. 2nd ed. Cape Town: Struik Nature.

Vidal-Matutano, P. (2017). Firewood and hearths: Middle Palaeolithic woody taxa distribution from El Salt, stratigraphic unit Xb (Eastern Iberia). *Quaternary International*, **457**, 74-84. https://doi.org/10.1016/j.quaint.2016.07.040.

Vogel, J., Fuls, A. and Visser, E. (1986). Pretoria Radiocarbon Dates III. *Radiocarbon*, **28**(3), 1133-1172. https://doi.org/10.1017/S003382220002018X.

Wadley, L., Backwell, L., d'Errico, F., Esteban, I., Lennox, S., Marine, W., Orange, F., Peña, P., Rosso, D., Sievers, C. and Stratford, D. (2020). Fire and grass-bedding construction 200 thousand years ago at Border Cave, South Africa. *Science,* **369**, 863-866. https://doi.org/10.1126/science.abc7239.

Wheeler, E.A., Baas, P. and Gasson, P.E. (1989). IAWA list of microscopic features for hardwood identification. *IAWA Bulletin,* **10**(3), 201- 232.

Wheeler, E.A. and Baas, P. (1993). The potentials and limitations of dicotyledonous wood anatomy for climatic reconstructions. *Paleobiology*, **19**, 487-498.

Wheeler, E.A., Baas, P. and Rodgers, S. (2007). Variations in Dicot Wood Anatomy: A Global Analysis Based on the Insidewood Database. *International Association of Wood Anatomists Journal*, **28**, 229-258.

Wheeler, E.A. (2011). InsIdeWood – A web resource for hardwood anatomy. *IAWA Journal*, **32**(2), 199-211. https://insidewood.lib.ncsu.edu/.

Wiemann, M.C., Wheeler, E.A., Manchester, S.R. and Portier, K.M. (1998). Dicotyledonous wood anatomical features as predictors of climate. *Palaeogeography, Palaeoclimatology, Palaeoecology*, **139**, 83-100.

Wolfe, J.A. and Upchurch, G.R. (1987). North American nonmarine climates and vegetation during the Late Cretaceous. *Palaeogeography, Palaeoclimatology, Palaeoecology*, **61**, 33-77.

Zamani Project Team (2023). Zamani Project. https://www.zamaniproject.org/site-south-africa-wonderwerk-cave.html/ (Accessed 4 December 2023).

Zheng J., Jansen S., Morris H. and Zhao X. (2019) Phylogeny Best Explains Latitudinal Patterns of Xylem Tissue Fractions for Woody Angiosperm Species Across China. *Frontiers in Plant Science*, **10**(556). https:doi.org/10.3389/fpls.2019.00556.

Zicherman, J.B. and Williamson, R.B. (1981). Microstructure of wood char. *Wood Science and Technology*, **15**, 237-249. https://doi.org/10.1007/BF00350942.

Zwane, B. and Bamford, M. (2021). A reconstruction of woody vegetation, environment and wood use at Sibudu Cave, South Africa, based on charcoal that is dated between 73 and 72 ka. *Quaternary International*, **593–594**, 95-103. https://doi.org/10.1016/j.quaint.2020.10.026.

Zwane, B. and Bamford, M. (2021). Wood charcoal from Border Cave's Member 1RGBS: Evidence for the environment and plant use during MIS 5. *African Archaeological Reviews,* **38,** 657-674. https://doi.org/10.1007/s10437-021-09448-4.

Appendix A: List of woody vegetation growing in the adjacent biozones; SVk 7, 8 and 9 (Rutherford *et al.,* 2006).

Plant type	**Ghaap Plateau Vaalbosveld (SVk 7)**	**Kuruman Vaalbosveld (SVk 8)**	**Kuruman Thornveld (SVk 9)**
Small trees	*Boscia albitrunca, Searsia lancea, Senegalia mellifera*	*Searsia lancea, Vachellia karroo, Ziziphus mucronata*	*Boscia albitrunca, Senegalia mellifera* subsp. *detinens*

	subsp. *detinens, Vachellia karroo, V. tortilis* subsp. *heteracantha*		
Tall trees	*Vachellia erioloba*	*Vachellia erioloba*	*Vachellia erioloba*
Low shrubs	*Aptosimum procumbens, Chrysocoma ciliata, Helichrysum zeyheri, Hermannia comosa, Lantana rugosa, Leucas capensis, Melolobium microphyllum, Peliostomum leucorrhizum, Pentzia globosa, P. viridis, Vachellia hebeclada* subsp. *hebeclada, Zygophyllum pubescens.*	*Amphiglossa triflora, Anthospermum rigidum* subsp. *pumilum, A. rigidum* subsp. *rigidum, Helichrysum zeyheri*	*Gnidia polycephala, Helichrysum zeyheri, Hermannia comosa, Monechma divaricatum, Pentzia calcarea, Plinthus sericeus, Vachellia hebeclada* subsp. *hebeclada*
Tall shrubs	*Diospyros austro-africana, D. pallens, Ehretia rigida* subsp. *rigida, Euclea crispa* subsp. *ovata, Grewia flava, Gymnosporia buxifolia, Lessertia*	*Cadaba aphylla, Diospyros austroafricana, D. lycioides* subsp. *lycioides, Grewia flava, Gymnosporia buxifolia,*	*Grewia flava, Gymnosporia buxifolia, Lycium hirsutum, Tarchonanthus camphoratus*

	frutescens, Olea europaea subsp. *africana, Rhigozum trichotomum, Searsia tridactyla, Tarchonanthus camphoratus, Ziziphus mucronata*	*Tarchonanthus camphoratus*	
Graminoids	*Aristida adscensionis, A. congesta, A. diffusa, Anthephora pubescens, Cenchrus ciliaris, Cymbopogon pospischilii, Digitaria eriantha* subsp. *eriantha, Enneapogon scoparius, E. cenchroides, E. desvauxii, Eragrostis echinochloidea, E. lehmanniana, E. obtusa, E. rigidior, E. superba, Fingerhuthia africana, Heteropogon contortus, Schmidtia pappophoroides, Sporobolus fimbriatus, Stipagrostis uniplumis, Themeda triandra,*	*Anthephora pubescens, Aristida meridionalis, A. stipitata* subsp. *spicata, Cymbopogon caesius, Digitaria eriantha* subsp. *eriantha, Eragrostis lehmanniana, uniplumis, Fingerhuthia africana, Pogonarthria squarrosa, Schmidtia pappophoroides, Themeda triandra, Tragus koelerioides*	*Aristida meridionalis, A. stipitata* subsp. *stipitata, Eragrostis lehmanniana, E. echinochloidea, Melinis repens*

	Tragus racemosus		

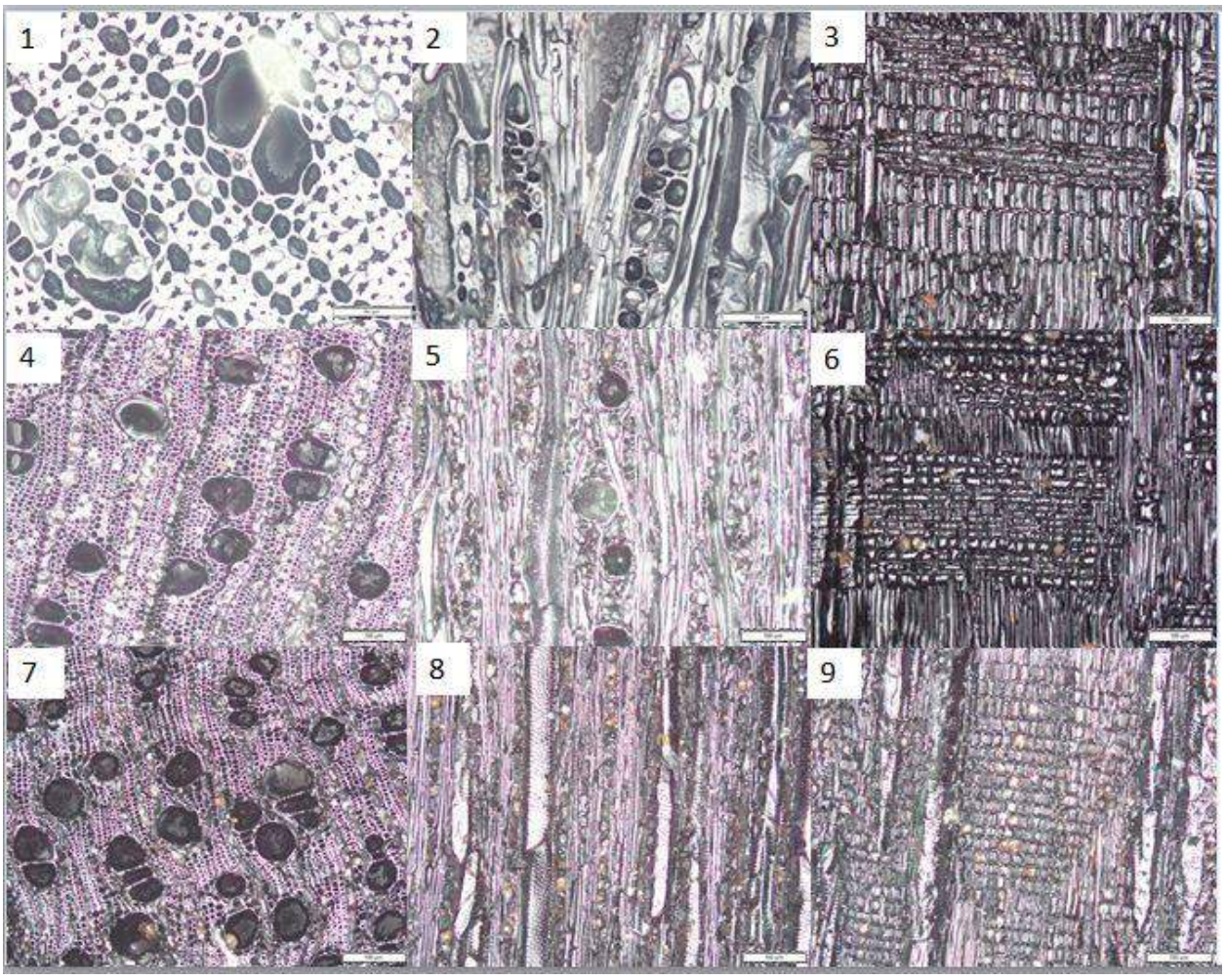
Appendix B: Summarized descriptions of the comparative charcoal anatomy. Charcoal described using the numbered features descriptions from Wheeler *et al.,* (1989).

Taxa	IAWA descriptions
Berchemia zeyheri (BPI/20/252)	2, 5, 7 (1-3 rm), 13, 22, 25, 30, 41, 49, 52, 58, 61, 66, 69, 71, 72, 78, 91, 92, 97, 107 (marginal cells upright), 115
Brachylaena discolor (BPI/20/721)	2, 5, 7, 10v, 11v, 13, 22, 24, 40, 49, 52, 61, 69, 78, 79v, 106, 116, 118, 136, 138
Commiphora schimperi (BPI/20/561)	2, 5, 7 (1-2 rm), 13, 22, 23, 24, 26v, 40, 48 (31 vessels/ mm^2), 52, 68, 75, 78, 97, 109, 115, 130, 136, 137
Diospyros abyssinica (InsideWood)	2, 5, 7v, 130v, 13, 22, 23, 25, 30, 40v, 41, 48, 49, 52v, 58, 61, 66, 69, 70, 71v, 76, 77, 78v, 86, 91v, 96, 106, 116
Diospyros austro-africana (BPI/20/574)	2, 5, 7 (1-3 rm), 13, 22, 25, 40 (45 µm), 47 (12 vessels/ mm^2), 52, 68, 78, 96, 105, 116
Ehretia rigida (Bamford, 2015b)	2, 5, 7 (1-3 vessels), 13, 22, 25, 30, 41 (80 µm), 48 (40 vessels/ mm^2), 52, 70, 80, 83, 93, 98 (4-8 cells), 106, 115
Euclea undulata (BPI/20/274)	2, 5, 10, 13, 22, 24, 30, 41, 47, 52, 61, 66, 68, 77, 78, 97, 105, 116, 136, 137
Euclea undulata (BPI/20/3)	2, 5, 7, 10, 13, 22, 24, 41 (60 µm), 49 (53 vessels/ mm^2), 52, 68, 78, 96, 98, 103, 105, 116
Grewia flava (BPI/20/691)	2, 4, 7 (1-3 rm), 13, 22, 27, 41, 48, 52, 69, 78, 79, 98, 107 (marginal cells upright), 115, 136, 137 (upright cells)
*Halleria lucida (*BPI/20/684)	2, 5, 7, 13, 22, 24, 30, 40v, 52, 61, 70, 75, 98, 102, 109, 115
Heteromorpha arborescens (InsideWood)	2, 5, 6, 7v, 8v, 11, 12v, 13, 20v, 21v, 22, 25, 26, 30, 36, 37, 40, 41, 49, 52, 53, 61, 65, 66, 68v, 69v, 71, 78, 106, 107, 110, 114, 115, 130v
Iboza riparia (BPI/20/605)	2, 5, 9, 13, 22, 25, 40, 49, 522, 70, 80, 83, 105, 115
Olea europaea subsp. *africana* (BPI/20/931)	2, 5, 7 (1-3 rm), 13, 22, 24, 30, 40, 49, 61, 66, 70, 78, 79, 107, 115
Olinia ventosa (BPI/20/308)	2, 5, 7 (1-3 rm), 13, 22, 24, 29, 30, 40, 41, 48 (29 vessels/ mm^2), 52, 61, 66, 70, 72, 78, 97, 100, 108, 115
Ozoroa paniculosa (BPI/20/15)	2, 5, 7 (1-3 rm), 13, 22, 26v, 27v, 41, 48 (28 vessels/ mm^2), 52, 61, 67, 78, 79, 97 (1-2 cells), 109, 115
Protea caffra (BPI/20/641)	2, 5, 9, 13, 22, 25v, 40, 49, 52, 70, 80, 83, 99, 108 (marginal upright cells), 115
Searsia lancea (BPI/20/537)	2, 5, 7 (1-3 rm), 13, 22, 25, 41 (80 µm), 49v (42 vessels/ mm^2), 52, 68, 78, 97, 107, 116, 130, 136, 137
Searsia pyroides (BPI/20/766)	2, 4, 7 (1-3 rm), 13, 22, 27, 41 (87 µm), 48 (36 vessels/ mm^2), 52, 68, 78, 97, 107 (body cells procumbent, marginal cells square), 116, 130, 136, 137 (square cells)

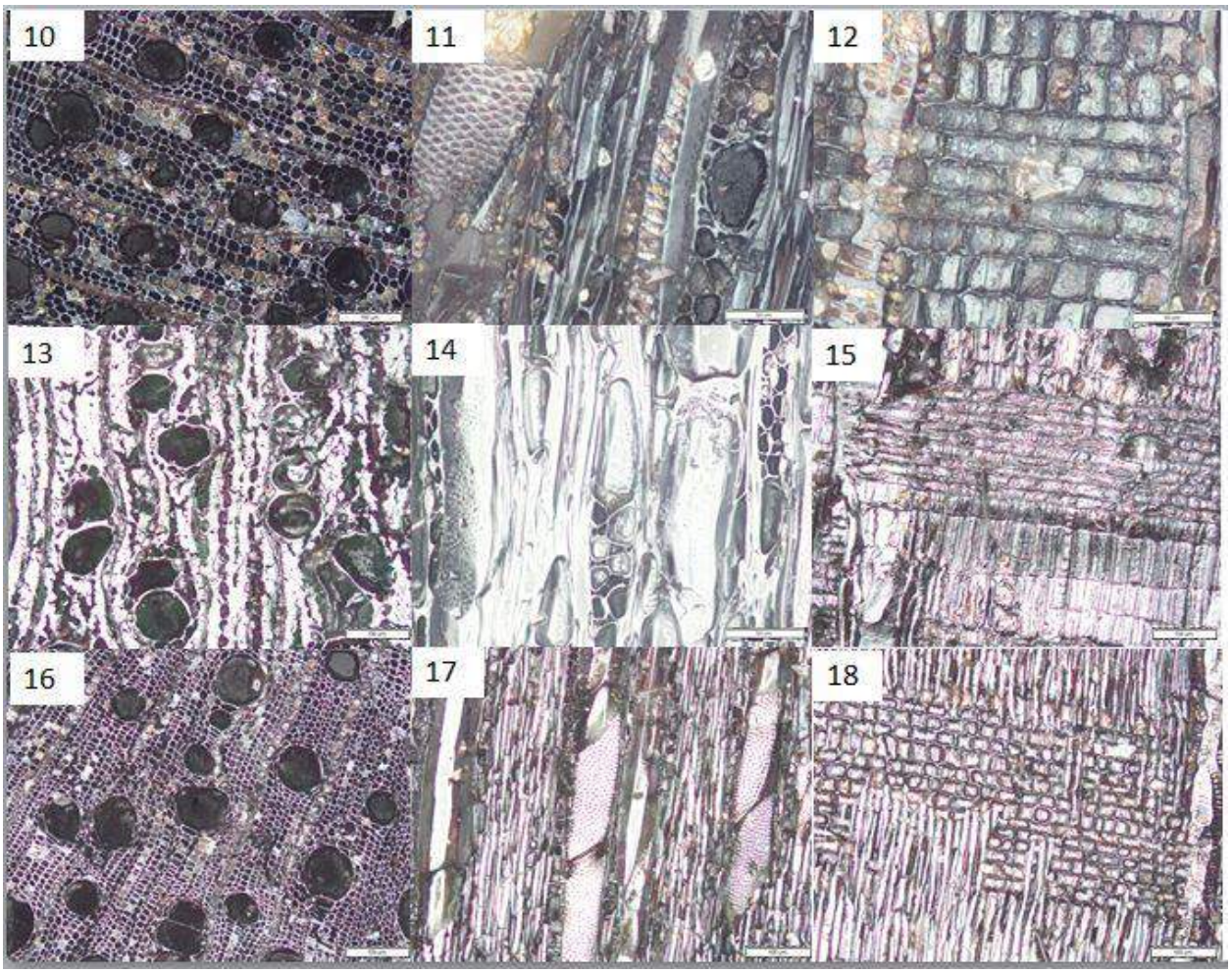
Senegalia caffra (BPI/20/716)	2, 5, 13, 22, 24, 29, 30, 42, 47 (10 vessels/ mm^2), 52, 61, 66, 69, 80, 81, 83, 98 (1-5 cells), 104, 115
Senegalia sieberiana (BPI/20/721)	2, 5, 13, 22, 24, 29, 30, 42, 47 (7 vessels/ mm^2), 52, 61, 66, 69, 80, 81, 83, 98, 102v (0.4-1.2 mm), 104, 115
Strychnos decussata (InsideWood)	2, 5, 7, 8, 10v, 11v, 13, 22, 25, 29, 30, 40v, 41v, 48v, 52, 1, 66, 70, 71v, 76, 77v, 78, 79, 86v, 93, 98, 107, 110, 115, 134, 136, 138, 139, 155v
Strychnos mitis (InsideWood)	2, 5, 7, 8, 10v, 13, 22, 24v, 25, 29, 30, 40v, 41, 48v, 49, 52v, 61, 66, 69, 71v, 76, 77v, 78, 79v, 83v, 86, 93, 94, 98, 107, 115, 134, 136, 138, 141v, 155v
Tarchonanthus camphoratus (BPI/20/421)	2, 5, 7 (1-3 rm), 11, 13, 22, 24, 40, 49, 52, 69, 76, 78, 97 (1-2 cells), 106, 115
Tarchonanthus littoralis (BPI/20/745)	2, 5, 7, 10, 13, 22, 24, 40, 49, 52, 69, 78, 97, 107 (2 rows of square marginal cells), 116
Tarchonanthus parvicapitulatus (BPI/20/454)	2, 5, 7, 10, 13, 22, 24, 40, 50 (120-150 vessels/ mm^2), 52, 69, 78, 97 (1-2 cells), 106, 115
Tarchonanthus trilobus (BPI/20/420)	2, 5, 7, 10, 13, 22, 24, 30, 41v, 49, 52, 61, 66, 69, 78, 97 (1-2 cells), 104, 116, 136, 138
Vachellia erioloba (BPI/20/717)	2, 5, 13, 22, 24, 29, 30, 41, 48, 52, 58, 61, 66, 70, 80, 81, 91, 98, 104, 115
Vachellia karroo (BPI/20/01)	2, 5, 13, 22, 26, 29, 30, 41, 47, 52, 62, 66, 69, 80, 81, 83, 85, 98 (2-8 cells), 104, 115
Vachellia tortilis (BPI/20/409)	2, 5, 13, 26, 29, 30, 41, 42V, 47 (32 vessels/ mm^2), 52, 61, 69, 70, 76, 80, 81, 83, 85, 98 (4-6 cells), 104, 115
Ziziphus mucronata (BPI/20/647)	2, 5, 10, 13, 22, 26, 30, 41 (72 µm), 49v (42 vessels/ mm^2), 52, 53, 61, 66, 68, 79, 96, 105, 116, 136, 137

v= variable, rm= radial multiples

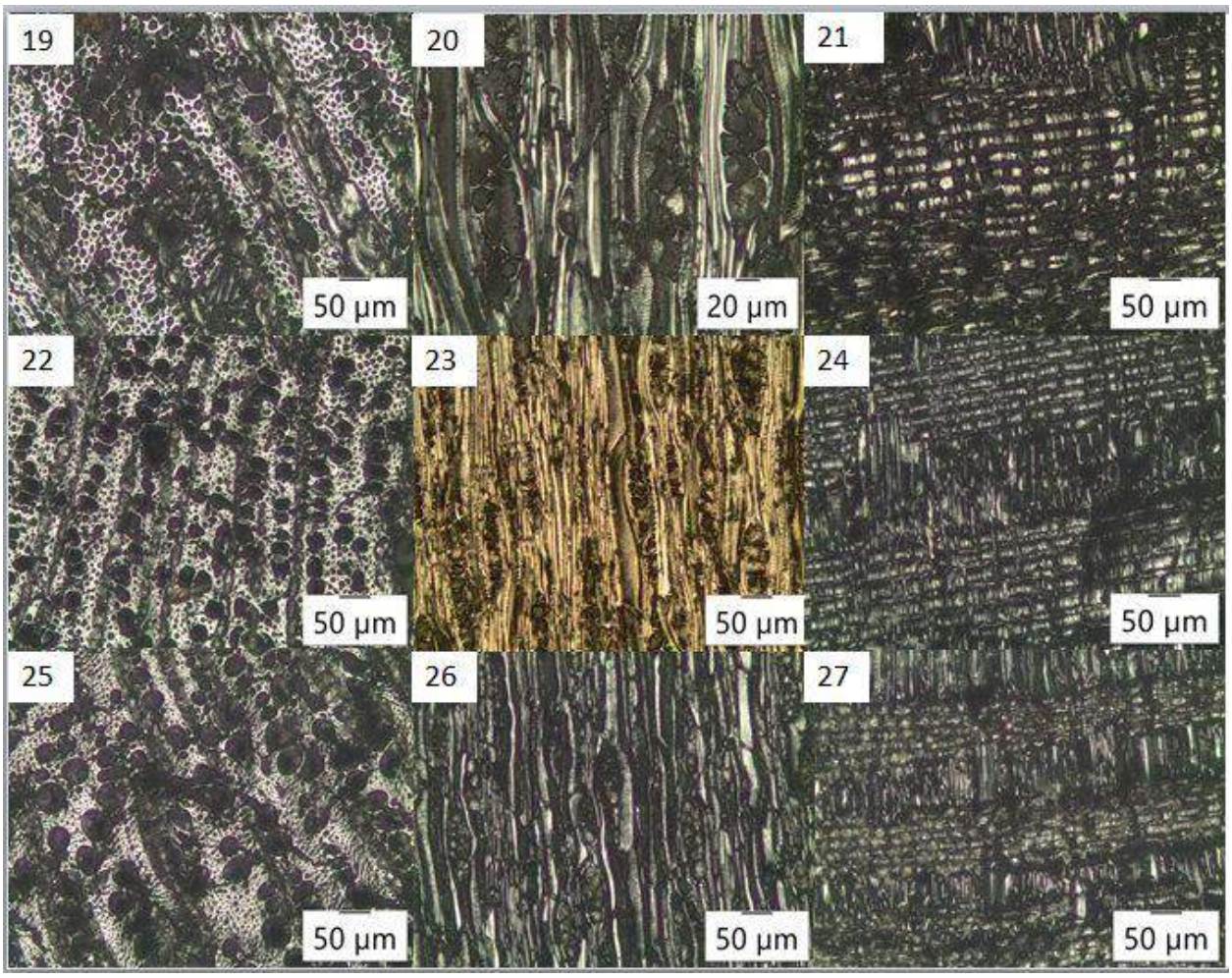
Appendix C: Photomicrographs of (1-3) *Olinia ventosa*, (4-6) *Searsia lancea* and (7-9) *Ziziphus mucronata.*



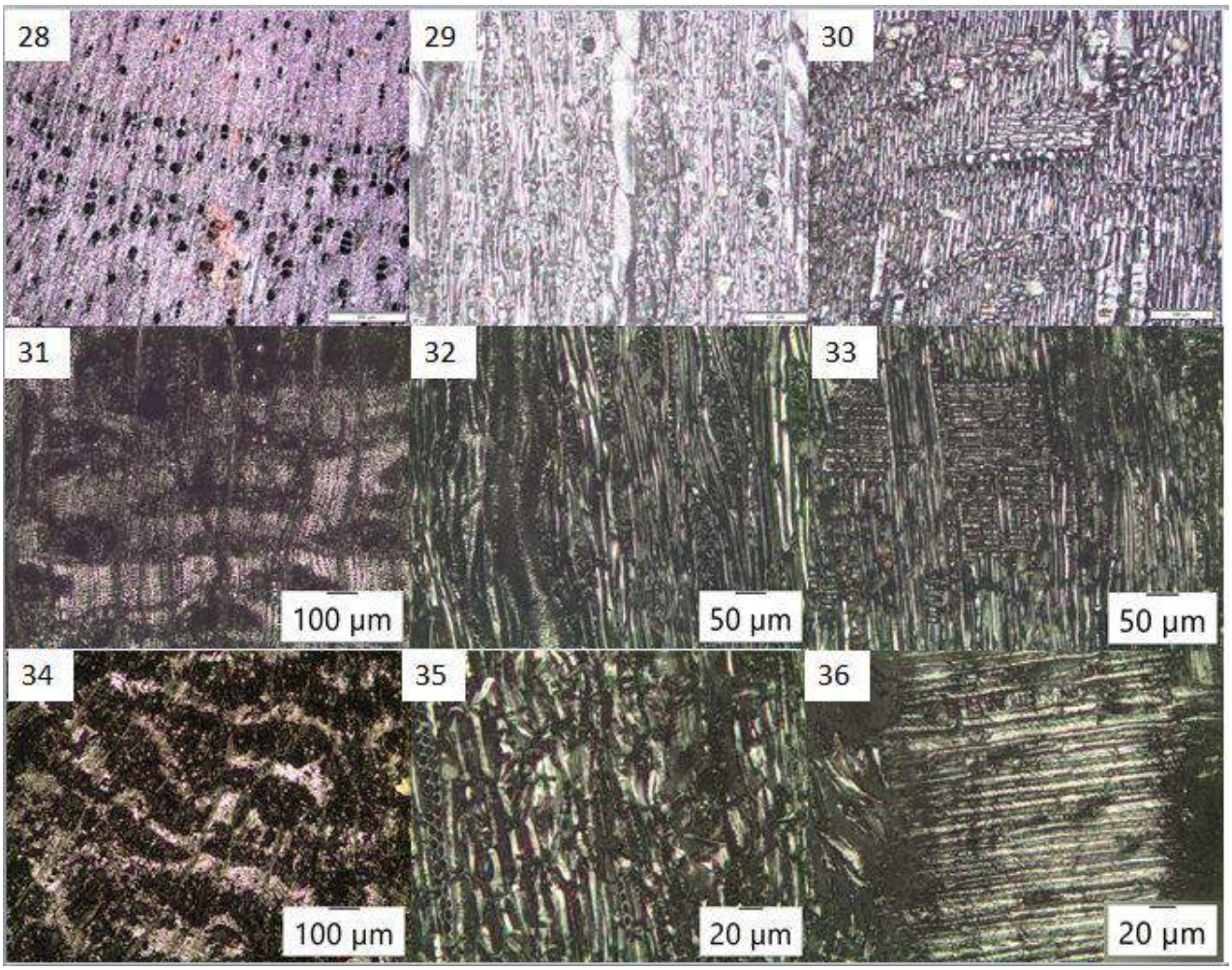
Appendix D: Photomicrographs of (10-12) *Commiphora schimperi*, (13-15) *Olea europaea* subsp. *africana* and (16-18) *Ozoroa paniculosa.*



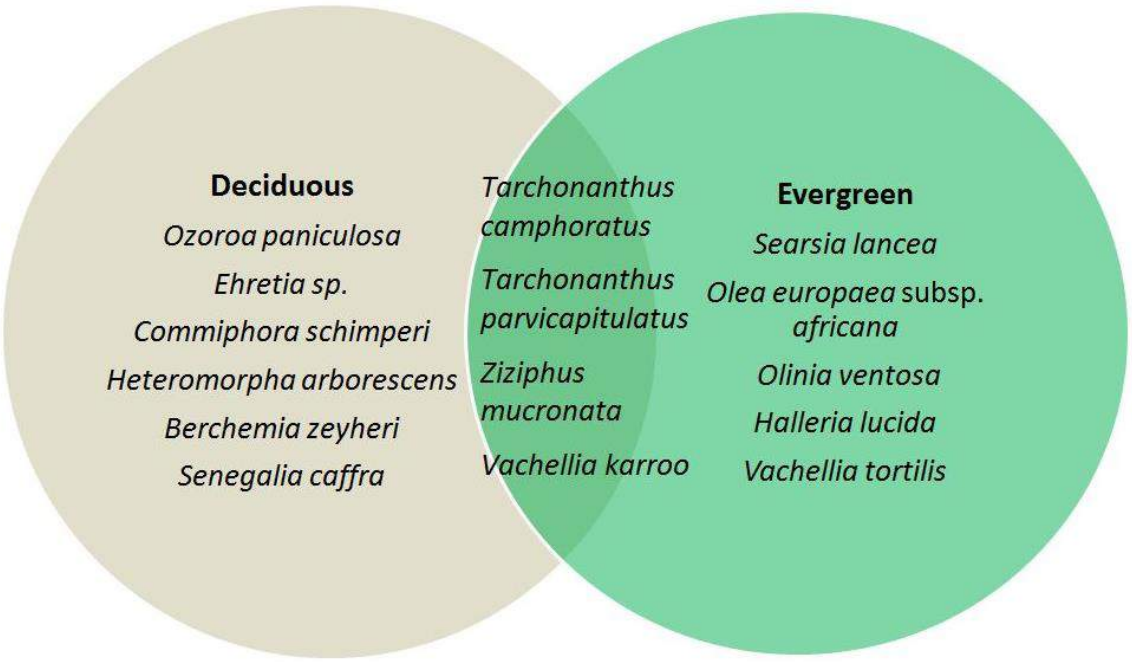
Appendix E: Photomicrographs of (19-21) *Tarchonanthus camphoratus*, (22-24) *T. parvicapitulatus* and (25-27) *T. trilobus.*



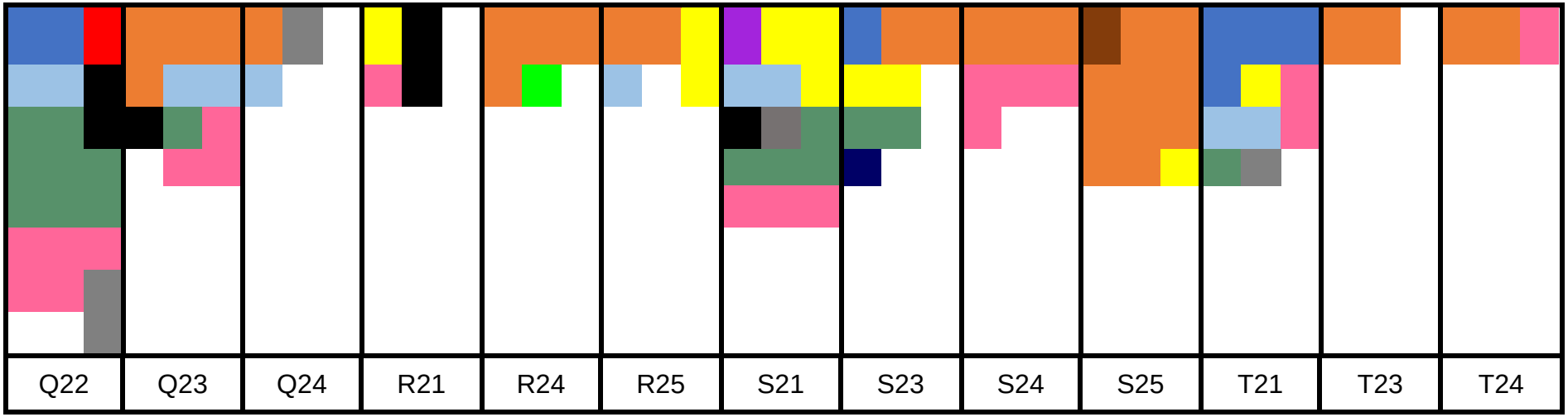
Appendix F: Photomicrographs of (28-30) *Searsia pyroides*, (31-33) *Vachellia mellifera* and (34-36) *V. tortilis.*



Appendix G: Venn diagram showing the deciduous and evergreen taxa identified in stratum 4b, Excavation 1, Wonderwerk Cave.



Appendix H: The distribution of the charcoal taxa across the cave floor.



Key		
		Berchemia cf. *zeyheri*
		Commiphora schimperi
		Halleria lucida
		Ehretia sp.
		Heteromorpha arborescens
		Olea europaea subsp. *africana*
		Ozoroa paniculosa
		Searsia lancea
		Senegalia caffra
		Tarchonanthus camphoratus
		Tarchonanthus parvicapitutalus
		Vachellia cf. *tortilis*
		Vachellia cf. *karroo*
		Ziziphus mucronata

Appendix I: Distribution of taxa in South African bioregions and biomes (Mucina and Rutherford, 2006; van Wykand van Wyk, 2013).

Taxa	Savanna	Grassland	Albany Thicket	Succulent Karoo	Desert	Nama-Karoo	Inland Azonal Vegetation	Forest	Fynbos
Berchemia* cf. *zeyheri	■								
Commiphora schimperi	■								
***Ehretia* sp.**	■	■	■	■	■	■	■		
Halleria lucida		■						■	
Heteromorpha arborescens	■	■	■						
Olea europaea* subsp. *africana	■	■	■						
Olinia ventosa								■	
Ozoroa paniculosa	■								
Searsia lancea	■	■	■						
Senegalia caffra	■	■							
Tarchonanthus camphoratus	■	■	■						
Tarchonanthus parvicapitutalus	■	■							
Vachellia* cf. *tortilis	■			■			■		
Vachellia* cf. *karroo	■	■	■				■		
Ziziphus mucronata	■	■	■			■	■		

Appendix J: Climate of the Wonderwerk Cave locality between 6.9-5.9 ka cal BP. SRZ = Summer Rainfall Zone, WRZ= Winter Rainfall Zone, YRZ= Year-Round Zone.

Taxa	**Climate tolerance** (Mucina and Rutherford, 2006)	**Rainfall zone** (Chase and Meadows, 2007)
Berchemia zeyheri	Warm, dry	SRZ
Commiphora schimperi	Hot, very dry	SRZ
***Ehretia* sp.**	Warm, dry-mesic	SRZ
Halleria lucida	Warm, moist-mesic	SRZ; WRZ
Heteromorpha arborescens	Warm, mesic	SRZ
Olea europaea* subsp. *africana	Warm, dry-mesic (drought & frost)	SRZ; WRZ; YRZ
Olinia ventosa	Warm, moist-mesic	WRZ; YRZ
Ozoroa paniculosa	Hot, dry	SRZ
Searsia lancea	Warm, dry (drought & frost)	SRZ; WRZ; YRZ
Senegalia caffra	Warm, dry-mesic (drought & frost)	SRZ
Tarchonanthus camphoratus	Warm, dry (drought)	SRZ
Tarchonanthus parvicapitutalus	Warm, dry	SRZ
Vachellia tortilis	Warm, dry (drought)	SRZ
Vachellia karroo	Mesic, (drought & frost)	SRZ; WRZ; YRZ
Ziziphus mucronata	Warm, dry-mesic (drought)	SRZ; YRZ